ABSTRACT

Title of Dissertation:	EFFECTS OF SLOPE RATIO, STRAW MULCHING, AND COMPOST AMENDMENT ON VEGETATION ESTABLISHMENT AND RUNOFF GENERATION
	Dylan Casey Owen Doctor of Philosophy, 2020
Dissertation directed by:	Professor Allen P. Davis, Department of Civil and Environmental Engineering Professor Ahmet Aydilek, Department of Civil and Environmental Engineering

Soil erosion management is a major environmental challenge facing highway construction. This study was undertaken to evaluate the effectiveness of compost use in lieu of topsoil for final grade turfgrass establishment on highway slopes. Two compost types, biosolids and greenwaste, and four compost/topsoil blends were compared with a topsoil standard (TS; with straw and fertilizer application) in their ability to reduce soil and nutrient loss and improve vegetation establishment. A series of greenhouse studies and field tests were conducted to analyze the effects of slope ratio, straw mulching, and compost mixing ratio on runoff by observing green vegetation (GV) establishment, runoff volume generation, and nutrient and sediment export. GV was measured using an innovative image segmentation and classification algorithm coupled with machine learning approaches with varying block size and classification acceptance thresholds. Algorithm classifications were compared to manual coverage classifications with R-squared values of 0.86 for GV, 0.87 for straw/dormant vegetation, and 0.96 for exposed soil, respectively. Straw mulching (≥95% straw cover) reduced evaporation rates and soil sealing and increased soil roughness and field capacity (FC), which significantly reduced volume runoff (34-99%) and mass export of sediment and nutrients (81-91%). With mulching, no statistical differences were found in GV establishment among the compost and TS treatments (≥95% cover in 60 days) while non-mulched media cover reached a maximum of 35%, due to limited moisture availability. Composted material (excluding 2:1 compost: topsoil mixtures) had higher hydraulic conductivity, FC, and shear strength than TS which, combined with straw mulching, reduced total runoff volume by 33-72%. This led to sediment and nutrient mass reductions of 57-97% and 6-82%, respectively, from standard TS. A general increase in runoff generation and decrease in GV was seen with slope ratio increase (41-96% more nutrient and sediment export and 81-97% lower GV from 20:1 to 2:1 slopes). However, benefits displayed at 25% slope were reduced at shallower slopes and enhanced at greater slopes. The use of compost as an additive or replacement to TS, with straw mulching, was seen to reduce runoff generation and improve runoff quality from the TS standard and is suggested as possible alternatives.

EFFECTS OF SLOPE RATIO, STRAW MULCHING, AND COMPOST AMENDMENT ON VEGETATION ESTABLISHMENT AND RUNOFF GENERATION

by

Dylan Casey Owen

Dissertation submitted to the Faculty of the Graduate School of the University of Maryland, College Park, in partial fulfillment of the requirements for the degree of Doctor of Philosophy
2020

Advisory Committee:
Professor Allen P. Davis, Chair
Professor Ahmet Aydilek
Assistant Professor Michelle Bensi
Professor Robert Hill
Assistant Professor Birthe Kjellerup

© Copyright by
Dylan Casey Owen
2020

Dedication

To my family and my best friend forever Cat.

Acknowledgements

I acknowledge the support of the Maryland Department of Transportation State Highway Administration (MDOT SHA) and the Aberdeen Wastewater Treatment Facility for donating biosolids compost.

Thank you to the committee members and my two fantastic advisors.

TABLE OF CONTENT

List of Tables

List of Figures

Chapter 1: Introduction

Soil erosion management is a major environmental challenge facing highway construction. Sediment and nutrient leaching from exposed roadway hillside construction sites can flow into streams and waterways, affecting entire water systems through deposition of sediments and creation of dead zones and eutrophication (USEPA, 2003). Power of rainfall impact, overland flow, and rill flow to erode hillslopes are controlled by soil cover, soil physical properties, and the slope steepness and length (Renard et al., 1997). Soil microtopography also plays a major role in the generation and dispersal of runoff (Abrahams et al., 1992; Liu and Singh, 2004). These studies suggest that irregular slopes, created by local soil minima and maxima, large particle size distributions, extensive soil coverage, and other factors can drastically affect the flow and resistance created by the soil surface.

Conventional stormwater management practices (SMPs) for exposed slope stabilization include synthetic erosion control blankets, turfgrass sod, straw mulching, and silt fence treatments with rapid permanent vegetation establishment being the goal. Permanent vegetation plays a key role in both protecting soil surfaces from rainfall impact and anchoring soil through extensive root systems (Mutchler et al., 1994; Robnison et al., 1996). To improve SMPs and increase the amount of renewable and reusable materials used in construction, compost addition has become the focus of many agencies due to its potential benefits to soil. Compost is a recycled, renewable resource that is high in organic and inorganic nutrients and can readily be found across the globe. Depending on the climate and availability, feedstocks for these composts include food waste, yard waste, and treated wastewater sludge. Each of these feedstocks results in a composted material with varying physical and nutrient compositions unique to the feedstock, composting method, and composting environment that can affect how well vegetation establishes and how effective the material is as an SMP amendment (Diaz et al., 2007).

The use of compost as an SMP for construction-related transportation projects has been studied and implemented in states across the U.S. (USEPA, 2003). Several researchers have found improvements to soil aggregation and hydraulic conductivity using compost and observed reductions in runoff volumes and sediment loss when compared to bare soil (Glanville et al. 2004; Faucette et al. 2005; Harrell and Miller, 2005; Curtis and Claassen, 2007; Mukhtar et al. 2008; Hansen et al., 2012; Chaganti and Crohn, 2014). Additionally, a review of 25 studies on compost effects to soil properties by Kranz et al. (2020) identifies a variety of improvements to soil physical properties, such as increased porosity and decreased bulk density, increased soil stability and aggregation, and increased field capacity (FC). Even though reductions in sediment and volume runoff have been observed, substantially greater (4-10-fold) nutrient concentrations in the runoff from compost amended soil surfaces, compared to bare topsoil, have been documented in past studies (Faucette et al., 2005; Muhktar et al., 2005; Chaganti and Crohn, 2014).

Straw mulching as an additional SMP to compost has the potential to increase surface roughness and moisture storage volume while reducing rainfall kinetic energy (KE) and momentum transfer to soil surfaces (Mannering and Meyer, 1963; Poesen and Lavee, 1991; Hillel, 2004; Jordan et al., 2010; Liu et al., 2012). The transfer of KE and momentum to soil structures breaks down soil aggregates and causes particle detachment which increases soil bulk density, entrains soil particles into surface flow, and reorganizes soil structure (Duley, 1939; Edwards, 1969; Hillel, 2004; Armenise et al., 2018). This often results in soil sealing of pores, which reduces hydraulic conductivity and infiltration. Many previous studies have focused on the use of uncovered composted material vis-à-vis some form of topsoil control, but few have analyzed composted material with additional SMPs (e.g., straw mulching).

Soil cover has long been identified as a crucial element in soil conservation, with cover factors identified specifically within many, if not all, erosion models (Wischmeier and Smith, 1978; Renard et al., 1997; Liu et al., 2004; Pandey et al., 2016). The type and abundance of different soil covers, including both green and dormant vegetation, in these scenarios is important during the initial establishment phase through the subsequent reestablishment in the second growth season. In this second season, green vegetation growth is intermingled with dormant growth and plant residue. Both residue and green vegetation growth are important to rainfall kinetic energy dispersion and kinematic flow resistance, each greatly affecting soil erodibility (Liu et al., 2004; Choi et al., 2017).

Providing accurate and quantifiable coverage information for regional mitigation, both green vegetation and straw(residue)/dormant vegetation, requires an efficient and effective approach for understanding current and evolving land cover in the target location. Digital image-based methods have increasingly been used to quantify land cover in an automated fashion due to their many advantages over manual coverage identification (increased precision, reliability, reproducibility, and rapid response), and processing of the captured images is often needed (Bauer and Strauss, 2014; Patrignani and Ochsner, 2015; Lottes et al., 2016; Mortensen et al., 2017; Riegler-Nurscher et al., 2018). As summarized by Hamuda et al. (2016), three common methods exist for segmentation of image components representing plant structures and background materials (e.g., soil and residue): color index-based, threshold-based, and learning-based approaches. Typically, color indexing and thresholding methods are fast and reliable to identify green vegetation cover under consistent photo conditions; e.g., lighting and photo angle; however, many of these methods are not designed to identify residue and litter (e.g. straw or dormant grass) as independent from the background (Gee et al., 2007; Montalvo et al., 2013; Hu et al., 2018; Riegler-Nurscher et al., 2018).

Beyond color thresholding, methods have been developed to use different feature descriptors to represent image objects that can then be used for classification through a learning algorithm, e.g. fuzzy logic, k nearest neighbors (KNN), or random forest (Bauer and Strauss, 2014; Mortensen et al., 2017; Lottes et al., 2017; Riegler-Nurscher et al., 2018). Although more information is provided through the learned algorithms, they often require greater processing power and many training samples to provide accurate classifications (Hamuda et al., 2016; Riegler-Nurscher et al., 2018; Hu et al., 2018).

1.1 Research Goal

While composted material has been seen to improve vegetation establishment and soil physical characteristics, use of compost magnifies the potential for excess nutrient runoff as an SMP. It was the goal of this project to determine the performance of select compost products with additional SMPs (straw) as part of construction site erosion prevention systems with focus on vegetation growth and nutrient and sediment management.

1.2 Research objectives

Compost comes from a variety of different feedstocks which contribute to the ultimate composition of the material. The current research study aimed to investigate two types of compost, greenwaste (Leafgro®) and biosolids (Aberdeen water treatment facility, MD), and the possible benefits or consequences of their use as an SMP for erosion management. Success of the chosen designs was based on the following criteria: 1) rapid and healthy green vegetative growth, 2) improved runoff retention and infiltration, 3) reduced sediment erosion, and 4) reduced nutrient leaching.

Specific research objectives for this study include:

1. Development of a method to measure ground coverage of green vegetation, straw/dormant vegetation, and exposed soil for the purpose of post-construction soil coverage measurements along highway systems with moderate to steep slopes for vegetation establishment, second stage growth, and slope stability.
2. Development of an algorithm using computer vision elements (color, texture, and oriented gradients) trained for the purposes of identifying ground cover data.
3. Optimization of the developed coverage algorithm to perform quickly and effectively for a variety of different ground covers, lighting, and angles.

4. Observation of field scale application of compost and compost mixtures versus standard topsoil to identify GV growth and runoff quality cycles over time, with the two-fold purpose of identifying critical elements for controlled greenhouse studies and identifying trends in long term observation.
5. Comparison of runoff nutrient concentrations and volumes from compost addition to topsoil within a controlled greenhouse setting, with the hypothesis that increased compost would decrease volume runoff but increase concentration runoff.
6. Analysis of the influence of straw mulching as an additional ground cover SMP to compost incorporation, the hypothesis being additional straw mulching will further reduce runoff volume to offset nutrient concentration increases with compost addition rendering reduced nutrient mass export.
7. Comparison of compost blankets to TS at a variety of slope ratios, with the hypothesis that slope ratio will change the relationships among different media by affecting total runoff quality and quantity differently depending on medium.
8. Synthesis of the observed field and greenhouse data to support or refute the advancement of compost amendment as a stormwater management practice for soil erosion control.

Chapter 2: Measuring soil coverage using image feature descriptors and the decision tree learning algorithm

Dylan Owen[1], Michelle T. Bensi[2], Allen P. Davis[3], and Ahmet H. Aydilek[4]

[1] Graduate Research Assistant, Dept. of Civil and Environmental Engineering, Univ. of Maryland, College Park, MD 20742.
[2] Assistant Professor, Dept. of Civil and Environmental Engineering, Dept. of Civil and Environmental Engineering, Univ. of Maryland, College Park, MD 20742, USA
[3] Professor and Charles A. Irish, Sr. Chair in Civil Engineering, Dept. of Civil and Environmental Engineering, Univ. of Maryland, College Park, MD 20742, USA.
[4] Professor, Dept. of Civil and Environmental Engineering, Dept. of Civil and Environmental Engineering, Univ. of Maryland, College Park, MD 20742, USA (corresponding author). E-mail: aydilek@umd.edu

2.1 Abstract

The quantification and identification of ground cover plays a key role in erosion modelling, weed measurement, plant disease identification and other environmental applications. Currently, a variety of methods are used to mechanically classify digital images for ground cover. Only a few of these methods can distinguish green vegetation, straw/dormant vegetation, and exposed soil using only the Red-Green-Blue (RGB) spectrum. This research presents an approach to classifying ground cover using standard JPEG images and readily available *Matlab* (2018b) functions. The approach uses block segmentation, as opposed to pixel-wise or object based segmentation, and compares multiple machine learning approaches with varying pixel block size and classification acceptance thresholds. The most successful classification approach found through this study was the decision tree algorithm with a 70-pixel block size and 60% classification acceptance threshold. Images were reduced to three feature descriptors: colour, texture,

and oriented gradients to represent the respective RGB spectrum for an image. Both the training set and test set images used in this research came from field and greenhouse studies done between 2016 and 2019. The produced classifications were compared to manual coverage classifications using *Samplepoint*, a grid-based method, with R-squared values of 0.86 for green vegetation, 0.87 for straw/dormant vegetation, and 0.96 for exposed soil, respectively. This method showed strong performance for images containing exposed soil and either green vegetation or straw/dormant vegetation. The method was less effective for images with large quantities of both green vegetation and straw/dormant vegetation likely due to their similar shape.

Keywords: Ground cover measurement, Decision trees, Computer vision

2.2 Introduction

Soil cover has long been identified as a crucial element in soil conservation, with cover factors identified specifically within many, if not all, erosion models (Wischmeier & Smith, 1978; Renard, Foster, Weesies, McCool, Yoder, 1997; Liu & Singh, 2004; Pandey, Himanshu, Mishra, Singh, 2016). Focusing on slope stability, the production of runoff and sediment yield from post construction can greatly be affected by vegetation establishment rates and total percentages (Pan & Shangguan, 2006). As an example, Maryland Department of Transportation (MDOT) requires 95% vegetation coverage before final acceptance as a means of runoff and sediment reduction. Evidence suggests that using soil conservation techniques, such as direct drill and mulching, can reduce soil loss by up to 80% and established vegetation can reduce runoff volume and sediment loss by up to 25% and 95%, respectively (Strauss et al., 2003; Pan & Shangguan, 2006). Providing the appropriate conservation technique along with accurate and quantifiable vegetation coverage information for regional mitigation requires an efficient and effective approach for understanding current and evolving land cover in the target location.

This research introduces a practical method for using photographs to estimate ground cover to support conservation efforts. Specifically, the objective of this research is to present a new method to measure ground coverage of green vegetation, straw (plant residue)/dormant vegetation, and exposed soil for the purpose of post-construction soil coverage measurements along embankments with moderate to steep slopes for vegetation establishment, second stage growth, and slope stability.

Measuring ground cover for ecological assessments has historically been done using on-site investigations through visual analysis or through digital image manipulation (Booth, Cox, Berryman, 2006). Commonly used strategies such as the line-intercept transect method, point frames, or lattice screen methods are often time-consuming and tend to lack precision and reproducibility (Sykes, Horrill, Mountford, 1983). Recent advancements in digital image analysis have improved quantification of growth analysis, plant disease identification, and weed measurement (Todd & Kommedahl, 1994; Glasbey & Horgan, 1995; Gee, Bossu, Jones, Truchetet, 2008). This process is quickly evolving as both satellite and digital imagery become more advanced and accurate (Burgos-Artizzu, Ribeiro, Tellaeche, Pajares, Fernández-Quintanilla, 2009).

Within the last two decades, there has been a push for quicker, more reliable and reproducible soil cover measurements through automation. Accurate and precise measurements of vast areas of land have spurred the evolution of a variety of different methods for gathering soil coverage information. Facilitating the growth of these methods has been the advancement of computer vision and, more recently, the use of machine learning. These topics have become ubiquitous in everyday life with the improvement of mobile technologies, image and facial recognition, self-driving technology, energy production, and natural language processing. The ubiquity has enhanced the application of these technologies to agricultural and environmental domains, including to help identify soil coverage information (Luscier, Horferlin, Sander, Stachniss, 2006; Gee, Bossu, Jones, Truchetet, 2008; Bauer & Strauss, 2014; Patrignani & Ochsner, 2015; Lottes, Horferlin, Sander, Stachniss, 2016; Mortensen, Dyrmann, Karstoft, Jorgensen, Gislum, 2017; Riegler-Nurscher, Prankl, Bauer, Strauss, Prankl, 2018).

The combination of computer and environmental sciences as well as the advancement of mobile technologies has brought about an abundance of accessible plant identification and land cover applications. As an example, the mobile application *PlantSnap*, uses machine learning to identify plants appearing in images. The underlying algorithms used over 150 million images to identify individual pictures of plants with 90% success (plantsnap.com, 2019). *Canopeo*, another mobile application, focuses on total coverage and allows the user to input various colour thresholds to attain all green vegetation coverage in an area (Patrignani & Ochsner, 2015). Several existing broader application technologies use various combinations of machine learning and computer vision to identify specific plant species (e.g., *Leafsnap*, *Google Goggles*) and occasionally crop coverage (e.g., *SoilCover*).

Many of the current field coverage computer vision and machine learning approaches in use today focus primarily on use of colours as the basis for image classification while few utilize other computer vision elements. As summarized by Hamuda, Glavin, and Jones (2016), three common methods exist for segmentation of image components representing plant structures and background materials (e.g., soil and residue): colour index-based, threshold-based, and learning-based approaches. Each of the colour index-based and threshold-based methods for distinguishing between the plant structure and background material take advantage of the predominant fact that living vegetation colour is typically green and can be readily distinguished from non-green soil, litter, and residue (Booth, Cox and Berryman 2006, C. Gee, et al. 2008, M. Montalvo, et al. 2013, Hamuda, Glavin and Jones 2016, Hu, Dai and Peng 2018). These methods focus on selecting either a static or dynamic intensity value at which pixels with greater intensity will be associated with vegetation and pixels with lower intensity are considered background. Typically, these methods are fast and reliable in identifying green vegetation cover under consistent photo conditions; e.g., lighting and photo angle; however, many of these methods are not designed to identify residue and litter (e.g. straw or dormant grass) as independent from the background (C. Gee, et al. 2008, M. Montalvo, et al. 2013, Hu, Dai and Peng 2018, Riegler-Nurscher, Prankl, et al., A machine learning approach for pixel wise classification of residue and vegetation cover under field conditions 2018). Most of these methods are designed for agricultural purposes and specifically for the initial growing period, when weeds have the most potential for damaging a crop (Zimdahl, 1988; Zimdahl, 1993). The identification of these residues is not a priority. Yet, residues can be important in erosion control and in many cases, ground cover such as straw or hay is placed as ground cover to protect bare soils from rain impact and to hold moisture to encourage seed germination.

Introducing additional computer vision elements has improved the ability for computers to identify coverage elements beyond green vegetation. Bauer and Strauss (2014) used *eCognition* 8.7 (Trimple Germany GmbH) for object-based image analysis. This method segmented the image using a multiresolution segmentation algorithm within the *eCognition* software and classified the segmented objects using fuzzy logic theory along with user-defined rules. Mortensen, Dyrmann, Karstoft, Jorgensen, and Gislum (2016) identified oil radish, barley, weed, stump, and soil using deep convolutional neural networks. Riegler-Nurscher, Prankl, Bauer, Strauss, and Prankl (2018) developed a method that utilized entangled random forests to train a computer for classification using colour, variance, pointness, linearness/pointness, and entangled features to identify stone, soil, living plant, biofilm and residue objects. Each of these provide more information on general soil cover beyond identifying green vegetation through manipulation of the colour spectrum.

Measuring coverage with slope stability as the primary focus presents a different problem from the focus of existing approaches used in agricultural applications. Specifically, identification of weeds and specific flora is less important than the accurate measurement of all plant growth and non-green protective residue. Post-construction slopes for MDOT SHA are designed with soil conservation as the major goal, without tillage or crop yield to contend with. Sites are initially established on shallow (less than 4:1, 25%), to often very steep slopes (greater than 4:1, 25%). As mentioned previously, the sites are then monitored regularly until final acceptance when 95% groundcover has been achieved (MDOT, 2019). Reaching 95% groundcover, however, may not occur uniformly with all flora remaining green throughout the observational period. The type and abundance of different soil covers, including both green and dormant vegetation, in these scenarios is important during the initial establishment phase through the subsequent reestablishment in the second growth season. In this second season, green vegetation growth is intermingled with dormant growth and plant residue. Both residue and green vegetation growth are important to rainfall kinetic energy dispersion and kinematic flow resistance, each greatly affecting soil erodibility (Sander, Hairsine, et al., Unsteady soil erosion model, analytical solutions and comparison with experimental results 1996, Liu and Singh 2004).

Beyond the colour thresholding mentioned previously, some methods use different feature descriptors to represent image objects that can then be used for classification through a learning algorithm, such as k nearest neighbours (KNN) and random forest (Bauer and Strauss 2014, Mortensen, et al. 2016, P. Lottes, et al. 2017, Riegler-Nurscher, Prankl, et al., A machine learning approach for pixel wise classification of residue and vegetation cover under field conditions 2018). Colour thresholding techniques are quick and can handle large batches of images over a short period of time, however, they do not leverage the abundance of information presented through a learned algorithm with additional feature descriptors. Although more information is provided with the learned algorithms, they often require greater processing power and many training samples to provide accurate classifications (Hamuda, Glavin and Jones 2016, Riegler-Nurscher, Prankl, et al., A machine learning approach for pixel wise classification of residue and vegetation cover under field conditions 2018, Hu, Dai and Peng 2018).

The procedure developed in this research extends beyond colour thresholding for green coverage but is not as computationally intensive as the more rigorous algorithms employed for plant identification. Under the proposed approach, RGB images and existing *Matlab* (2018b) functions were used to extract image feature descriptors for three image objects of interest (exposed soil, green vegetation, and straw/dormant vegetation) in the images captured from two field and four greenhouse studies. These descriptors were then used to train an algorithm and to classify image coverage.

The method described in this study follows the learned algorithm approach, and utilizes the standard RGB spectrum, a grid of set pixel size for segmentation, and several different feature descriptors identified from previous studies. Existing *Matlab* functions are used to extract image colour, texture, and histogram of gradients (HOG) as feature descriptors; to take advantage of known differences between residue, vegetation, and soil.

2.3 Methods

Two stages for model development were used in this study: 1) a classifier model was trained based solely on example images with only one type of object (exposed soil, straw/dormant vegetation, or green vegetation); and 2) the model was tested by seeking to identify multiple types of objects within a single image. A flow chart of the process used in this study is given in Figure 2-1 and further described below.

Initially, images underwent two processing steps, 1) the original images were cropped to the region of interest (ROI) and 2) the images were segmented into smaller subsets (pixel blocks). Following processing of the images, feature descriptors were extracted (based on green colour, texture, and oriented gradients) from the subsets to represent the image segments. Images were then split into (1) testing dataset and (2) the validation and training dataset for classification learning. The validation and training set was then further partitioned into (a) the training set used to fit several candidate models (i.e., decision tree, K-nearest neighbour, support vector machine, and ensemble random under-sampling boosting models) and (b) the validation set used to optimize (tune) model parameters using six-fold cross validation. The "tuned" trained models were then applied to predict image classification using the "unseen" testing set and performance was compared to manual classification. Specifically, to test the accuracy of the classification models, 73 manually classified images; with a range of different exposed soil, green vegetation, and straw/dormant vegetation coverage percentages; were compared to the algorithm-derived percent coverage classifications. Feature extraction, model training, and image classification utilized *Matlab* (2018b) applications and functions. Additional information regarding each step of the modeling process is provided below.

2.3.1 Image acquisition

A series of digital images were captured between 2016 and 2019 from field and greenhouse experiments constructed to study use of compost in lieu of topsoil in highway slopes. Figure 2-2 provides examples of the field and greenhouse designs. In both the field and greenhouse experiments, the designs used 5 different soil media with straw and without straw application. The media included topsoil, biosolids compost, greenwaste compost, 2:1 topsoil: biosolids compost blend, and 2:1 topsoil: greenwaste compost blend. Field slopes had similar angles (1.5±0.5:1) while greenhouse images came from 3 different slope angles; 20:1, 4:1, and 2:1. Images were taken by hand at an angle and height of 30º from vertical and 1.8 m, respectively, in the field images and 0º from vertical and 1.2 m in the greenhouse images, respectively. Figure 2-3 is an example of field and greenhouse image capture focusing on material growth and properties. Field images were taken between August 2016 and August 2017 to capture low soil coverage, the initial vegetation growth stage, and the second growth stage with low soil coverage and high residuals (dormant vegetation). Greenhouse images focused only on the initial growth stage over the first 3 months of growth and included low soil coverage, the initial growth stage, as well as heavy straw (residuals) application with various degrees of growth.

A Nikon D7100 digital camera with an AF-S DX NIKKOR 18-140mm f/3.5-5.6G ED VR lens was used to capture the images in JPG format with the auto focus feature, maximum pixel size of 4000 x 6000, without lens zoom, and at a hard sharpness and normal saturation.

After image capture, photos were cropped to include only the region of interest (ROI) and exclude elements of the image that were not necessary in the coverage classification process or that were repeated in multiple images. For example, Figure 2-4 shows the representative portions of images extract from Figure 2-3. These images represent a section of slope that corresponds to approximately 110 x 183 cm and 61 x 91.4 cm for the field and greenhouse setup, respectively. This produces an image size of approximately 2000 x 3500 pixels.

Over the testing period, thousands of images were taken from both field and greenhouse sites. For the purpose of developing this methodology, 123 of the images captured, including the training set (50 images) and testing set (73 images), were chosen to represent the varying degrees of coverage for the three objects of interest; green vegetation, straw/dormant vegetation, and exposed soil; and the five different soil types. These images were both manually classified and classified via the trained algorithm.

2.3.2 Image Segmentation and Feature Extraction

All images used in training or testing were manually classified using *SamplePoint* (SamplePoint.org), a widely used standard for validation of automated methods, in order to determine the plot coverage based on the grid method (Hu, Dai and Peng 2018, Riegler-Nurscher, Prankl, et al., A machine learning approach for pixel wise classification of residue and vegetation cover under field conditions 2018). A grid size of 12 x 12 blocks was used (approximately 167 x 292 pixels/grid block), resulting in 144 total blocks per image. Each of these blocks was manually classified as either exposed soil, straw/dormant vegetation, or green vegetation. Anything not classified as belonging to one of those three categories was labeled 'not classified'; this included leaves, trash, etc. that may be found in either the field or greenhouse images. The process was repeated by 6 different observers using 35 of the 73 selected images. These results were used to provide standard deviations for the manual observations. Other measures of performance (e.g., correlations) were calculating using the results from the 35 image/6 observer testing set as well as the results from one observer that manually classifying the remaining 38 images.

All 123 images, whether used for training (50 images) or testing (73 images) the algorithm, underwent the same segmentation and feature descriptor extractions, as demonstrated in Figure 2-5. Each image (*I*) was segmented into n pixel blocks of equal size (I_n) with r remainder blocks (I_r) representing pixel blocks smaller than the preset pixel block size, where the total image can be represented as $I = \sum I_n + \sum I_r$. In Figure 2-5, I_1through I_6 are equal block sizes and, together, represent $\sum I_n$ while I_7 and I_8 are both smaller than the preset pixel block size and represent $\sum I_r$. Each pixel block contains the visual RGB colour spectrum data originally found in I. In final classification, segments I_n and I_r were multiplied by the respective percentage of the total image, to prevent over estimation of coverage due to remainder image blocks.

From each pixel block I_n and I_r, feature descriptors were extracted based on colour (greenness), texture, and oriented gradients (Figure 2-5 shows this process for image block I_2). To represent each of these descriptive images, the mean, median, mode, and standard deviation for each feature descriptor of the pixel block I_n or I_r was calculated. This process led to each image segment being represented by 12 discrete values, four for each of the three feature descriptors.

Green colour representation of each pixel block I_n or I_r was done using (1) normalized RGB data and (2) the excess green (ExG, vegetation contrast index defined by Woebbecke et al., 1995 for plant region identification) and excess red (ExR, red vegetative index developed by Meyer et al., 1998 to reduce interference from background or camera operation) indices, as illustrated in Figure 2-6. All RGB data were normalized for colour extraction to reduce illumination and angle effects. This process takes advantage of differences in green vegetation and, generally, yellow straw compared to the, typically, darker soil.

Specifically, for each pixel within I_n or I_r the green colour is defined as the average of the ExG and the ExGr (i.e., ExG minus the ExR) (Meyer & Camargo-Neto, 2008)

$$Green\ Color = \frac{ExGr + ExG}{2} \qquad \text{Eqn. 1}$$

Where: ExG and the ExGr were calculated to represent the colour of the pixel block, based on the following equations:

$$ExR = 1.4 * r - g \qquad ExG = 2 * g - r - b \qquad ExGr = 3 * g - 2.4 * r - b \qquad \text{Eqn. 2}$$

where the r, g, and b are the normalized original R, G, and B spectral values defined as:

$$R = I_{k,k=n,r}(:,:,1) \qquad G = I_k(:,:,2) \qquad B = I_k(:,:,3) \qquad \text{Eqn. 3}$$

$$r = \frac{R}{R+G+B} \qquad g = \frac{G}{R+G+B} \qquad b = \frac{B}{R+G+B} \qquad \text{Eqn. 4}$$

This resulted in a single array of 2 dimensions with the same length and width as $I_n$or I_r filled with a new set of colour values. All these values were then reduced to the four different representative values for each image shown in the final block of Figure 2-6: mean, median, mode, and standard deviation.

For the extraction of non-colour features, both the oriented gradients and texture elements were extracted using the default settings for the *Matlab (2018b)* functions, *extractHOGFeatures* and *entropyfilt*, respectively. These functions were applied to the grayscale of pixel block $I_n$or I_r. Similar to the colour feature extraction, both oriented gradients and texture returned arrays similar to the initial $I_n$or I_r which was reduced to the four different mean, median, mode, and standard deviation values.

Figure 2-7 gives an example of the resulting oriented gradient vectors and the entropy filter for two example pixel blocks. Oriented gradient values represented the magnitude and direction of gradient vectors within an 8 x 8 pixel neighbourhood. Each of these values was binned into 9 core directions, 0, 45, 90, 180 etc., which can be seen in the middle images in Figure 2-7 as a compass rose. These values represented the linearity of an image segment and take advantage of the general shape of both vegetation and straw compared to soil; vegetation and straw oriented gradients were more clustered while soil was generally more dispersed.

Like the oriented gradient, texture values were calculated based on an 8 x 8-pixel neighbourhood. This method represents texture as the total entropy within an image, calculated as the number of 'edges' or sharp changes in intensity within an image segment (Gonzalez, Woods and Eddins 2003). The final images on the right side of Figure 2-7 show the entropy filtered original images, greater textural changes with high contrast between edges (such as sharp contrast between blades of grass) corresponded to greater entropy values compared to more uniform surfaces which had lower intensity values (like soil). Entropy images had greater intensity values and brighter images for grass and lower intensity values and darker images for soil.

2.3.3 Classification Training and Optimization

To develop the learned algorithm, a set of training images that could represent each of the three image objects was necessary. To facilitate the large amount of information needed to train the algorithm, 50 captured images from the field and greenhouse studies were manually classified, using SamplePoint with 12 x 12 grid size. These 50 images were selected because they had greater than 95% exposed soil, straw/dormant vegetation, or green vegetation. The images were then broken into smaller image pixel blocks, based on the pixel block size chosen from Table 2-1. Each of the presented categories were represented by 21 exposed soil, 19 straw/dormant vegetation, and 10 green vegetation raw images. After image pixel block segmentation, the categories were represented by over 30,000 soil, 21,000 straw/dormant vegetation, and 14,000 green vegetation representative image pixel blocks, respectively. Example images for each category that contain greater than 95% coverage are shown in Figure 2-8 along with the number of available raw images and the minimum number of image blocks generated for each category. The minimum number of available image segments was based on the largest pixel block size shown in Table 2-1.

The algorithms considered in this study (and listed in Table 2-1) are as follows: (1) support vector machine, which segments the desired classification objects into representative dimensional spaces separated by hyperplanes whereby future classifications are made based on similarity to the dimensional space; (2) K-nearest neighbours, which classifies an image element based on its proximity to the most common trained data points; (3) decision tree, which makes a series of binary decisions at various 'nodes' until a final decision is made; and (4) ensemble random undersampling boosting, which balances training data sets and utilizes multiple learning algorithms to develop a single algorithm. Models based on all four algorithms were trained using the training set, based on varying pixel block size, and using a 6-fold cross-validation within the 'Classification Learner' application from *Matlab*. All four algorithms use the default *Matlab* settings and were chosen based on the best percentage 'Accuracy' score given by the program for validation activities (i.e., the percent the algorithm correctly placed an unknown image into the corresponding classification).

Changes in the pixel block size used for classification, shown in the middle column of Table 2-1, corresponds to the accuracy of the total representation of a single image. Larger pixel blocks will include larger sections of the original image and reduce clarity on specific image objects within the image. Smaller image blocks will have fewer image objects but break the original image into far more pieces to be analyzed (ex. 100 x 100 image divided by 10 x 10 pixel blocks produces 100 total blocks, divided by 5 x 5 pixel blocks produces 400 total blocks). Image blocks between 30 and 100 were chosen to determine the effects of altering this feature on image classification accuracy.

The threshold values presented in Table 2-1 correspond to a minimum value at which the computer can classify the image segment as one of the three defined categories (exposed soil, straw/dormant vegetation, and green vegetation). Values that do not reach that threshold are labeled ‘unknown’.

2.3.4 Analysis of Model Performance

Optimum results were chosen based on a series of tests varying algorithms, pixel block size, and classification threshold. The list of factors considered in model optimization are presented in Table 2-1. Performance of each model (i.e., combination of algorithm, pixel block size, and classification threshold) was assessed based on the original objectives of this study and determined by: 1) the R-squared values for predicted compared to manually observed classification for coverage percentage of green vegetation, straw/dormant vegetation, and exposed soil, 2) the average absolute value of the difference between the manual and algorithm calculated coverage percentages, and 3) the execution time for classification of a single image normalized to the 100-pixel block size, based on an Intel® Core™ i5-4460 CPU @ 3.20GHz. To reduce the volume of results, the performance of all algorithms was initially compared with no thresholding at all pixel block sizes; algorithms or pixel block sizes that performed significantly worse than other algorithm and pixel block size combinations were not tested at varying thresholds. Algorithm optimization was based on the comparisons between values of performance for each algorithm at the corresponding pixel block sizes and thresholds using the Welch's t-test (Welch, 1947).

2.4 Results

2.4.1 Optimization and Validation of Models

The most common methods used for initial image segmentation with the purpose of object classification are pixel- and object-wise segmentation (J. Luscier, et al. 2006, Riegler-Nurscher, Prankl, et al., A machine learning approach for pixel wise classification of residue and vegetation cover under field conditions 2018). The research presented here deviated from the common methods by using a set block segmentation method. The chosen method provided more information on shape and texture of image objects than pixel-wise segmentation by inclusion of a larger visual area. However, the method used here becomes equivalent to pixel-wise segmentation when the pixel block size is set to 1 x 1. However, as discussed later, the decrease in pixel block size requires additional computational time and may result in a loss of clear visual distinctions between image objects. By choosing set pixel block sizes, vis-à-vis object-wise segmentation, the method provided similar shape and texture information but on a more general scale with the goal of reducing computational demands.

Figure 2-9 shows the comparison of model performance (R-squared and average difference between manual and calculated coverage percentages) for all four algorithms and considering the 100-, 80-, 70-, 50-, and 30-pixel block sizes with a threshold of 0% for green vegetation, straw/dormant vegetation, and exposed soil. As can be seen in the figure, all pixel block sizes, except the 50-block size, produced similar R-squared and average differences between manual coverage percentages and calculated coverage percentages based on the three classifications. The 50-pixel block size performed consistently well using the ENS algorithm but showed fluctuations for green vegetation and straw/dormant vegetation for other algorithms. As discussed later, the approach proposed in this paper had a slightly lower success rate when classifying green vegetation and straw/dormant vegetation compared to classification of exposed soil. It was judged that this was due to the similarity between green vegetation and straw/dormant vegetation in terms of shape factors (texture and histogram of oriented gradients). It was unclear why the 50-pixel block size appeared to magnify this issue. However, as shown in Figure 2-10, with a reduction in pixel block size, the shape and texture contrasts become limited. Specifically, with the reduction in pixel block size, Figure 2-10 shows reduced shape information for both straw/dormant vegetation and green vegetation.

Considering the algorithm classification duration (a measure of computational demands), the 30- and 50-pixel block sizes took longer to classify per image, as shown by the classification times presented in Figure 2-11. Based on time required for classification for the 30-pixel block size and the poor R-squared and average differences values for the 50-pixel block, the 30- and 50-pixel block sizes were eliminated from further comparisons. Also, based on the student t-test performed on the average differences between manual and calculated coverage percentages over all 73 testing images, the SVM method consistently had statistically larger differences from manual observations than other algorithms at all larger pixel block sizes (values not presented); because of this, the SVM method was not analyzed further.

Times required for classification across the algorithms considered are seen in Figure 2-11. In general, the choice of classification algorithm had only a minor effect on the computational time, especially at larger pixel block sizes. However, with reduced pixel block size (i.e. 30-pixel block size) the DT algorithm performed faster than the other algorithms. Error bars for each test represent algorithm duration deviation at each pixel block size determined from multiple testing of the single 2000 x 3500 pixel image.

The DT, KNN, and ENS methods were then compared at the 70-, 80-, and 100-pixel block sizes using the range of thresholding values presented in Table 2-1. As an example of these results, Figure 2-12 shows the performance of the three algorithms using the 100-pixel block size for all five threshold values. For all the algorithms tested at each pixel block size, the average R-squared and average differences for the three coverage classification categories together changed very little with threshold changes; (average value and standard deviation taken across green vegetation, straw/dormant vegetation, and exposed soil) 0.88 ± 0.04 (R-squared) and 9.1 ± 1.1 (average difference) for KNN, 0.86 ± 0.03 and 9.3 ± 1.5 for DT, and 0.85 ± 0.06 and 10.5 ± 2.0 for ENS, for the 100-pixel block size. However, the greater overall R-squared and smaller overall differences both occurred using the DT algorithm at the 70-pixel block size; 0.89 ± 0.05 and 8.56 ± 1.36, respectively. Since none of the thresholding values resulted in a statistically more successful DT algorithm, the threshold that produced the greatest R-squared and least average difference was chosen which occurred for the 60% threshold.

Both R-squared and the overall differences were found to be optimal for the DT algorithm at the 70-pixel block scale and the image classification duration only increased by 52% and 17% from the 100- and 80-pixel block sizes, respectively. Therefore, the DT algorithm at the 70-pixel block scale with a 60% threshold was chosen as the optimal model and used for testing overall model performance.

2.4.2 Decision Tree Algorithm Performance

Model performance was assessed by comparison against manual (human) classification. Specifically, 35 representative images were manually classified by 6 independent observers. One observer manually classified all 73 images. The calculated percent coverage as a function of the manual percent coverage is presented in Figure 2-13 along with the standard deviation taken across the 6 manual observers. Error bars within graphs represent the percentage of cover not classified for the algorithm-based (calculated) coverage (y-axis) or the standard deviation between observations for the manual classifications (x-axis).

Correlations between manual and calculated coverage percentages for all three coverage types are presented in Figure 2-13. From the presented results, the derived algorithm slightly overpredicted the green vegetation at increasing actual coverage values and consistently underpredicted exposed soil with decreasing actual coverage. Straw/dormant vegetation coverage showed a general trend for underprediction at values <50% and overprediction at values >50%. The R-squared values and the calculated regression are presented in Table 2-2. Exposed soil had the greatest correlation followed by straw/dormant vegetation, and green vegetation.

To serve as an illustration, Figure 2-14 presents selected images that were analyzed manually and using the developed algorithm. The top three images represent 'successful' images, i.e., ones that matched closely with the manual coverage. For these images, on average, the calculated coverage percent differed from manual classification percentages by 1.9, 1.8, and 1.4% respectively, and the bottom three images represent less 'successful' images with average differences of 21, 20, and 19% respectively. As seen in the presented examples, and observed in other similar images, the algorithm typically matched exposed soil well regardless of other coverage types. Green vegetation and straw/dormant vegetation were accurately measured when one or the other was present but was less successful when both were present at high percentages (e.g 50% straw/dormant vegetation and 50% green vegetation). In high percentage cases, the percentage of green vegetation was consistently overpredicted, reducing the estimated percentage of straw/dormant vegetation.

2.5 Discussion

The proposed method makes classifications based on colour, texture, and histogram of oriented gradient information extracted from segmented pixel blocks. For both straw and grass, many of the values for oriented gradients and texture were similar. This can be seen in Figure 2-15, which shows texture mean values (y-axis) as a function of the mean histogram of oriented gradient mean values (x-axis) for a random selection of 10% of the test data. As seen in Figure 2-15, with both green vegetation and straw/dormant vegetation in the image, two of the three computer vision tools used in this study view the image object as generally similar. Therefore, the only remaining distinguishing feature for image classification was colour.

The use of colour as a classification tool is often affected by light exposure (Hu et al., 2018). For the separation of straw/dormant vegetation and green vegetation, lighting conditions likely affected the classification results (e.g., green vegetation with high exposure has higher red spectrum values leading to a more yellow colour similar to straw/dormant vegetation). Additionally, the pixel blocks average all image elements within the block, which could further "blur" the distinction in colour values when both green vegetation and straw/dormant vegetation were present in the same pixel block.

Although colour and lighting aspects may have affected the classification of green vegetation and straw/dormant vegetation, it did not appear to affect the classification of exposed soil. Figure 2-15 shows a clear separation of exposed soil from both green vegetation and straw/dormant vegetation based on the two computer vision tools used (histogram of oriented gradients and texture). Using these additional tools reduced the classification power of colour alone, which resulted in more consistent exposed soil results.

The specific algorithm produced through this study was designed using images from the Nikkon D7100 camera and was not tested on images captured with other cameras during the study period with no additional images available. It is possible that the method may not work as well with images captured from other cameras due largely to pixel to real world ratio, lens distortion, and color spectrum representation. The use of both histogram of oriented gradients and texture are highly dependent on pixel neighbourhoods which could be vastly different depending on camera quality. However, the method of feature extraction and model development were not dependent on the specific camera used in this study. One purpose of the study was to demonstrate a ground cover measurement method that utilized multiple computer vision tools, the method developed can then be implemented again with any camera.

Images captured in the field (Figure 2-4a) were taken at an angle. Perspective has the potential to affect the final ground cover measurement via unequal image spatial resolution and should be adjusted prior to algorithm application. For the purpose of algorithm development however, we judged that the angle shouldn't affect the correlations between manual and computer-based measurements, presented here, as both values were obtained using the same distorted images. With initial image adjustment to an undistorted frame the algorithm will more accurately represent actual ground cover values.

As stated by both Laflen, Amemiya, and Hintz (1981) and Riegler-Nurscher, Prankl, Bauer, Strauss, and Prankl (2018), and observed in the current study, using human observers for manual classification can lead to a large deviations in observed percent coverage, which provides important context when validating automated classification performance against manual observations. To further compare the derived classifications to the manual deviation, the average standard deviation between the 6 observers for each class and the average absolute value of the difference between actual and algorithm-derived percent coverage for each class are compared in Table 2-3. From the images and classifications presented, the average absolute value of the difference between manual and algorithm-derived percent coverage are greater than the average standard deviation between the 6 manual observations. This indicates that the algorithm did not perform within the deviation of manual observation. However, when only images without large coverage values for both green vegetation and straw/dormant vegetation are compared, the average absolute values decrease to 3.5, 2.3, and 3.2%, respectively, which puts the presented values within the standard deviation for both soil and green vegetation. Riegler-Nurscher, Prankl, Bauer, Strauss, and Prankl (2018) used 10 observers and 10 images, resulting in standard deviations of 4.2, 3.5, and 5.5% for green vegetation, straw/dormant vegetation, and exposed soil; their observations indicate higher average standard deviations than the results presented here.

2.6 Conclusions

The research presented was designed to produce an automated ground cover measurement tool using readily available software tools for standard JPEG images. Success of this tool was based on the following: production of quantitative ground cover data that is both accurate and precise, an algorithm that uses limited processing power, quick responses to limited input information, and production of reliable and consistent data. Three different image feature descriptors, colour, texture, and oriented gradients, were used to assess alternative modeling options and to ultimately train a decision tree algorithm for classification purposes.

Results showed good correlation for all three coverage classifications with R-squared values of 0.86, 0.87, and 0.96 between predicted and manually classified percent coverage for green vegetation, straw/dormant vegetation, and exposed soil, respectively. However, the average absolute value of the difference between manual and algorithm-derived classifications was greater than the average standard deviation between 6 different observers over 35 different images: 2.4, 3.3, and 1.2 times greater, respectively. The algorithm performed poorly for images with large manual observations of both green vegetation and straw/dormant vegetation in the same image, $20 \pm 2\%$ average difference between manual and algorithm, but well for most other images, $2 \pm 1\%$ average difference between manual and algorithm.

Based on correlation alone, this method is a suitable determinant of ground coverage data. However, when considering the standard deviation between observers and the absolute value of the difference between actual and algorithm-derived classifications, images with high coverage percent of both green vegetation and straw/dormant vegetation were not consistently well-represented. This research chose to segment images into pre-determined pixel block sizes to reduce computational time. It is possible that an attempt of segmenting the image into objects vis-à-vis the proposed set regions prior to algorithm training and object classification may improve the performance of the algorithms, however this change will also increase the computational need and classification time, which could offset potential benefits.

2.7 Acknowledgement

Dr. John Aloimonos, Professor at the University of Maryland Computer Science department, offered insight and discussion over computer vision elements presented.
Funding: The research reported in this paper was financially supported by the Maryland Department of Transportation -State Highway Administration (MDOT SHA) and the National Transportation Center at Maryland (NTC) [Project number SHAUM423] Endorsement by MDOT SHA and NTC is not implied and should not be assumed.

2.8 List of Tables

Table 2-1: Algorithms, pixel block sizes, and classification thresholds chosen for optimization.

Algorithm	Pixel Block Size	Threshold
Support Vector Machine (SVM)	30	0
K-nearest neighbours (KNN)	50	20%
Decision trees (DT)	70	40%
Ensemble Random	80	60%
Undersampling Boosting (ENS)	100	80%

Table 2-2: R squared and linear regression line for algorithm calculated as a function of manual observations for the three classification types.

Image object	Green vegetation	Straw/dormant vegetation	Exposed soil
R squared	0.86	0.87	0.96
Linear regression	$y = 1.1x + 1.1$	$y = 0.98x + 1.4$	$y = 1.1x - 7.2$

Table 2-3: Average standard deviation between the 6 observer classifications for each classification type and the average absolute value of the difference between manual and algorithm-derived percent coverage.

	Green vegetation	**Straw/dormant vegetation**	**Exposed soil**
Manual standard deviation	3.5	1.7	3.9
Abs (manual - algorithm)	8.3	5.6	4.6

2.9 List of Figures

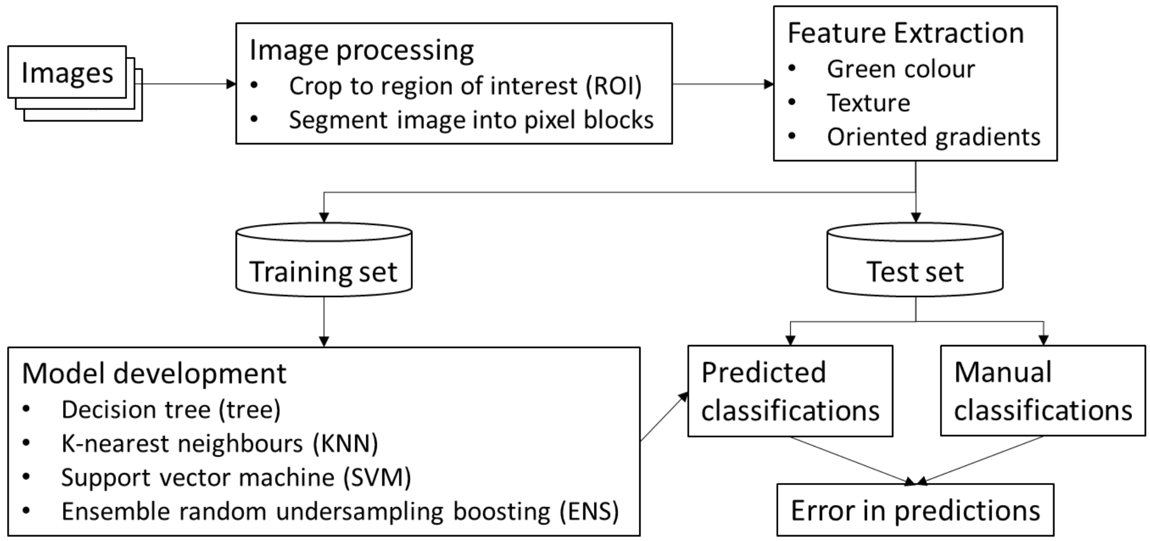

Figure 2-1: Methodology flow chart depicting classification training and application based on manual classification.

Figure 2-2:a) Field image taken from the 2016 experimental setup and b) example of greenhouse experimental setup.

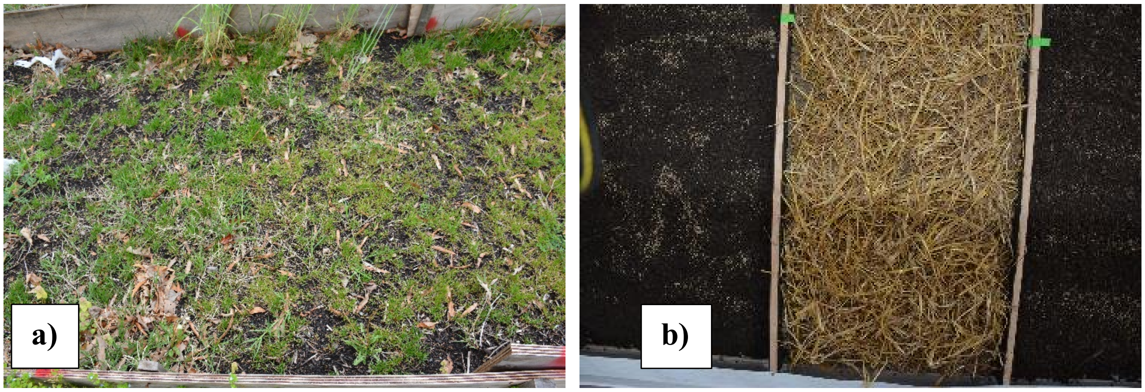

Figure 2-3: Captured images from a) the field site and b) the greenhouse experiment.

Figure 2-4: Images from Figure 2-3 after ROI cropping, a) field site image and b) greenhouse image. Due to the angle in the field image a) the shape is slightly trapezoidal.

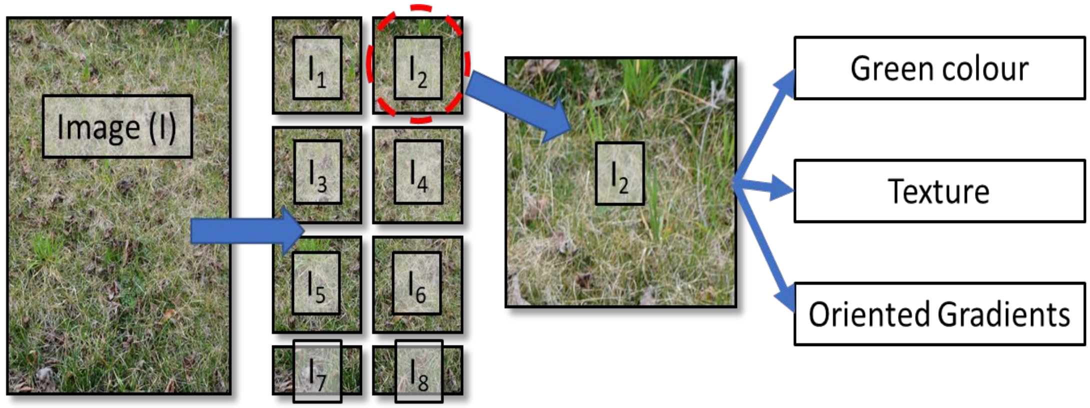

Figure 2-5: Flow chart of image segmentation and image feature extraction.

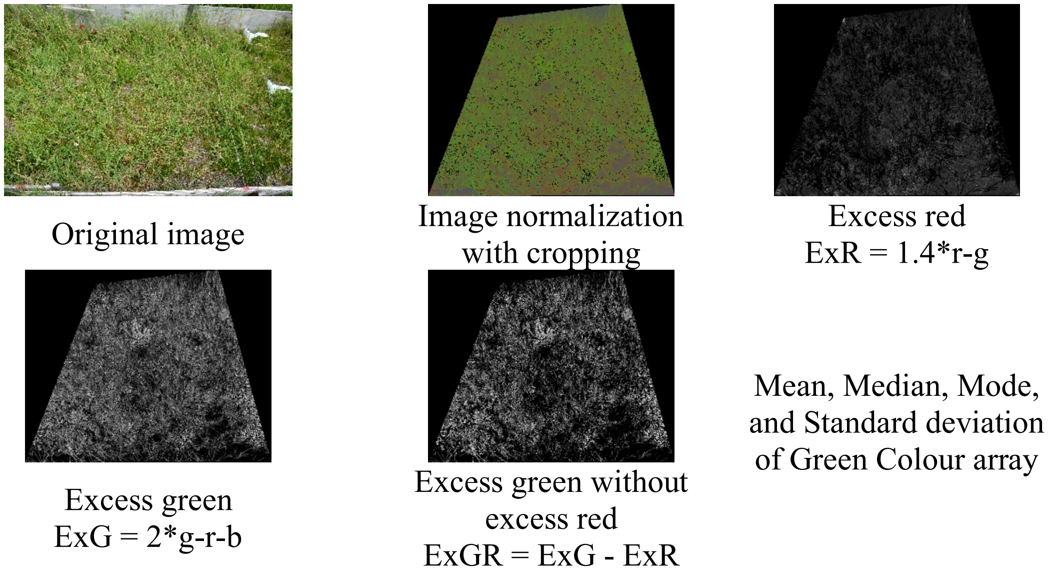

Figure 2-6: Image manipulation for Green colour. Average greenness for all images was calculated and used to determine a final thresholding value

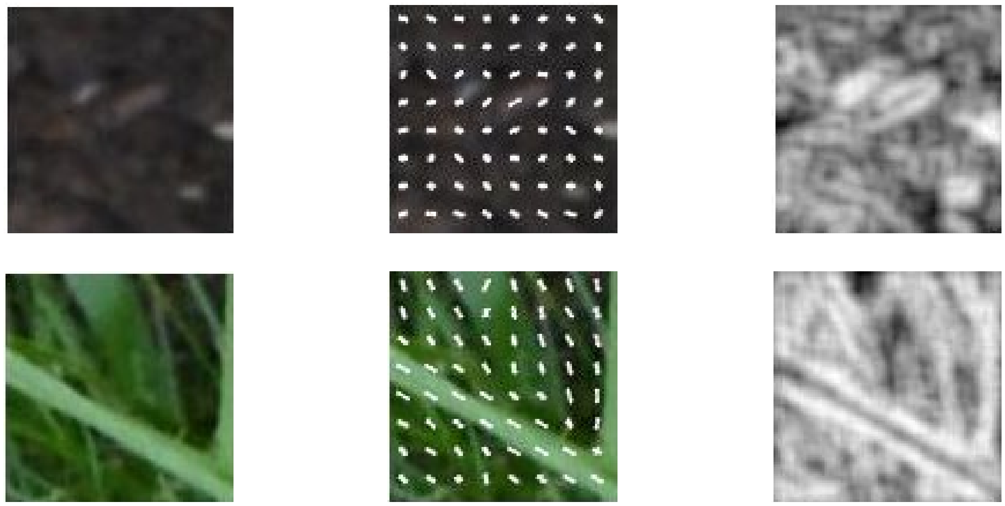

Original 100 x 100 pixel segment | Oriented gradient vectors | Entropy filtered image

Figure 2-7: Soil (top) and grass (bottom) image segments analyzed for histogram of oriented gradients and texture.

	Exposed soil	Straw/dormant vegetation	Green vegetation
Example image (>95% class based on manual observation)			
Number of raw images	21	19	10
Number of segmented images	>30,000	>21,000	>14,000

Figure 2-8:Training set image availability. Images come from both field and greenhouse experiments.

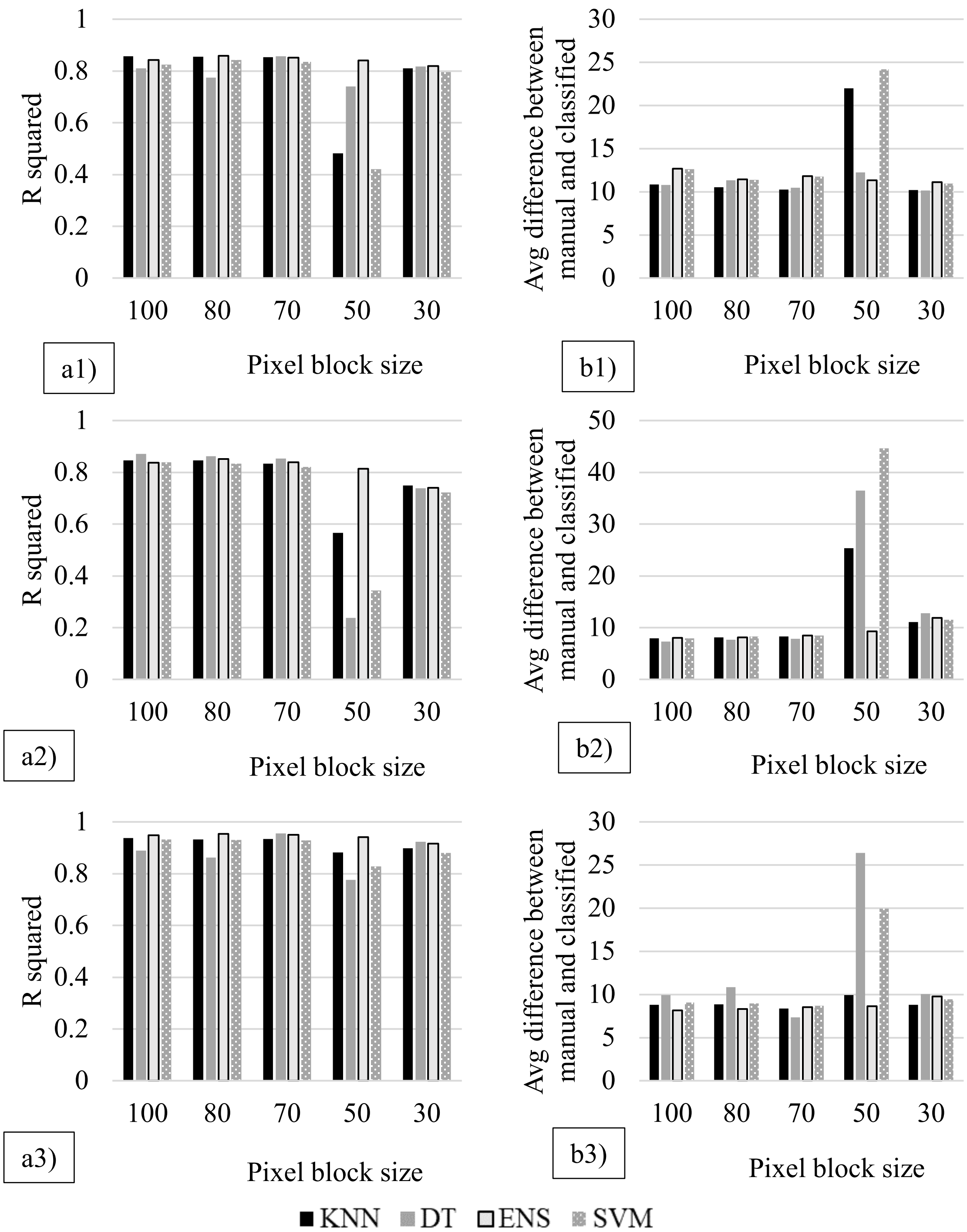

Figure 2-9: Validation performance of four algorithms at the five pixel block sizes a) Coefficient of determination for (a1) green vegetation, (a2) straw/dormant vegetation and (a3) exposed soil and b) average differences between manual and calculated classifications for (b1) green vegetation, (b2) straw/dormant vegetation, and (b3) exposed soil. KNN = K-nearest neighbour, SVM = Support vector machine, DT = Decision tree, ENS = Ensemble random undersampling boosting

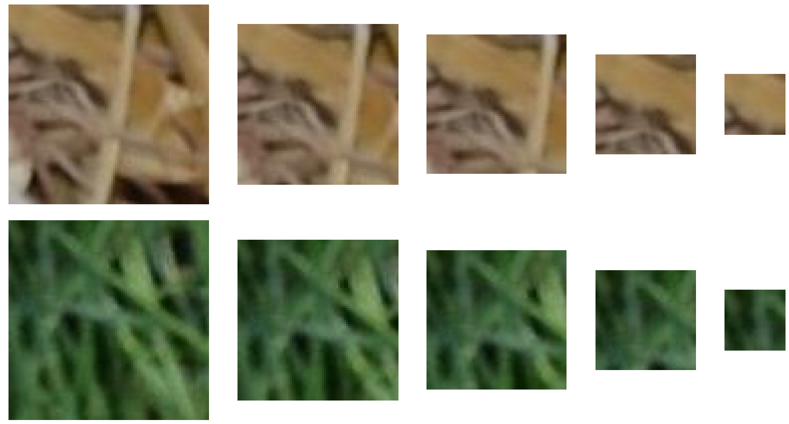

Straw/dormant vegetation

Green vegetation

Pixel block size 100 80 70 50 30

Figure 2-10: Pixel block size effects on image elements at the 100-, 80-, 70-, 50-, and 30- pixel block sizes.

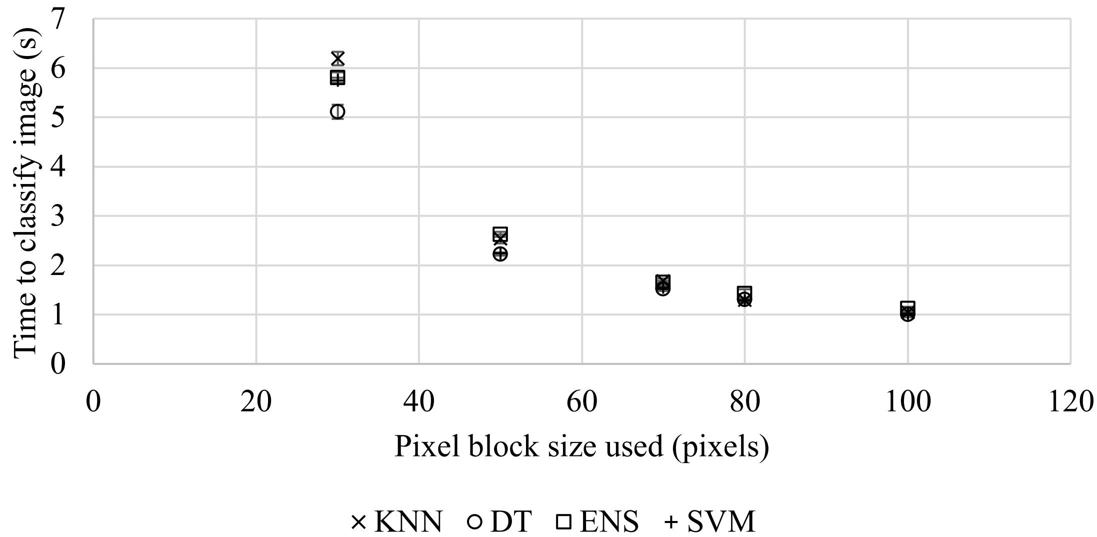

Figure 2-11: Average duration to classify an image of size 2000 x 3500 pixels for each tested algorithm at each pixel block size normalized to the DT algorithm at the 100 pixel block size. KNN = K-nearest neighbour, SVM = Support vector machine, DT = Decision tree, ENS = Ensemble random undersampling boosting

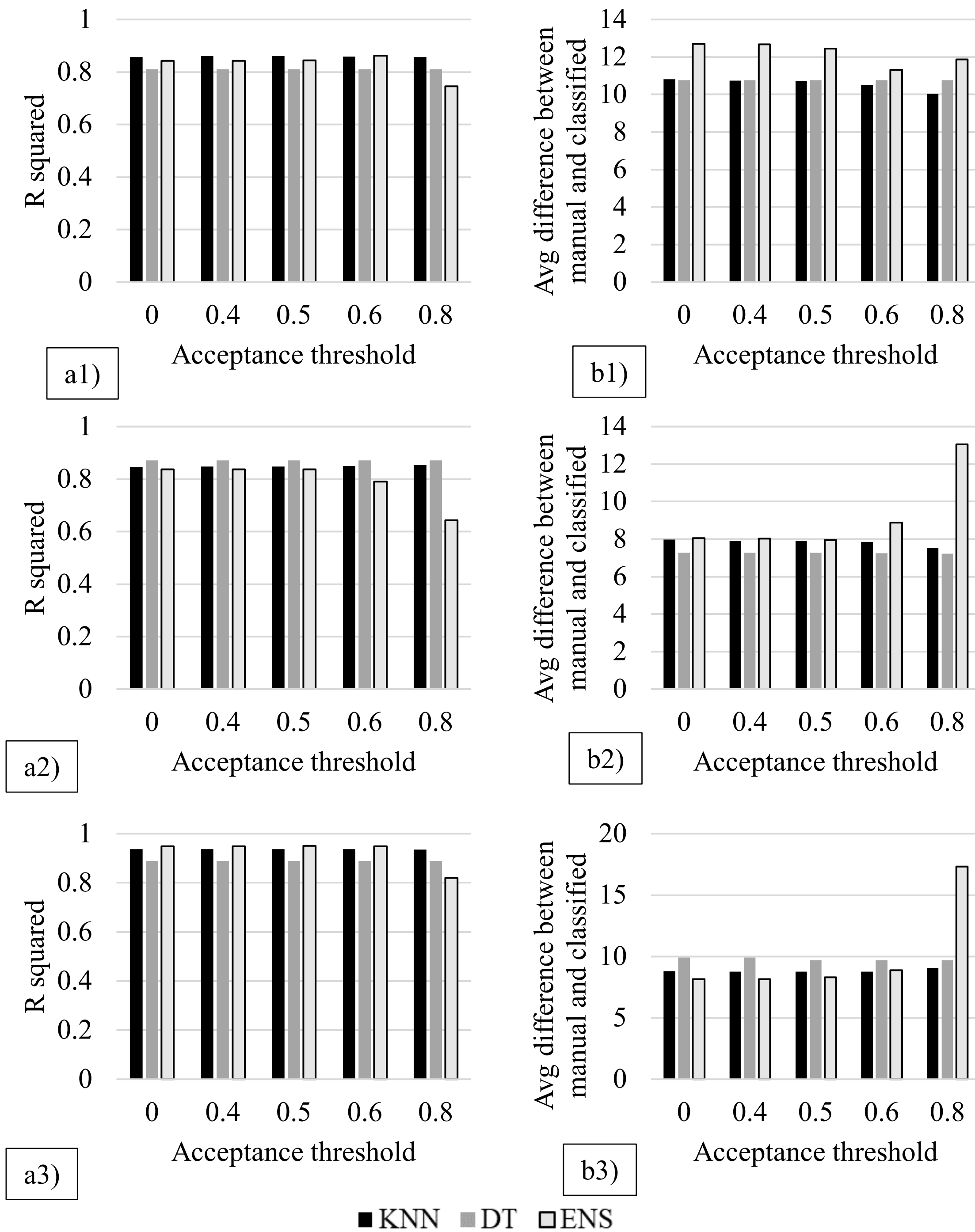

Figure 2-12: Validation performance of four algorithms at the five acceptance thresholds; a) Coefficient of determination for (a1) green vegetation, (a2) straw/dormant vegetation and (a3) exposed soil and b) average differences between manual and calculated classifications for (b1) green vegetation, (b2) straw/dormant vegetation, and (b3) exposed soil for three algorithms at the 100-pixel block size for five different acceptance thresholds. KNN = K-nearest neighbour, DT = Decision tree, ENS = Ensemble random undersampling boosting

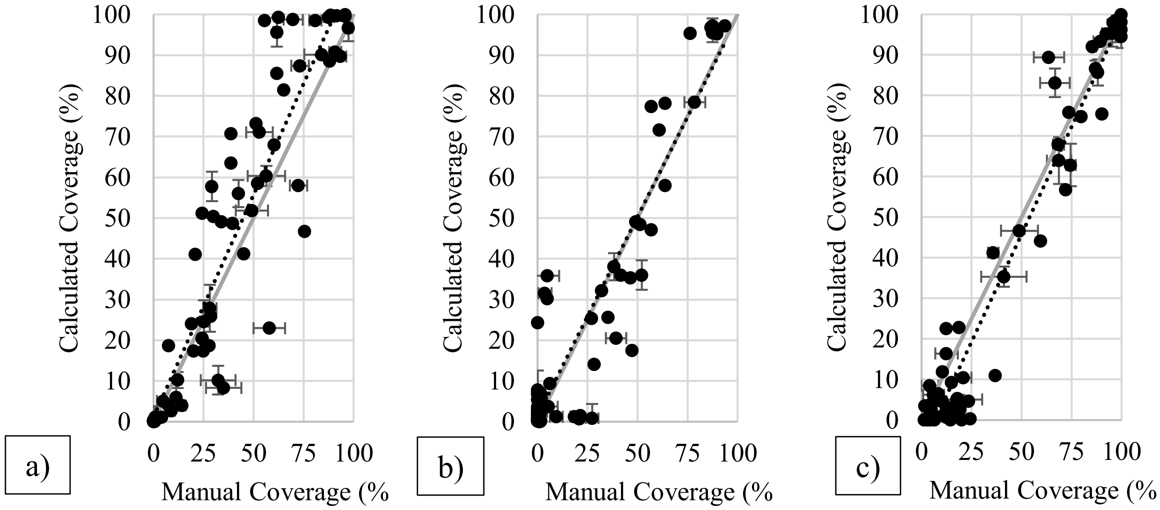

Figure 2-13: Correlation between algorithm classifications (calculated) and manual classifications using the decision Tree algorithm at the 70-pixel block size for a) green vegetation, b) straw/dormant vegetation, and c) exposed soil coverage. The solid line represents the ideal 1 to 1 ratio and the dashed line represents the calculated correlation.

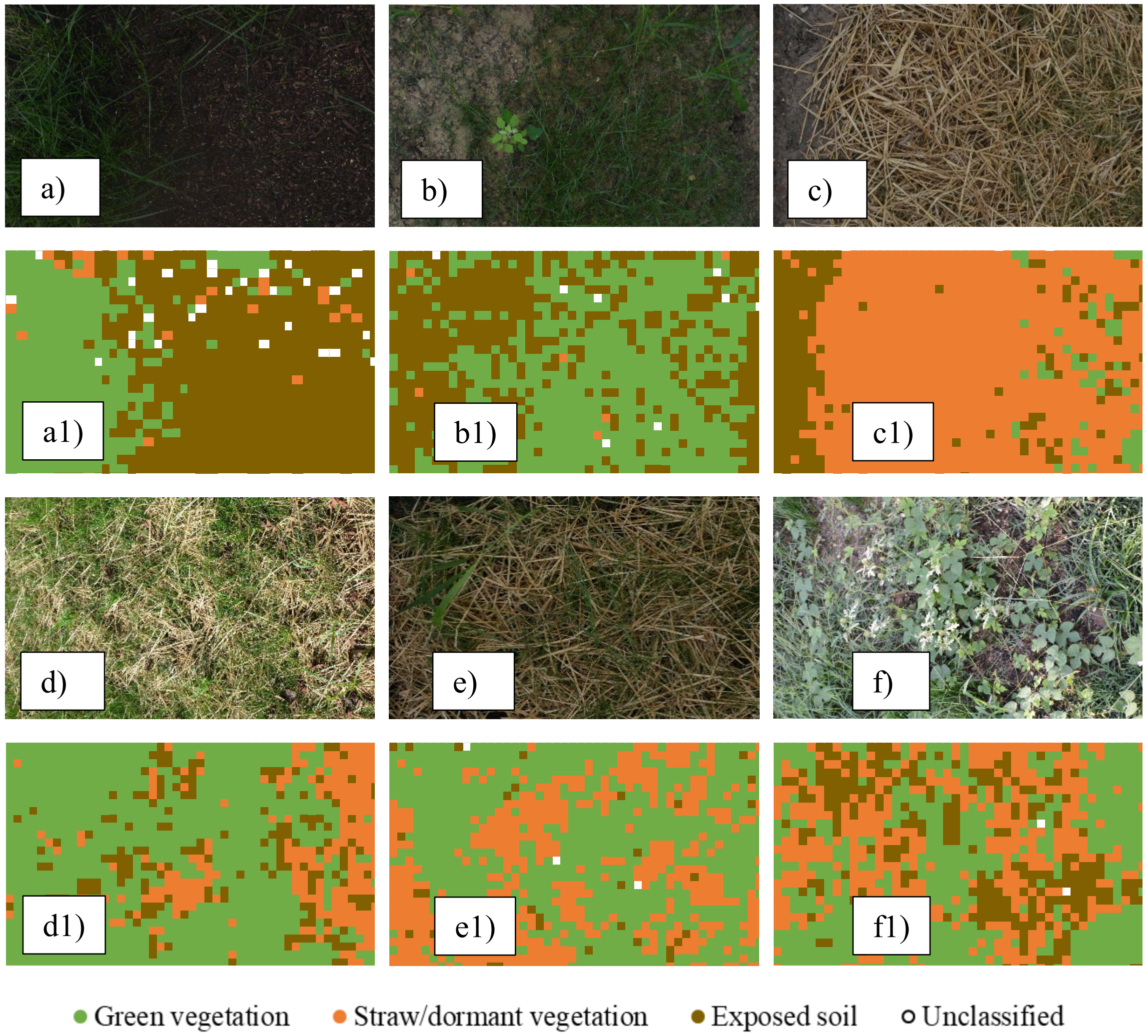

Figure 2-14: Various coverage results for both field and greenhouse images. The original images are labeled a, b, c, d, e, and f and their respective algorithm derived classifications are labeled a1, b1, c1, d1, e1, and f1.

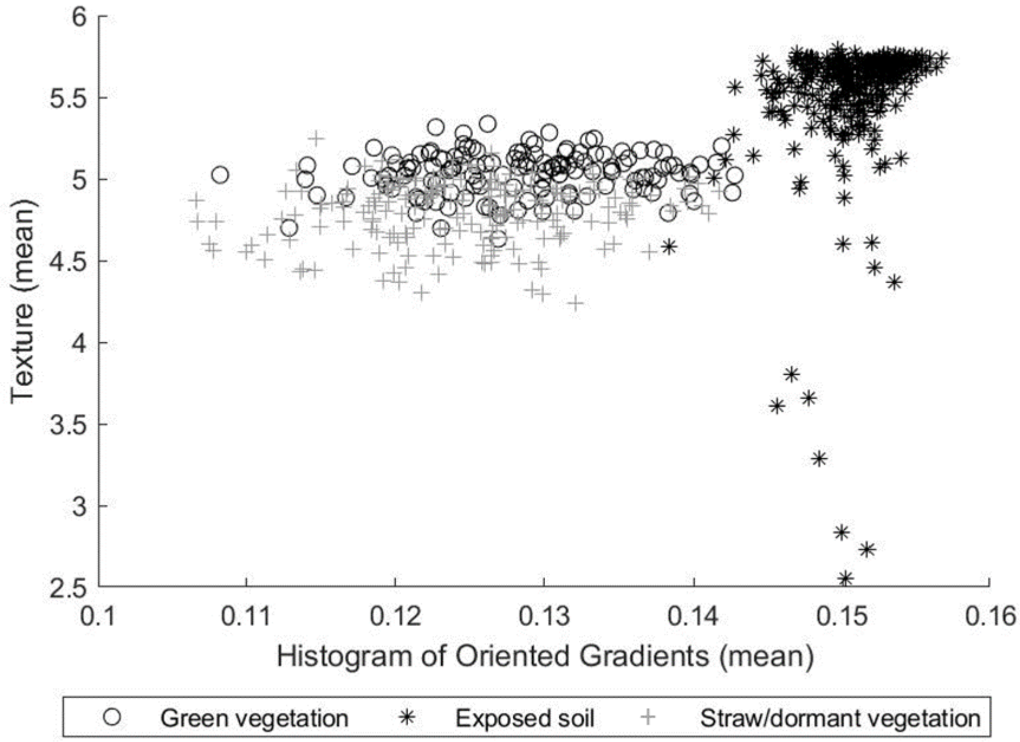

Figure 2-15 Texture and histogram of oriented gradients (HOG) mean values for green vegetation, straw/dormant vegetation and exposed soil extracted from 1% of the training images.

Chapter 3: Compost for Permanent Vegetation Establishment and Erosion Control Along Highway Embankments

3.1 Abstract

Erosion management is a major environmental challenge facing highway construction. A research study was undertaken to analyze possible sustainable improvements to current standard procedures for final grade turfgrass establishment on disturbed lands at both field and greenhouse scale. Pure compost, biosolids and greenwaste, and two topsoil/compost blends were compared with a topsoil standard (with additional straw and fertilizer application) in their ability to reduce sediment and nutrient runoff and improve green vegetation (GV) establishment. Differences in field GV rates were only observed during initial establishment (biosolids and topsoil had 11-35% greater GV). This period coincided with an initial flush of nutrients and sediment that was 3-17-fold greater than later phase runoff. After this initial runoff phase, tested materials exported largely comparable nutrient and sediment runoff. Both the topsoil/compost blends and the pure compost treatments had higher measured hydraulic conductivity and moisture holding capacity compared to topsoil, however, greenhouse studies showed runoff volume reduction only for biosolids treatment (40-98%); it was hypothesized that the additional straw mulch layer offered increased water storage, surface resistance, and physical protection from rainfall impact and surface flow compared to non-mulched compost. Evidence of soil sealing from rainfall impact was seen for topsoil/compost mixtures resulting in 20 to 28-fold greater runoff volume than topsoil which, combined with

rainfall splash, led to 28 to 224-fold greater sediment export. Nutrient export was greater with compost addition (1.5 to 51-fold and 2.2 to 3.3-fold greater phosphorus and nitrogen, respectively) due to concentration increases for pure compost and volume increases for topsoil/compost mixtures.

3.2 Introduction

Following large-scale highway construction projects, sizable land areas may be left unvegetated and exposed to rainfall. Common practices may cover these slopes with topsoil, a fertilizer blend, turfgrass seed, and straw to reduce erosion through promotion of rapid vegetative growth. This practice uses a non-renewable resource (topsoil), can be costly for both purchase and transportation of materials, and can potentially leach nutrients into existing waterways from land-applied chemical fertilizers during rainfall events. The increase in available nutrients in these waterways can directly lead to eutrophication and dead zones (Davis and McCuen 2005). Thus, there is need for a more sustainable approach to slope stabilization.

Major elements that determine the erosive potential of a storm event are rainfall impact and overland water flow (Hairsine and Rose 1991). The power of these elements to erode are controlled by soil cover, soil physical properties, and the slope steepness and length (K. Renard, et al. 1997); soil microtopography may also play a major role in the generation and dispersal of runoff (Abrahams, Parson and Hirsch, Field and laboratory studies of resistance to interrill overland flow on semi-arid hillslopes, southern Arizona 1992, Liu and Singh, Effect of microtopography, slope length and gradient, and vegetative cover on overland flow through simulation 2004). These studies suggest that irregular slopes, created by local soil minima and maxima, larger particle sizes, and extensive soil coverage can drastically affect the flow and resistance created by the soil surface. Therefore, it is important to quickly establish vegetation and increase soil structural stability, soil roughness, and moisture retention to reduce rainfall impact, increase flow resistance, and increase water storage.

Compost is a recycled, renewable resource that is readily available in the form of yard waste, food waste, manure, and wastewater treatment byproduct. Additionally, according to the U.S. Environmental Protection Agency nearly 30% of municipal solid waste produced in the U.S. is compostable; incorporation of more permissive composting policies can reduce the total volume of waste produced nationwide. Depending on the composting method and type of feedstock utilized, organic material will decompose into an earthy humic material with unique chemical and physical properties high in both macro- and micro-nutrients beneficial for plant growth (Diaz, De Bertoldi and Bidlingmaier 2007). Using composted material, departments of transportation can incorporate renewable, locally sourced materials without the use of chemical fertilizers while supporting an alternative treatment for various municipal waste products.

Compost use in transportation related projects is becoming increasingly common across the U.S. (USEPA, 2003). The use of composted material as a means of increased vegetation establishment and reduced runoff sediment loss has been reported in many studies (e.g., (Glanville, et al. 2004, Harrell and Miller, Composted yard waste affects soil displacement and roadside vegetation 2005, Curtis and Claassen, Using compost to increase infiltration and improve the revegetation of a decomposed granite roadcut. 2007, Mukhtar, McFarland and Wagner, Runoff and water quality from inorganic fertilizer and erosion control compost treatments on roadway sideslopes 2008, Hansen, et al. 2012, Chaganti and Crohn 2014). In a review of 25 different studies on compost effects to soil properties, Kranz, McLaughlin, Johnson, Miller, and Heitman (2020) identifies a variety of improvements to soil physical properties, such as increased porosity, soil stability, aggregation, and moisture retention with decreased bulk density.

The goal of this project was to determine the performance of select compost products as part of construction site erosion prevention systems. Both biosolids compost, a byproduct of the wastewater treatment process defined as dewatered and composted wastewater residual material that is combined with a bulking agent (like wood chips or peanut husks), and greenwaste compost, material that includes yard trimmings and grass clippings, were chosen for the study.

The desired performance of potential compost amendments compared to standard topsoil (with straw and fertilizer) application for soil erosion management were met in this study through collection and subsequent analysis of digital images and stormwater runoff samples (measured for sediment, nitrogen, and phosphorus). The data was collected from two field studies over the course of three growing seasons (Fall 2016, Spring 2017, and Fall 2017) and seven greenhouse platform studies. Success of the chosen treatments was based on the following criteria: 1) rapid and healthy green vegetative (GV) establishment and growth, 2) reduced erosion through soil stabilization, and 3) improved runoff retention and quality. Controlled studies provided comparative evaluation of five different topsoil and compost medium treatments, in order to describe the advantages and disadvantages of the compost-based products for erosion control.

3.3 Materials and Methods

All materials used adhere to the current Maryland Department of Transportation State Highway Administration specifications (MDOTSHA, Standard specifications for construction and materials 2019). Topsoil came from a local landscape supply store; greenwaste compost was Leafgro® (produced from yardwaste collected from local counties) purchased from a home improvement store. Biosolids compost came from a wastewater treatment facility in Aberdeen, Maryland. Both biosolids and greenwaste composted materials for this study were produced aerobically. The field and greenhouse studies compared the same five media covers: topsoil with straw and fertilizer application (TS), greenwaste compost (GNS), biosolids compost (BNS), 2:1 topsoil:greenwaste compost (TGNS), and 2:1 topsoil:biosolids compost (TBNS). All topsoil/compost mixtures were prepared on a volume basis and corresponded to 9% compost by dry mass.

Table 3-1 shows properties of the media, including the Mehlich-3 phosphorus (performed by AgroLab, Inc.), loss on ignition (organic matter content; performed by AgroLab, Inc.), KCl nitrogen (Castle, 2009), and particle diameter for 50% pass through (D_{50}) and 10% pass through (D_{10}) (values do not include the additional fertilizer used on the topsoil treatment). Particle diameter was based on ASTM D6913 particle-size analysis (detailed results in Figure 3-8) using an average dry mass of 278 ± 92.2 g. Based on Table 3-1, BNS had the highest levels of organic matter, nitrogen, phosphorus, and particle size among the media studied. Based on the USDA soil texture classifications system, all media tested were classified as sandy loam (United States Natural Resources Conservation Service Soil Science Division, 2017).

All media were seeded with a turf grass mixture of 95% tall fescue and 5% Kentucky bluegrass from Chesapeake Valley Seed, Inc. Only the topsoil layers received additional fertilizer (20: 16: 12, 83% ureaform with monoammonium phosphate and sulfate of potash) from Keymar Fertilizer, Inc. applied at a rate of 0.022 kg/m^2 and covered with bailed wheat straw from the a local home supply store at a rate of 0.448 kg/m^2. All applications were based on current MDOT SHA practices for slope stabilization and permanent turfgrass establishment (MDOTSHA, Standard specifications for construction and materials 2019).

3.3.1 Field Site Design

Two field sites were constructed in July (Hanover, Maryland, designated as HA) and August 2016 (Upper Marlboro, Maryland, designated as UM). Both sites were built facing NE at a slope of 1.6 H:1 V ($71 \pm 20\%$) with all five medium types applied in triplicate and monitored for one full year, 3 growing seasons. Sites were excavated to approximately 10 cm below the original soil height and separated by 30 cm -tall plywood, with the test media placed on top. Figure 3-9 shows the experimental setup for the HA and UM sites. GNS and BNS blankets were applied at 2.5 cm depth to the sub-surface while all other medium types were loaded at 5.0 cm depth above the subsurface. Medium treatment placement was chosen in a semi-random way to reduce the effects of neighboring plots on growth and runoff. The HA site plots were 1.8 m wide and 5.8 m long and the UM site plots were 2.4 m wide and 12 m long; both had 0.9 m gaps that separated every two plots.

Samples of soil and water runoff and digital image capture, to represent grass growth, were collected from these sites every two weeks or after runoff generating storm events. Stormwater samples were collected from 1 L sample bottles placed at the bottom of eight different slopes in each of the two field locations; sample locations are indicated in Figure 3-2. Three sets of 13 cm by 28 cm muslin bags with a mesh size of ~1 mm were placed at the bottom left, middle, and right of each treatment slope (for a total of 45 bags per site) and used to capture large sediment at both field sites, based on the method derived from Hsieh, Grant, and Bugna, (2009). Each bag covered 15 cm of width at the bottom of the slope with a total of 45 cm per plot; this accounts for 25% and 19% of the total width of the HA and UM sites, respectively. All bottles and bags were picked up and replaced every two weeks or after runoff generating storm events. Sediment samples from the bags were dried and weighed for total sediments captured. Water samples were analyzed for total phosphorus (TP) and total nitrogen (TN). Some storm events did not produce enough runoff volume to transport sediment and bags were left in the field for further collection.

Rainfall data for the field sites were collected from the PRISM climate group at 39.1558 latitude and -76.6769 longitude and 38.7978 latitude and -76.7391 longitude for HA and UM, respectively (Northwest Alliance for Computational Science and Engineering 2013). Hourly precipitation data were obtained from the National Oceanic and Atmospheric Administration using their Local Climatological Data. The nearest location for this information came from Baltimore Washington International Airport, Maryland for HA, approximately 2.4 km from the site, and Washington Reagan National Airport, Virginia for UM, approximately 34 km from the site.

3.3.2 Greenhouse Experimental Design

Platforms were built at the University of Maryland temperature-controlled greenhouse to monitor variables different from the field study. Figure 3-10 shows the rainfall simulator and platforms used for the experiments. Two 1.8 m by 1.8 m boxes were constructed with three separate sections in each. These sections were 0.6 m wide and 1.8 m long with wooden dividers covered in a granular surfaced roof leak barrier to provide surface friction to the underdrain area and prevent water movement between sections. A 5-cm drainage layer of 1:1 gravel/sand mixture was used on top of the roof leak barrier to reduce subsurface flow and export all infiltrated water. Test media were then loaded to 5 cm above the drainage layer. All five medium types tested in the field were replicated at a 4 H:1 V (25%) slope in the greenhouse study. A gutter system (Figure 3-10a) was built at the bottom of each section to allow the collection of all surface runoff. To prevent pooling and allow all infiltrated water to escape, a 12.5-mm gap covered in a 1 mm mesh was added below the gutter.

Simulated rainfall was applied at two-week intervals for 12 weeks following the timeline and storm durations established in Table 3-4. A single 12.5 mm HH-30 W SQ Fulljet® nozzle, shown in Figure 3-10b, was centered ~ 2.75 m above the platform to administer rain at a constant pressure of 27.6 kPa, based on the designs of Humphry, Daniel, Edwards, and Sharpley (2002). With this height and pressure, the simulator produced rainfall intensity of 10 cm/hr with similar diameter and within 2% terminal velocity of actual rainfall (Shelton, von Bernuth and Rajbhandari 1985, Humphry, Daniel, et al., A portable rainfall simulator for plot-scale runoff studies 2002). Tap water was used for these experiments due to the volume and pressure of water required. Tap water used was measured for nutrients throughout the study and had average concentrations of 1.9 ± 1.2 mg-N/L total nitrogen and 0.51 ± 0.52 mg-P/L total phosphorus with no measurable suspended solids. Most of the nitrogen was in the form of nitrate at $75 \pm 24\%$ (1.4 mg-N/L) and most of the phosphorus was orthophosphate at $81 \pm 29\%$ (0.41mg-P/L). Based on data obtained from the National Atmospheric Deposition Program (NADP) (http://nadp.slh.wisc.edu/) in Somerset County, MD (collected per rainfall between 1995-2014) atmospheric rainfall had average nitrate concentrations of 2.0 ± 2.1 mg-N/L and phosphate concentrations of 0.01 ± 0.03 mg-P/L. The applied tap water had similar nitrate composition with 40-fold greater phosphate when compared to the average concentrations of rainfall in the field, based on the nearest Maryland data.

Total runoff volume from the greenhouse applied rainfall events was collected and analyzed for sediment, TN and TP, and N and P speciation concentrations. Periodic grab samples were also taken throughout each applied rainfall event to determine any trends that developed within events. In both the field and greenhouse studies, there were instances where runoff volume was not large enough for analysis.

3.3.3 Plant Growth and Analysis

In order to accurately quantify growth rates and establishment of vegetation in the field and greenhouse studies, images were captured approximately every 14 days via a Nikon D7100 digital camera with an AF-S DX NIKKOR 18-140mm f/3.5-5.6G ED VR lens in JPG format with the auto focus feature, maximum pixel size of 4000 x 6000, without a lens zoom, and at a hard sharpness and normal saturation. Image capture was paused in the field during the winter months when plants were dormant and growth changes were at a minimum.

Before image capture, both greenhouse and field sites were divided into smaller sections for improved image quality. Each field site plot was segmented into 1.1 m sections and greenhouse plots were divided into 0.9 m sections along the length of the slope. This resulted in 4 images per plot at HA, 10 images per plot at UM, and 2 images per plot in the greenhouse. Field images were taken 1.8 m above the ground at a 30^o angle while greenhouse images were taken at a height of 1.2 m and a 0^o angle.

After image capture, total plot coverage was measured based on the method described in Chapter 2. The method segmented captured images into smaller subsets (pixel blocks) and extracted feature descriptors based on green color, texture, and oriented gradients to represent each subset. These feature descriptors were then input into a decision tree-trained algorithm to classify coverage for each subset; these values were then combined with all subsets from the original image to return a total ground coverage per image. Coverage results included green vegetation (GV), straw/dormant vegetation, and exposed soil.

3.3.4 Analytical Procedures

Due to the collection process/holding time for field water quality samples, only totals for nitrogen and phosphorus were measured. However, complete analysis was done for all greenhouse collected samples which included: TN, TP, nitrate, nitrite, ammonium, organic N, soluble reactive phosphorus (orthophosphate), dissolved organic phosphorus (DOP), particulate P, and sediment concentration. TN and TP measurements were taken with unfiltered vortexed samples. All speciation measurements were taken after vacuum filtration through a 0.22-μm membrane.

Sediment measurements for the greenhouse studies followed the total suspended solids (TSS) standard method 2540D (Standard methods for the examination of water and wastewater 2005) using 30-50 mL of runoff sample. Field sediment runoff was measured based on the mesh bags described earlier and presented as mass transport per slope area (mg/m^2). Field nutrient/sediment export was presented as the first flush.

TP and dissolved phosphorus (DP) were measured using the persulfate oxidation method and the ascorbic acid method based on the Murphy and Riley (1977) colorimetric method. Orthophosphate was measured using the ascorbic acid method without oxidation. DOP was calculated as the difference between DP and orthophosphate; particulate P was the difference between TP and DP.

Measurements for TN were made using a Shimadzu SSM-5000A with a total nitrogen measuring unit. Nitrate measurements were taken using ion chromatography on a Dionex ICS-1100 with ASRS 4 mm suppressor and a Dionex IonPac AS22 column.

The 4500-NH_3 F phenate standard method and 4500-NO_2-B colorimetric standard method were used for ammonium and nitrite, respectively, using 10 mL of sample instead of the requested 25 mL; the methods were altered to accommodate for reduced sample volume. Organic N was calculated as the difference between TN and all measured nitrogen species.

Captured runoff volumes were measured before testing to determine total volume runoff for the applied rainfall event and multiplied by the associated pollutant concentration to obtain the total mass of nutrient exported. The EMC was then calculated as the total mass over the total volume for that applied rainfall event. These calculations were only possible for the greenhouse data (with known volume runoff).

3.3.5 Statistical Analysis

All values presented are the average plus/minus the standard deviation from three measurements, unless otherwise noted. Acceptance or rejection of the null hypothesis was based on a 5% level of significance; however, all p-values are also included. Sample independence and treatment comparisons were determined using the nonparametric Wilcoxan rank-sums test. A one-tailed test was used to determine acceptance or rejection of the null hypothesis that the two samples were from the same set and equal (Hollander and Wolfe, 1999).

Trends within data sets were determined using the nonparametric Kendall's Tau one-tailed test. The test was used to determine general increase or decrease in sample concentration values with the null hypothesis being no discernable trend in the sample data and sample concentrations did not change over the x-axis (Gibbons, 1985).

The modified Thompson Tau test was used to determine single variable outliers in sample sets with n variables, with the null hypothesis being the sample point exists within the data set. Sample points that may have been outliers were tested individually using the τ-distribution with the degrees of freedom equal to (n-2). Samples outside of the Thompson τ value were eliminated systematically and a new τ value was calculated until all values fit within the range (Cimbala, 2011).

3.4 Results and Discussion

3.4.1 Grass Coverage

Observations were taken every two weeks for 435 and 402 (field) and 78 and 77 (greenhouse) days after initial establishment. Three visible growth periods were seen during the field monitoring phase: Fall 2016, Spring 2017, and Fall 2017; these growth periods can be seen in Figure 3-1, which displays the average percent GV for both field locations. GV cover reached a maximum around 90, 300, and 400 days after establishment for both field sites; these corresponded to early November, early May, and mid-September.

The data in Figure 3-1 represent the mean GV cover for each slope with the variation coming from the differences among the three slopes with the same treatment at each site. These plots combine the variability among the three treated slopes at the site as well as the variability between the bottom and top of each slope. Ranges are often very wide, 50% at some points, and indicate that a single coverage value does not necessarily represent the makeup of the entire slope.

During the initial phase of growth, BNS at HA and TS at UM had statistically greater rates of GV establishment ($p \leq 0.013$ and $p \leq 0.018$, respectively) than the other treatments. In the second growth phase, TGNS had statistically lower growth rates at HA and UM ($p \leq 0.006$ and $p \leq 0.04$, respectively), GNS was also slower to establish at HA ($p \leq 0.006$). No other statistical differences in GV were found among treatments.

GV cover for both field and the greenhouse are compared in Table 3-2 at 69-78 days since establishment. Table 3-2 shows that field growth was more successful than greenhouse growth for all media at UM and all but TS at HA. In the greenhouse, limited GV growth was seen after 60 days for BNS, GNS, TBNS, and TGNS. This difference is likely due to lower soil moisture in the greenhouse study compared to the field. A clear difference between the field and greenhouse studies was the frequency and duration of rainfall application; rainfall intensity, volume, and intermittent drying periods between storms was very different. The greenhouse study had consistent 10 cm/hr intensity storm events with a 14-day drying period while the field sites included multiple days of rain with a maximum intensity of 1.8 cm/hr and had average drying periods of 2.8 days with a maximum of 16 days.

In the greenhouse setup, average volumetric water contents of $24 \pm 1.4\%$, $21 \pm 2.6\%$, and $14 \pm 4.9\%$ (for BNS, GNS, and TS, respectively) were measured prior to rainfall application. Duzgun, Hatipoglu, and Aydilek (2020) found that the wilting points for BNS, GNS, and TS were 49%, 48%, and 21%, respectively. The measured volumetric water content prior to rainfall application, in the greenhouse setup, were far below the wilting point presented in Duzgun, Hatipoglu, and Aydilek (2020) for all materials and indicated that greenhouse slopes in this study were likely well below the wilting point for some time. Multiple days below the wilting point would greatly hinder plant growth and add further explanation to the reduced growth found in the greenhouse.

3.4.2 Water Quality

All treatments in the greenhouse studies showed some degree of rainfall infiltration throughout the 30 cm of applied rainfall (330 L), as seen in Table 3-3, but BNS was the most successful at reducing runoff volume. Compared to the TS (with straw) standard, BNS treatment reduced runoff volume by 43% ($p = 0.20$). Conversely, all other medium treatments increased runoff volume, as seen in Table 3-4, by 1.5-, 14-, and 20- fold for GNS, TBNS, and TGNS, respectively.

Runoff volume is largely influenced by the infiltration rate and the water holding capacity of the soil; faster infiltration with higher holding capacity produces lower runoff volume. Water holding capacity is defined as the moisture content at field capacity minus the initial moisture content. Duzgun, Hatipoglu, and Aydilek (2020) found that both the saturated hydraulic conductivity (K_s) and field capacity correlated positively with increased percentage of compost. They reported that pure biosolids and greenwaste composts (same media as BNS and GNS used in this study) had K_s values 3 orders of magnitude greater than topsoil (same media as TS used in this study) and had field capacity 2.4-2.6-fold greater than topsoil. Results for topsoil/compost mixtures investigated in Duzgun, Hatipoglu, and Aydilek (2020) had one order of magnitude increase in K_s and 1.4-1.7- fold increase in field capacity compared to topsoil.

With higher K_s and field capacity, both compost and topsoil/compost mixtures were expected to have far greater infiltration than TS. However, these characteristics only establish a baseline for each soil medium. The data presented in Duzgun, Hatipoglu, and Aydilek (2020) does not consider rainfall impact on soil hydraulics or the additional protective straw mulch layer applied to the topsoil layer. Straw mulching not only provides additional storage space for rainfall moisture but also, based on the daily Morgan-Morgan Finney model, provides both increased surface roughness and protection from rainfall kinetic energy (KE) and momentum transfer to soil surfaces (Mannering & Meyer, 1963; Poesen & Lavee, 1991; Hillel, 2004; Jordan et al., 2010; Liu et al., 2012; Choi et al., 2017). The transference of rainfall KE and momentum to soil structures breaks down soil aggregates and causes particle detachment, which increases soil bulk density, entrains soil particles, and reorganizes soil structure (Hillel, 2004; Armenise et al., 2018). This often results in soil sealing of pores, which reduces hydraulic conductivity and infiltration. Without the straw mulching, compost treatments were more susceptible to this soil sealing phenomenon. Evidence of this was seen in both compost mixtures; normalized runoff volume to influent volume of both TBNS and TGNS temporally increased 10-28- fold (from 0.02 L to 8.2 L and from 1.08 L to 11 L, respectively) with applied rainfall. The gradual increase in runoff volume strongly indicated reduced infiltration likely due to soil sealing.

Unlike both TBNS and TGNS, temporal characteristics of runoff volumes for both BNS and GNS were not seen to increase. Armenise et al. (2018) found that both increased grain size and organic matter content have been found to decrease the impact of soil sealing. Based on organic matter and particle size distribution (Table 3-1 and Figure 3-8), GNS had 22-69% smaller soil particles than TS but 29-37% greater organic matter content. GNS did not show evidence of soil sealing despite the reduced particle size distribution, which suggests that organic matter content, as opposed to particle size distribution, likely played a more dominating role in reduction of soil sealing.

With reduced soil sealing for both composts, via increased organic matter content, and topsoil, via straw mulching, the particle size distribution then offers explanation to the remaining runoff generation. BNS generated the lowest runoff volume and had the greatest particle size distribution (Table 3-1 and Figure 3-8) while GNS had the smallest particle size distribution with greater runoff volume, excluding the mixtures that observed soil sealing. The percentage of compost in TBNS and TGNS was likely too low (9-10% compost by dry mass with organic matter content of 9.2-10%) to have the protective benefits seen for pure compost treatment and supply further evidence that the organic matter content, with non-mulched media, played a major role in soil seal prevention.

3.4.2.1 Sediment

Field sediment capture occurred for 290 days at HA and 283 days at UM; by that time ground cover had accumulated to the point that sediment bags could not be placed in contact with the soil surface. Figure 3-2 shows sediment loss for both field locations as a function of cumulative rainfall. No statistical trend was noted in the data with respect to cumulative rainfall. Field applied TBNS and TGNS had the greatest average sediment export (3.5 g/m^2 and 6.2 g/m^2 at HA and 15 g/m^2 and 16 g/m^2 at UM, respectively). However, these values were only statistically greater than the TS treatment (1.9 g/m^2 and 2.3 g/m^2 at HA and UM, respectively). No other treatments showed statistical differences. No statistical differences were found between the two field sites for the same treatment type.

Like the field observations, sediment loss for the greenhouse studies did not appear to be associated strongly with applied rainfall (Figure 3-3). This was checked within individual applied rainfall events (using runoff grab samples) and using EMCs for the six applied rainfall events. Occasionally, a 'first flush' of sediment was seen within storm events of 30 to 45-min for BNS and GNS, but this was not consistent.

From Figure 3-3a, the TGNS treatment produced statistically greater sediment export than all other treatments ($p \leq 0.04$); average EMC of 3140 ± 2068 mg-sediment/L. The TS, BNS, GNS, and TBNS were not statistically different from each other and had sediment average EMCs of 356 ± 358, 1940 ± 3844, 483 ± 242, and 1178 ± 409 mg-sediment/L, respectively. Both TGNS and TBNS sediment masses (Figure 3-3b) were statistically greater than all other treatments ($p \leq 0.008$) with total mass sediment export after 30 cm measured as 47- and 182- fold greater than TS. TBNS was greater than BNS by 27-fold and TGNS was greater than GNS by 152-fold.

In one or two instances, large concentrations of solids were flushed out within a single applied rainfall event that did not necessarily represent the normal sediment transport found for that treatment. This occurred at the 25% slope for both BNS and TGNS at 15 cm and 10 cm of applied rainfall, respectively. These BNS and TGNS spikes were 14 and 2 times larger ($10{,}520$ and 7360 mg-sediment/L, respectively) than the second largest solids EMC. Such spikes likely occur when rainfall impact and micro-topography changes form small rills in the soil surface, similar to the more extreme rill erosion seen in the field (Figure 3-11). These rills increase runoff velocity and volume within a small area during a storm event which can transfer greater sediment volume (Hillel, 2004; Liu and Singh, 2004). Evidence of large rill creation (Figure 3-11) was only found at the UM field site but was found on both topsoil/compost treatment slopes. The operating assumption behind the sediment bags used in this study was that sheet flow across the surface would be uniform (Hsieh, Grant and Bugna, A field method for soil erosion measurements in agricultural and natural lands 2009). Evidence of rills and preferential flow either into or past sediment capture bags demonstrates a potential to under or overestimate sediment loss at the field sites.

From greenhouse and field evidence, both TGNS and TBNS had greater sediment export than their respective pure composts. The low sediment transport for both composts can largely be attributed to the runoff volume reduction discussed previously. Elevated runoff volume and flow leads to greater runoff force; which, paired with soil splash from rainfall kinetic energy transference to soil particles, causes more frequent entrainment of soil particles with longer distances required for soil particle settling (Sander, Hairsine, et al., Unsteady soil erosion model, analytical solutions and comparison with experimental results 1996, Singh 1996, Liu and Singh, Effect of microtopography, slope length and gradient, and vegetative cover on overland flow through simulation 2004). Additionally, organic matter increases soil aggregation through the increase in physico-chemical clay and oxide interactions as well as microbiological binding (physical entanglement, adsorption, and cementation by mucilaginous products) which naturally resists soil splash, compaction, fragmentation, and scouring (Hillel, 2005).

Many studies have compared the benefits of composted material on the reduction of sediment erosion on slopes when compared to bare topsoil (Harrell and Miller, Composted yard waste affects soil displacement and roadside vegetation 2005, Reinsch, et al. 2007, Faucette, et al. 2007, Hansen, et al. 2012) but compared to straw mulching (which was used as the control in the current study) the results are less clear. Edwards, Burney, Richter, and MacRae (2000) found that, while straw reduced soil loss by 50%, compost amendment had no effect on soil loss. Faucette et al. (2007) found that using compost reduced storm runoff on bare soils by 60% compared to straw mulched, which reduced volume by 34%, but sediment loss reductions were not statistically different (93% vs 81%, respectively).

The addition of a straw mulch layer has been seen to greatly reduce runoff volume and sediment transport. Based on the daily Morgan-Morgan Finney model for soil erosion, straw addition decreases the effects of rainfall impact (based on KE) and runoff velocity (which is inversely proportional to an adjusted Manning's roughness coefficient) by the governing equations:

$$KE = R_{eff} * \{(1 - CC) * U_{DT}\} \tag{1}$$

$$v = \left(\frac{1}{n'}\right) d^{\frac{2}{3}} * \sqrt{\tan(S)} \tag{2}$$

$$n' = \left(n^2 + \frac{D * NV * d^{\frac{4}{3}}}{2 * g}\right)^{\frac{1}{2}} \tag{3}$$

where KE is a function of effective rainfall (mm) (adjusted for slope ratio; R_{eff}), direct throughfall (rain that bypasses the coverage layer; U_{DT}) based on the universal power law equation (Shin, Park and Choi 2016), and canopy cover (CC); runoff velocity (v), is a function of slope (S), Manning's roughness coefficient based on soil surface roughness (n), gravity (g), flow depth (d), plant stem diameter (D), and number of stems per unit area (NV).

Reduction in flow velocity and KE of rainfall impact through straw addition (when compared to bare soils) directly reduces sediment transport (Jordán, Zavala and Gil 2010, Wang, et al. 2011, Liu, Tao, et al., Runoff and nutrient losses in citrus orchards on sloping land subjected to different surface mulching practices in the Danjiangkou Reservoir area of China 2012). This can explain why compost addition, which was seen to greatly improve sediment runoff in previous studies when compared to bare soil (Harrell and Miller, Composted yard waste affects soil displacement and roadside vegetation 2005, Reinsch, et al. 2007, Faucette, et al. 2007, Hansen, et al. 2012), did not show significant improvement from the TS control in the current study.

3.4.2.2 Phosphorus

Phosphorus (P) measurements for field locations had no discernable temporal trend over the 402-day measurement period, indicating that field runoff concentrations had reached a steady-state for each plot. Results are presented as mean concentrations in Figure 3-4. Two data points from the TGNS and one from TS at HA and one from each treatment at UM were excluded using the modified Thompson tau test for outliers.

Like observations found in previous studies, compost amendment increased P runoff concentrations from the TS medium both in the field and greenhouse (Glanville, et al. 2004, Faucette, et al. 2005, Mukhtar, McFarland and Wagner, Runoff and water quality from inorganic fertilizer and erosion control compost treatments on roadway sideslopes 2008, Hansen, et al. 2012). Furthermore, the current study found no significant differences between P runoff from yard waste and biosolids compost, also seen by Faucette et al. (2005).

From Figure 3-4, different letters above bar values denote statistical differences in average concentrations, based on the 5% acceptance value. Only runoff P concentrations found at the UM site showed statistical differences. At the UM site, P concentrations collected from TS, TBNS, and TGNS treatments, after outlier exclusion, were statistically similar ($p > 0.28$). However, only TS, had statistically lower P than both BNS and GNS ($p < 0.001$). All treatments at the HA site were found to be statistically similar ($p > 0.08$).

Many greenhouse grab samples within individual applied rainfall events observed a 'first flush' phenomena (Thornton & Saul, 1987) (Figure 3-12). The initial flush of nutrients was likely caused by high concentration gradients between soil moisture pockets and initial rainfall, which led to higher P concentration release. As rainfall was applied, the concentration gradient declined resulting in reduced runoff concentrations throughout the storm event.

Observed in the TS, BNS, and GNS treatments (but not for TBNS or TGNS) in the greenhouse (Figure 3-5a) was a decrease in overall effluent P EMCs as simulated rainfall was applied to the medium. Based on the continued decrease in P EMCs throughout the six applied rainfall events, it was unclear whether the greenhouse experiments (within the 30 cm of applied rainfall) reached a final steady state as seen in the field. The asymptotic decrease in P over time, seen in Figures 3-12 and 3-5a, suggests that runoff export of P may approach a mineralization steady state with the organic material in the media. Further support of this theory was seen in BNS and GNS speciation (average speciation percentages for the study can be found in Figure 3-14). Over time, an increase in orthophosphate percent of total P was seen for both BNS and GNS (46 to 57% and 63 to 88% increase, respectively). The slow mineralization of organic material would continue to contribute orthophosphate while other forms of P would not be replenished. Mukhtar, McFarland, and Wagner (2008) also found that non-vegetated (initial) plots compared to vegetated (older) plots observed a statistical decrease in runoff P over time.

The increase of orthophosphate fraction of total P over time was not seen for TS, TBNS, or TGNS. For TS, the percent of orthophosphate decreased by 24%, likely due to initial fertilizer washoff. Monoammonium phosphate was applied to the TS slope which would have changed the species characterization of the natural soil runoff. Both TBNS and TGNS had large runoff volume and sediment loss, as discussed previously. For these treatments, particulate P was found to be the dominant P species, transported through the increased sediment runoff. The export of sediment and particulate P (which is highly sorbed to soil particles (Fu, et al. 2009)) for both TBNS and TGNS likely obscured any evidence of an approach to steady state, slow organic material mineralization that was seen in the pure compost treatments.

BNS and TBNS had the highest Mehlich-3 extractable P (Table 3-1), with GNS, TGNS, and TS having lower values. This suggests that BNS and TBNS should have higher runoff concentrations (which was true for BNS but not TBNS). However, TBNS and TGNS also discharged the greatest volume of runoff. With greater volume runoff, higher concentrations of P found in the ‘first flush’ would be diluted by lower concentrations found later in the steady state phase of runoff, as discussed previously. Figure 3-5b displays P mass export for the greenhouse studies. Although EMCs were lower for TBNS and TGNS than both pure composts, the mass export for these media were much greater than BNS (17-35-fold) or GNS (9-19-fold) due to the increased runoff volume found for both topsoil/compost blends. Based on mass export, BNS and GNS still exported more P than TS but exported less P than both TBNS ($p = 0.12$ and $p = 0.20$, respectively) and TGNS ($p = 0.002$ and $p = 0.008$, respectively).

The lack of a discernable decreasing trend found in the P field data may be due to the volume of applied rainfall and the timing of field measurements. Faucette et al. (2005) found significantly higher P values from runoff on day 1 than 3-12 months after installation which indicates a general reduction in P prior to a steady state phase like the one observed in the greenhouse studies. The steady state phase represents a near constant release of nutrients likely based on decomposition rates of organic matter occurring after initial washoff or movement into the soil profile of initial inorganic, mobile nutrients. Runoff volumes prior to 8.6 cm and 23 cm of rainfall at UM and HA, respectively, were not captured, which correspond to 52-59 days after installation and likely missed the first-flush phenomenon observed in the greenhouse. All decreasing trends found in the greenhouse were measured within the first 30 cm and were most exaggerated within the first 10 cm for both the TS and GNS slopes. Only one data point from UM was collected within the 10 cm period and three within 30 cm. Declines in TP like the ones seen in the greenhouse may have occurred, but samples could not be acquired to demonstrate this change statistically.

Despite the lack of a declining trend, observations for all media, except TS at HA, had statistically smaller P concentrations than the accompanying greenhouse studies, which may indicate a lower steady state phase that greenhouse experiments did not reach. Lower values in the field were also likely due in part to the 40-fold greater P concentrations in the tap water applied rainfall used in the greenhouse experiments vis a vis natural rainfall, discussed previously.

3.4.2.3 Nitrogen

Unlike the field P observations, high nitrogen (N) concentrations were seen within the first 25-30 cm of applied water at both field test sites (Figure 3-6). Initial concentrations were 3-17 times higher than the mean concentrations in the (apparent) steady state phase. Faucette et al. (2005) and Mukhtar, McFarland, and Wagner (2008) observed similar increased nutrient runoff toward the beginning of their study followed by lower runoff concentrations. TGNS at UM had the highest initial concentration of 67 mg-N/L. Beyond these initial measurements, like the P data, no discernable trend was apparent in observations for any treatment.

Assuming values reached a steady state beyond the initial washoff within the first 25 cm of rainfall, the remainder of the points are averaged as the expected continuous export of N from each site. Within this steady state, one point from TS, TGNS, and BNS and three from TBNS at the HA site and one point from the TS and TBNS treatments at UM were classified as outliers.

Similar statistical differences were found for N that were found for P. Figure 3-6 shows that TS, TGNS, and TBNS discharged lower concentrations than both pure composts at UM, but only TGNS was statistically lower than BNS ($p = 0.02$) and GNS ($p = 0.05$). TS, TBNS, and TGNS were not statistically different from each other ($p \geq 0.12$), with average concentrations 2.5 ± 2.2, 2.3 ± 1.1, and 4.0 ± 1.4 mg-N/L, respectfully. At the HA site, TS and TBNS had lower concentrations than other treatments, but only TS was found to be statistically lower than TGNS (2.7 ± 1.8 mg-N/L vis-à-vis 4.9 ± 3.6 mg-N/L). All other media had steady state concentrations from 3.4 to 4.6 mg-N/L and were not statistically different from one another. Only the TGNS steady state N concentration at HA was statistically greater than the TGNS mean at UM, 2.3 ± 1.1 mg-N/L and 5.5 ± 3.7 mg-N/L, respectively.

The quick reduction in N concentration found at both field sites was also seen in the greenhouse studies. EMC values for all media declined throughout the 30 cm of applied rainfall. Like the greenhouse P data, the concentrations within each applied rainfall event (with high enough effluent volume) also produced a first flush of N concentrations for all media observed (Figure 3-13). This, similar to P, was also likely due to a large concentration gradient between initial soil moisture and incoming rainfall which produced higher initial concentrations of N followed by a steady-state release of decomposed organic matter. N EMCs and mass export are presented in Figure 3-7. A reduction in overall N export occurred within the first 30 cm of applied water. Both

Faucette et al. (2005) and Mukhtar, McFarland, and Wagner (2008) also observed decreases in N concentrations throughout their experimental observations.

From Figure 3-7a, EMCs for both TBNS ($p \leq 0.002$) and TGNS ($p \leq 0.002$) were consistently lower than all other treatments, with average EMCs of 16 ± 7.1 mg-N/L and 12 ± 16 mg-N/L, respectively. Concentrations for BNS were consistently the highest (average EMC 311 ± 110 mg-N/L) while GNS and TS were not found to be statistically different (173 ± 242 and 93 ± 86 mg-N/L, respectively). TGNS was statistically lower ($p = 0.03$) than TBNS. Although all media had decreasing trends, BNS showed the greatest reduction (328 to 101 mg-N/L). Like the P mass export, volume of runoff for both TBNS and TGNS becomes a major factor controlling mass export of N (Figure 3-7b). Because of high runoff volume, despite significantly lower concentrations, the mass export of these media are similar to BNS ($p \geq 0.8$) and GNS ($p \geq 0.6$).

The greenhouse platforms did not clearly reach a steady-state N value like the field data, for any medium treatment since concentrations appeared to continue to decline throughout the trial. However, evidence of an approach to a mineralization steady state, like the orthophosphate data presented earlier, was seen for BNS and GNS (mean speciation concentrations are presented in Figure 3-14b). For these treatments nitrate percent of total N increased by as much as 44%. The fertilizer used in the TS treatment included ureaform and monoammonium phosphate and evidence of fertilizer washoff was seen in the ammonium percent of total N, which reduced by 22% as rainfall was applied. This initially high concentration of ammonium likely obscured an approach to mineralization steady state. For both TBNS and TGNS sediment transport led to high organic N export ($36 \pm 4\%$ and $47 \pm 25\%$, respectively) (Figure 3-14b) as organic N is highly bound with sediment particles, especially silt and clay (Neitsch, et al. 2011). The transport of this sediment and organic N likely obscured the approach to steady state seen for the pure compost treatments.

The increased runoff N concentration agrees with observations from Glanville, Persyn, Richard, Laflen, and Dixon (2004), Faucette et al. (2005), and Hansen, Vietor, Munster, White, and Provin (2012), who also found that compost addition led to greater N runoff concentrations. N extractions in Table 3-1 show that KCl extractable N was highest in BNS, with GNS having the least. Although extractions showed higher TBNS and TGNS extractable N than GNS, both TBNS and TGNS EMCs were likely diluted by steady-state effluent after the first flush, as described previously.

Comparing the first few data points from the field (corresponding to <30 cm applied rainfall) and the greenhouse experiments; TS, BNS, and GNS greenhouse concentrations were 5 to 14 times greater than the observed field concentrations, however, both compost/topsoil mixtures had statistically similar concentrations.

3.5 Conclusions

Composted materials (biosolids and greenwaste), topsoil/compost blends, and a standard topsoil treatment (with additional fertilizer and straw application) were compared in their ability to provide slope stability and reduce soil erosion. Through field and controlled greenhouse study, runoff quality and quantity was compared both during the critical vegetation establishment phase and the extended post establishment phase.

Compost application increased soil hydraulic conductivity, aggregation, and moisture holding capacity while it reduced soil bulk density (Duzgun, Hatipoglu and Aydilek 2020). This led to an aversion to soil sealing for both pure composts that consistently reduced both volume and sediment runoff. Due to the increase in organic matter, pure compost was seen to decrease both sediment mass (96-99% reduction) and volume runoff (89-98% reduction) when compared to their respective topsoil/compost blends. However, the reduction in volume and sediment was coupled with an increase in runoff nutrient concentrations for both P (1.1- to 2.0-fold) and N (11- to 27- fold), compared to the topsoil/compost blends. Nonetheless, with both the increase in nutrient concentration and decrease in volume and sediment, the pure compost treatment ultimately had similar (for N export) or reduced (for P export) nutrient export compared to the respective topsoil/compost blend.

Although compost addition has been shown to reduce runoff volume, sediment, and nutrient export when compared to a bare topsoil (Harrell and Miller, Composted yard waste affects soil displacement and roadside vegetation 2005, Reinsch, et al. 2007, Faucette, et al. 2007, Hansen, et al. 2012), the performance of compost compared to a straw mulch layer, done in this study, proved to be less effective. Compared to the TS standard, runoff volume was reduced only for the BNS treatment (40-98% reduction) while all other compost treatments significantly increased runoff volume (4- to 22- fold). Without a straw mulch layer, compost treatments did not have the additional water storage, surface roughness, and surface physical protection that was provided to the topsoil treatment. This was most evident for both topsoil/compost blends, which showed evidence of soil sealing.

Although significant performance differences were found throughout the greenhouse studies, many of the comparisons did not translate directly to the field application. This was largely due to the duration differences in both studies (3-months vs 1-year, respectively). While the greenhouse focused on the initial establishment phase, where soil is most vulnerable to rainfall erosive potential, the field study looked largely at post-establishment characteristics. From the field data collected, application of the tested materials for slope stability resulted in similar N, P, sediment, and GV establishment with few variations. After establishment, the vegetation provided surface protection, additional storage, and surface roughness to all treatment blankets, similar to the straw mulch applied to TS. With the established vegetation, field results showed that all blankets produced similar runoff quality. It is likely that with an initial straw mulch layer applied to the compost treatments, the initially greater runoff volume, sediment and nutrient export found for the compost treatments, compared to the TS treatment, may be eliminated.

3.5.1 Acknowledgement

This research was financially supported by the Maryland Department of Transportation - State Highway Administration (MDOT SHA) and the National Transportation Center at Maryland (NTC) [Project number SHAUM423] Endorsement by MDOT SHA and NTC is not implied and should not be assumed.

3.5.2 Data Availability Statement

All data, models, and code generated or used during the study appear in the submitted article.

3.6 List of Tables

Table 3-1: Soil media organic matter, mehlich-3 extractable phosphorus, and KCl extractable nitrogen. (Mean ± standard deviation from three measurements).

Soil media	Organic matter content	KCl, Nitrogen (mg-N/kg-dry media)	Mehlich-3, Phosphorus (mg-P/kg-dry media)	D_{50}	D_{10}
TS	$2.5 \pm 0.1\%$	183 ± 146	147 ± 22	1.7	0.30
BNS	$47 \pm 0.1\%$	3468 ± 236	881 ± 209	2.3	0.70
GNS	$39 \pm 1.0\%$	84 ± 8.8	522 ± 116	0.71 ± 0.02	0.19 ± 0.02
TBNS	$10 \pm 7.3\%$	193 ± 40	568 ± 110	1.5 ± 0.4	0.35 ± 0.06
TGNS	$9.2 \pm 3.8\%$	169 ± 78	206 ± 47	0.91 ± 0.06	0.18 ± 0.02

Table 3-2: Percent GV coverage after 69-78 days of growth at UM, HA, and the greenhouse and the total runoff volume measured in the greenhouse.

	UM	**HA**	**Greenhouse**
TS	$100 \pm 5.6\%$	$53 \pm 13\%$	$77 \pm 35\%$
BNS	$73 \pm 17\%$	$86 \pm 11\%$	$2.8 \pm 1.4\%$
GNS	$67 \pm 16\%$	$62 \pm 24\%$	$2.9 \pm 1.4\%$
TBNS	$61 \pm 28\%$	$50 \pm 36\%$	$35 \pm 29\%$
TGNS	$73 \pm 15\%$	$40 \pm 22\%$	$29 \pm 21\%$

Table 3-3: Total runoff volume and total mass export per unit area for TSS, TP, and TN for all greenhouse media tested at the 25% slope after 30 cm. of applied rainfall and sediment mass export per unit area for UM and HA after 30 cm rainfall.

	Runoff volume	**TN ($mg\text{-}N/m^2$)**	**TP ($mg\text{-}P/m^2$)**	**TSS ($g\text{-}Sediment/m^2$)**	**TSS UM ($g\text{-}sediment/m^2$)**	**TSS HA ($g\text{-}sediment/m^2$)**
TS	4.1 ± 1.8	255 ± 218	8.6 ± 4.0	1.7 ± 1.4	5.9 ± 0.53	5.9 ± 0.12
BNS	2.3	569	13	3.0	9.5 ± 0.18	4.6 ± 0.09
GNS	7.3	828	24	2.0	50 ± 1.1	4.3 ± 0.02
TBNS	72	650	218	79	94 ± 1.4	11 ± 0.04
TGNS	102	600	450	309	96 ± 3.6	31 ± 0.78

3.7 List of Figures

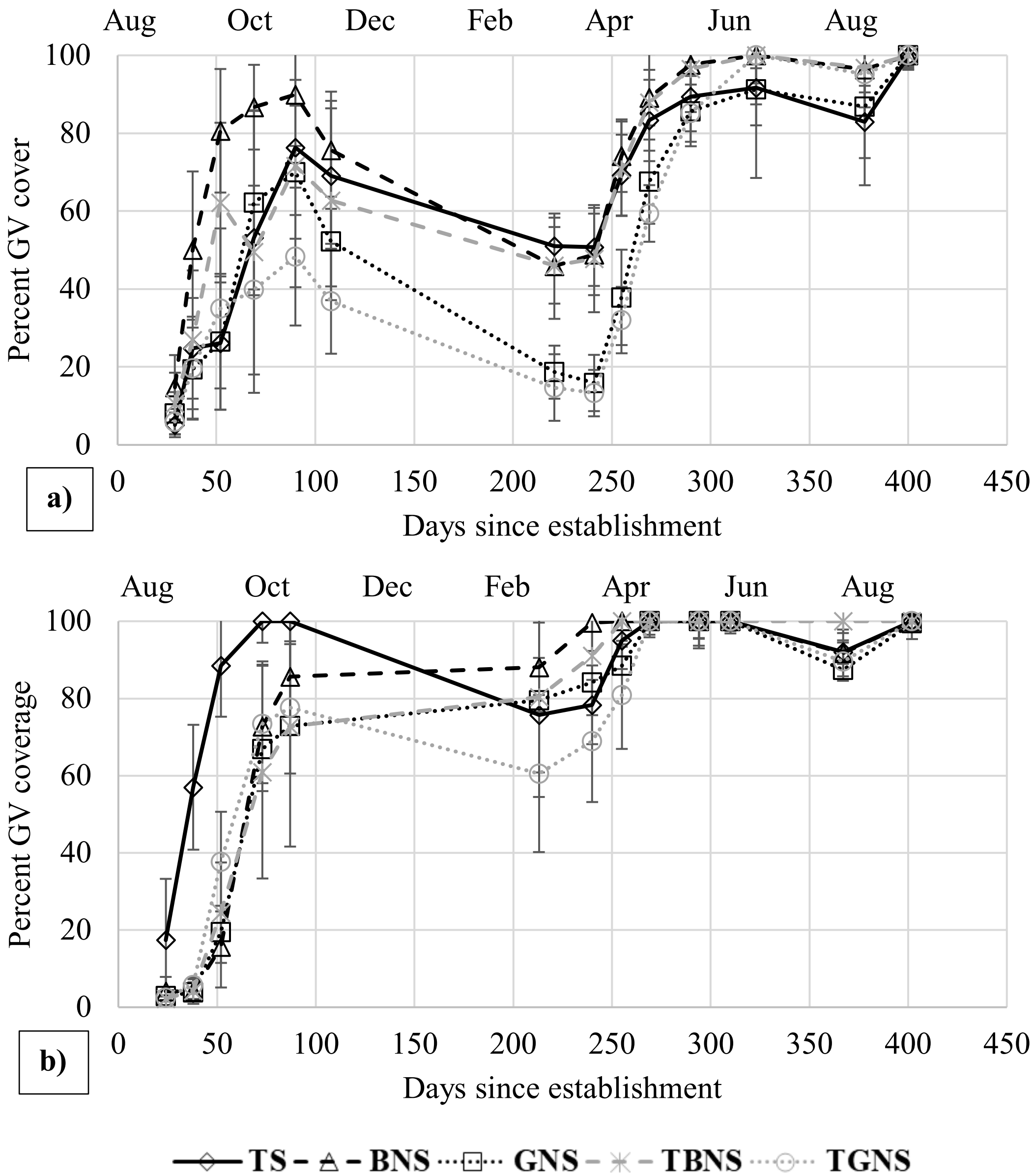

Figure 3-1: (a) Hanover (HA) and (b) Upper Marlboro (UM) green vegetation values for the three distinct growth periods. Green vegetation coverage after the second growth period becomes statistically similar for both biosolids media types and the topsoil/greenwaste mixtures.

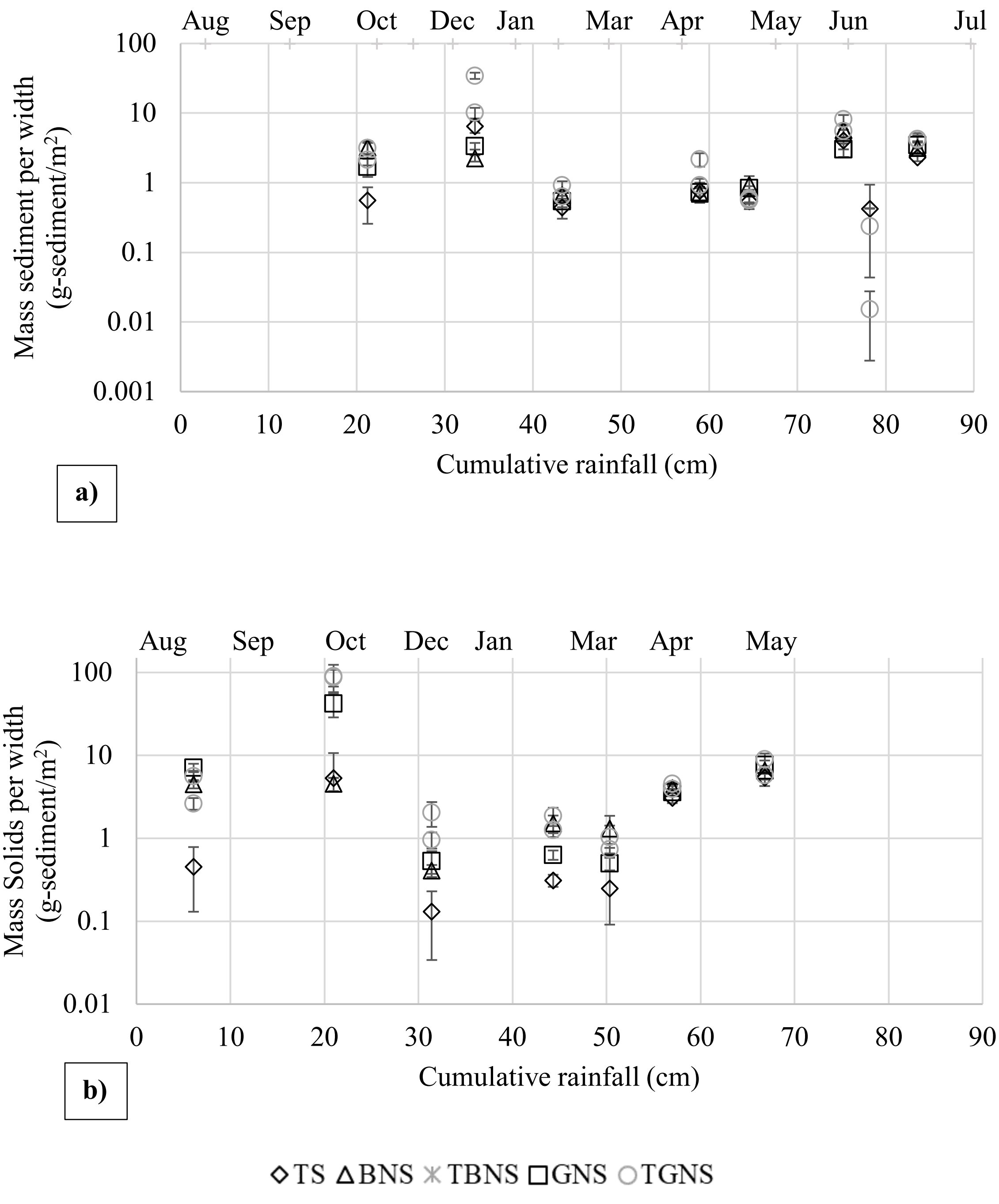

Figure 3-2: Capture of sediment from (a) UM and (b) HA slopes. Error bars represent deviation between the three mesh bags/slope in triplicate at each site.

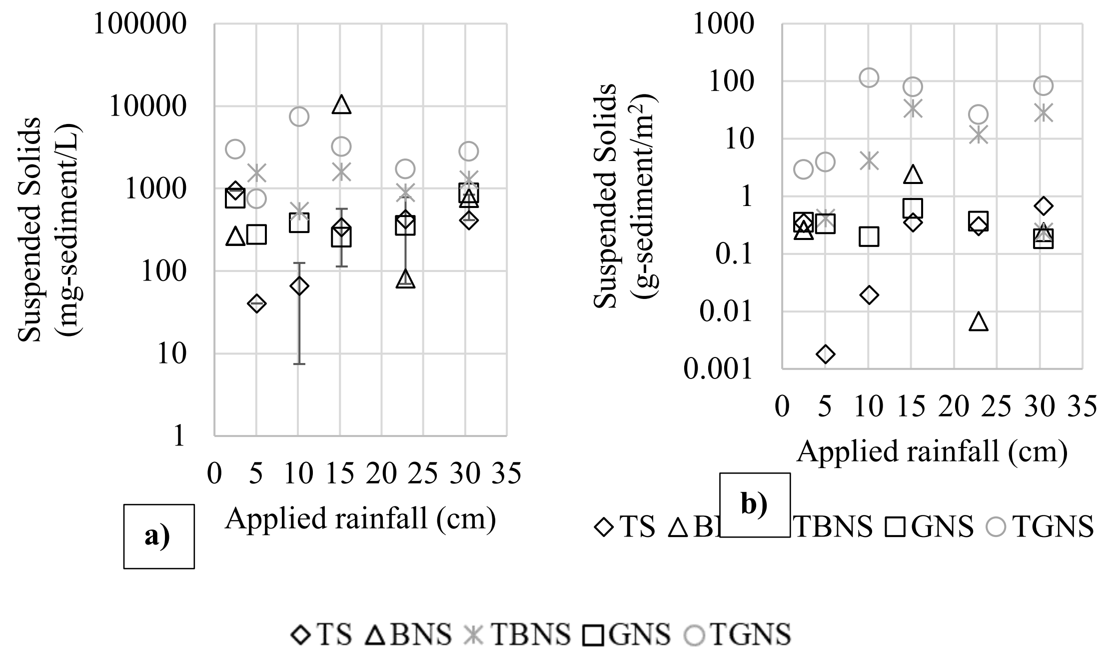

Figure 3-3: Sediment (a) EMCs and (b) mass export/m^2 for all medium applications at the 25% slope.

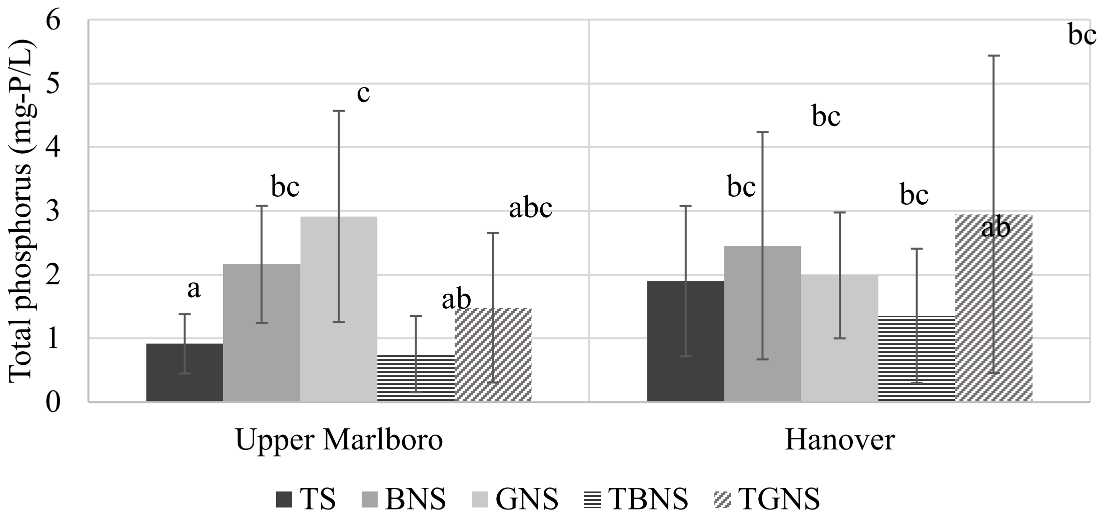

Figure 3-4: Average phosphorus concentrations for both UM and HA with all outlier points excluded. Different letters above bar values denote statistical differences in values based on the 5% significance. Error bars represent the standard deviation over the course of the experimental observation period.

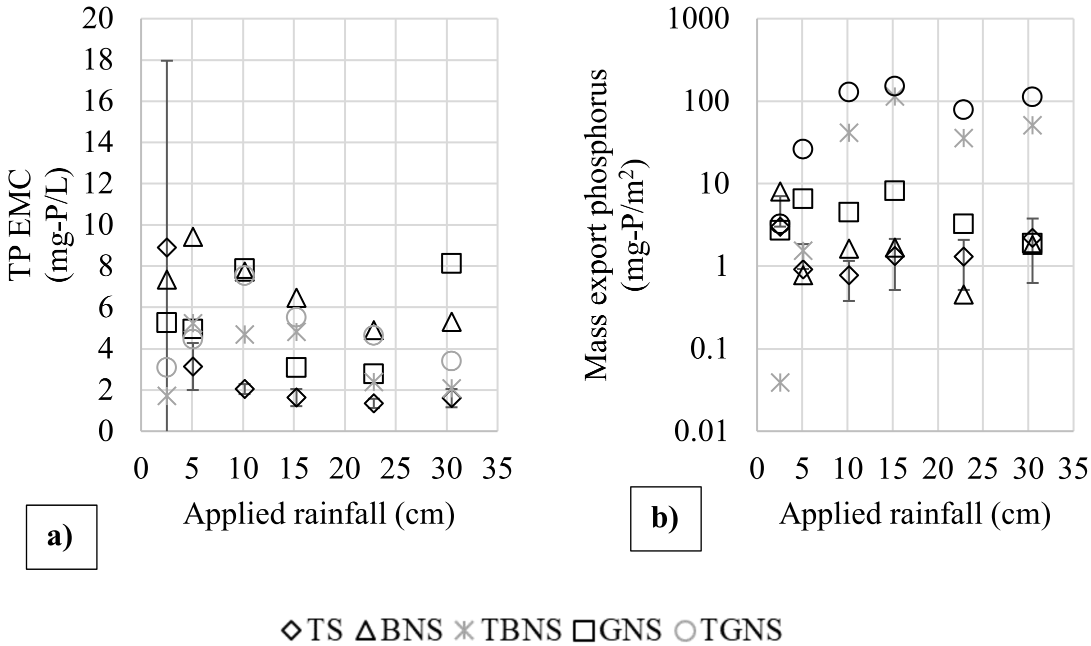

Figure 3-5: Phosphorus (a) EMCs and (b) mass export for all media runoff captured throughout the greenhouse study at the 25% slope. Error bars for TS come from the study done in triplicate.

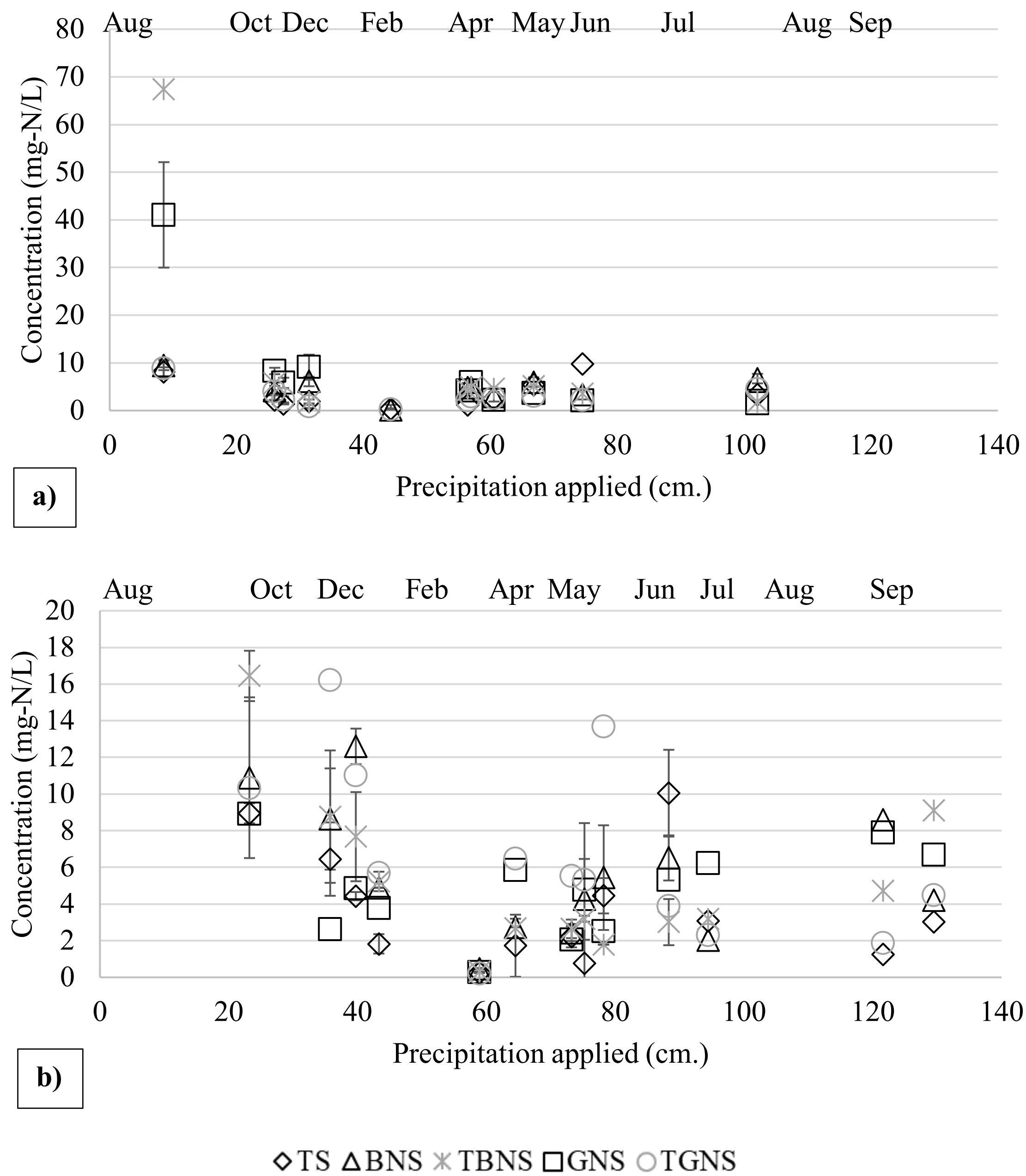

Figure 3-6: Total nitrogen concentrations for the (a) UM and (b) HA field sites. Months are not aligned because sites received different rainfall amounts.

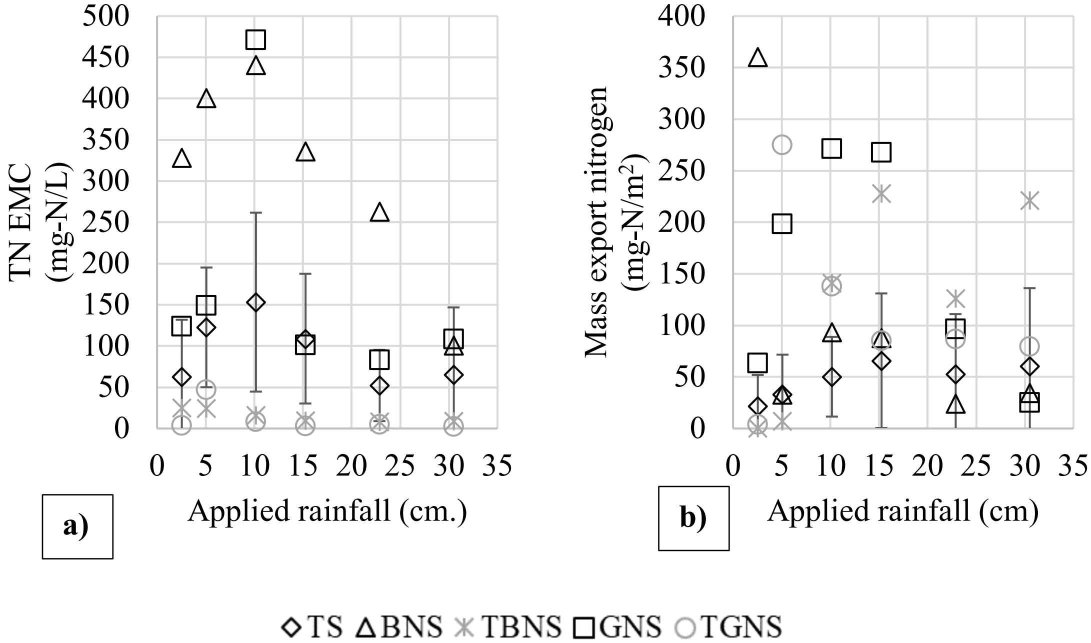

Figure 3-7: Nitrogen (a) EMCs and (b) mass export for all media runoff captured throughout the greenhouse study at the 25% slope. Error bars for TS come from the study done in triplicate.

3.8 Supplemental Information

Table 3-4: Synthetic stormwater application schedule and durations for greenhouse simulations.

Days since seeding	6-8	20-22	34-39	48-50	62-64	69-79
Duration	15-min	15-min	30-min	30-min	45-min	45-min
Rainfall Volume (in.)	1	1	2	2	3	3

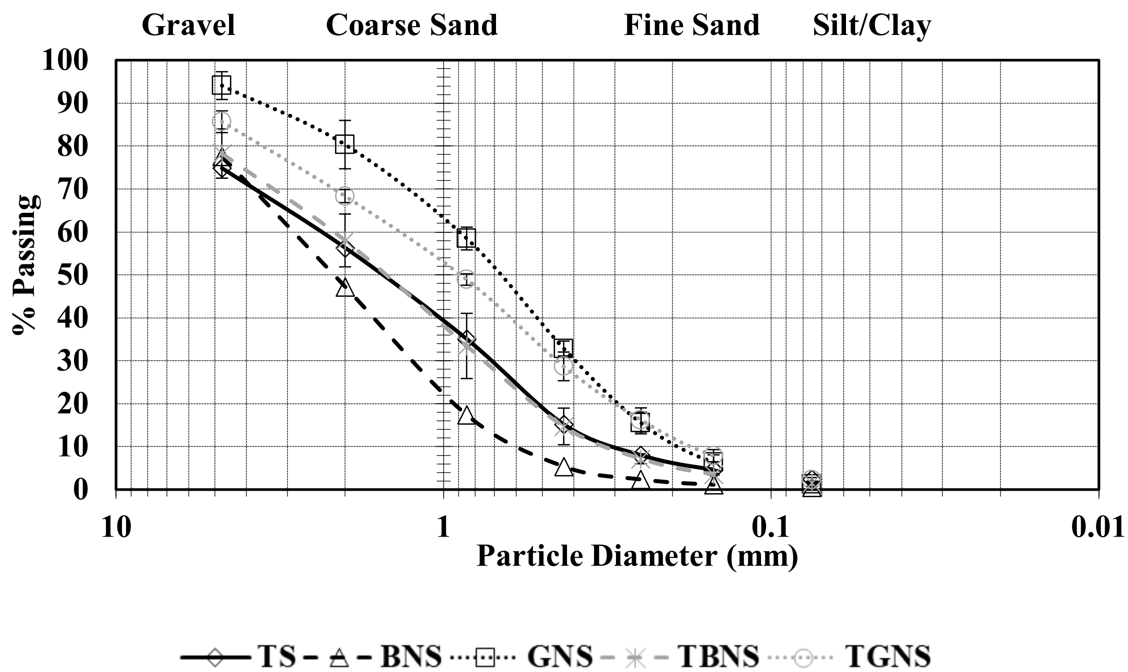

Figure 3-8: Particle size distribution for the materials used in this study.

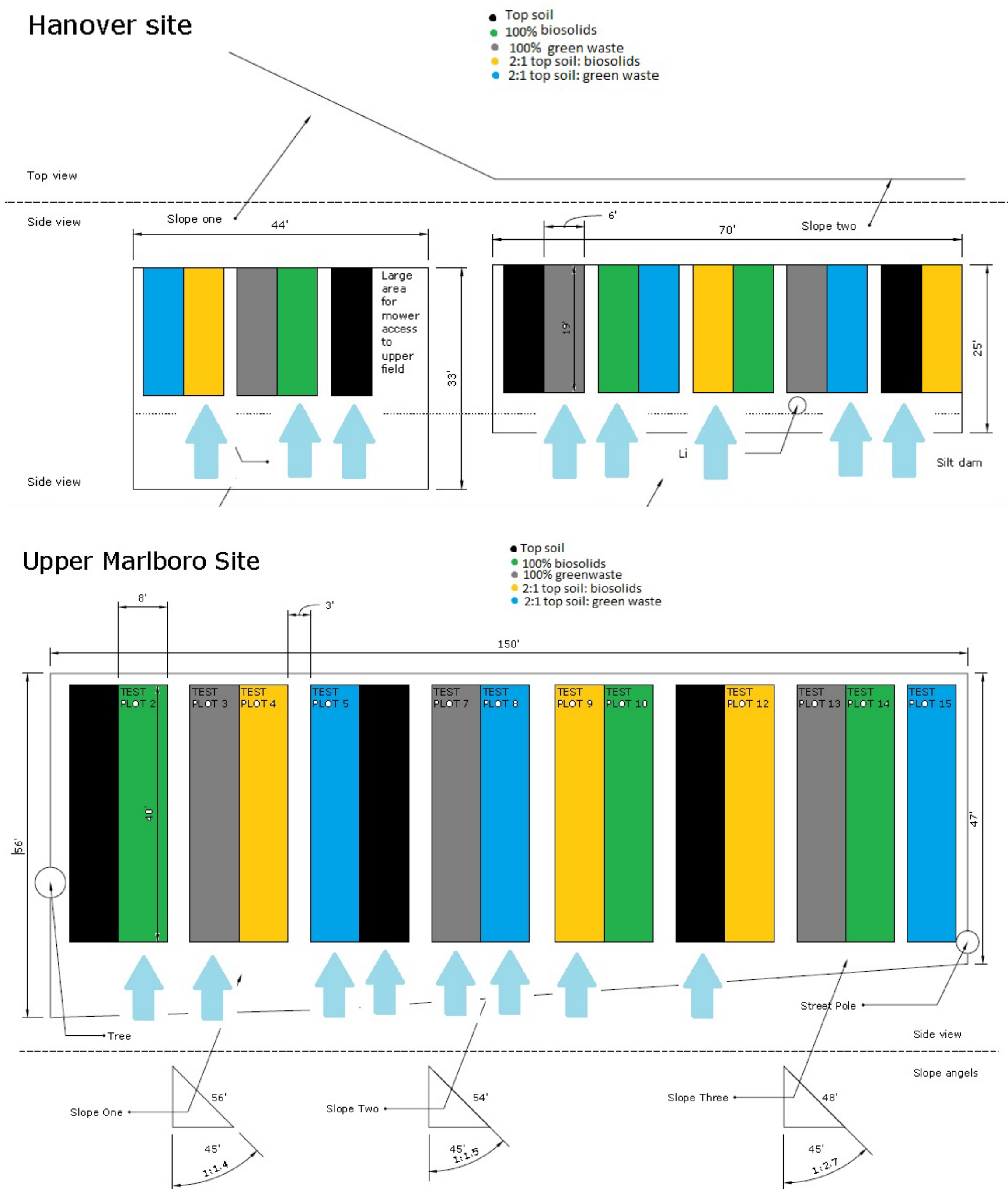

Figure 3-9: (a) Hanover, MD and (b) Upper Marlboro, MD field site designs. Blue arrows indicate locations for water runoff sampling bottles.

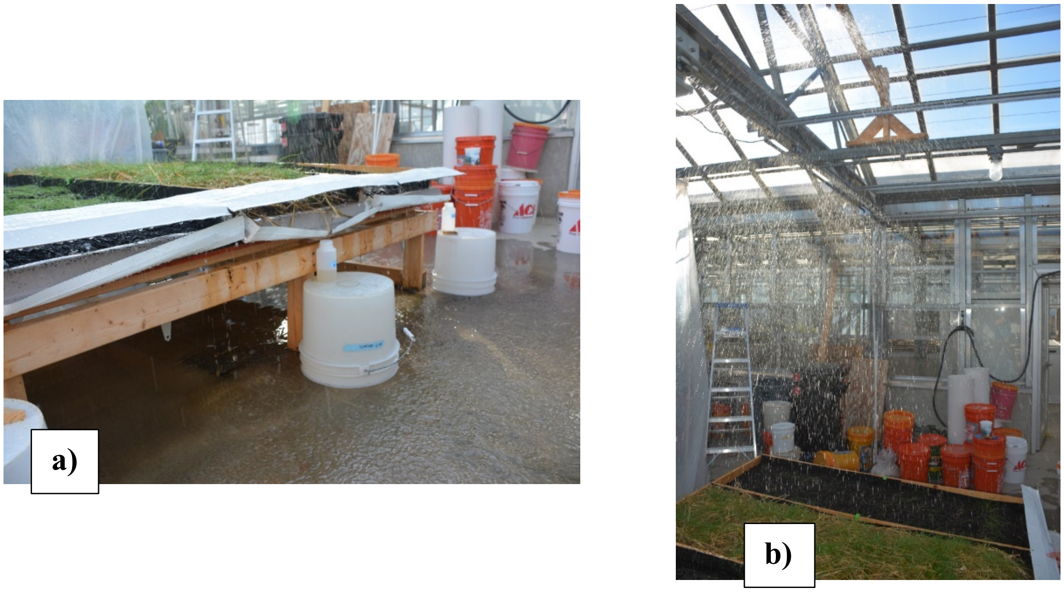

Figure 3-10: (a) Rainfall simulator (b) producing the runoff collected in the gutter system and sample bottles.

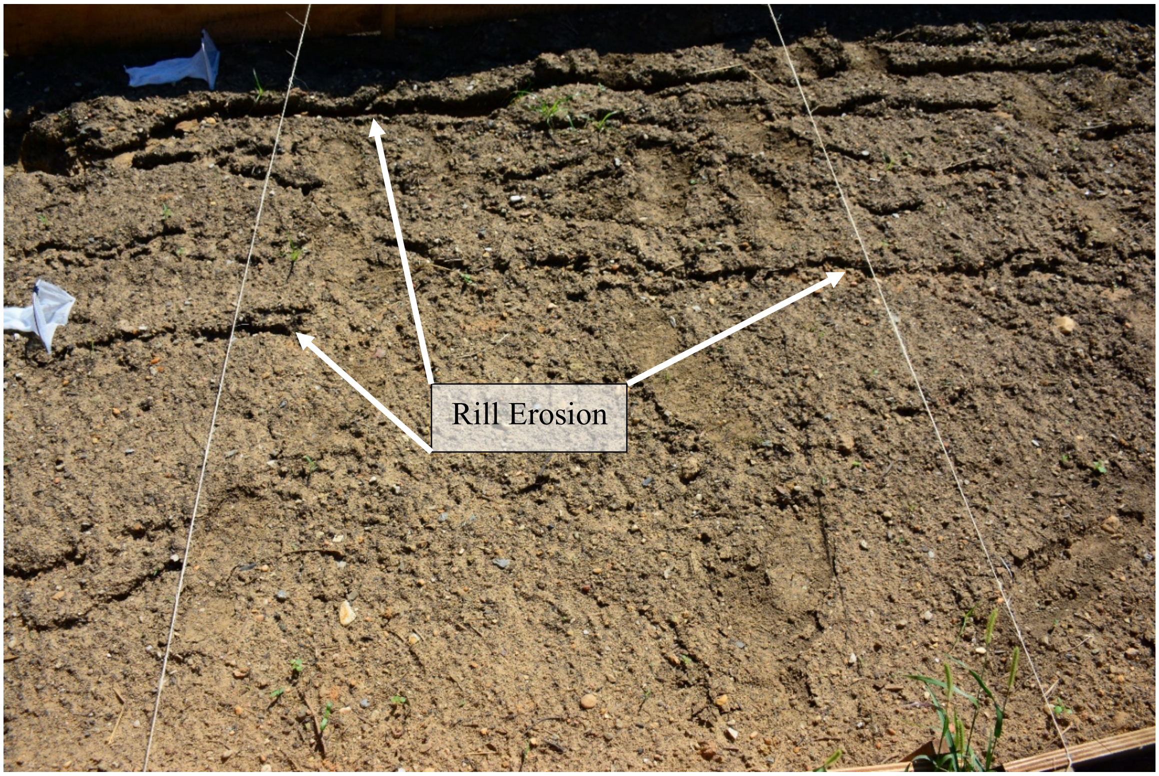

Figure 3-11: Example of rill erosion in one of the TGNS plots at UM. The top most rill avoids the sediment bag placed on the left side of the slope while the middle rill flows directly into the bag location.

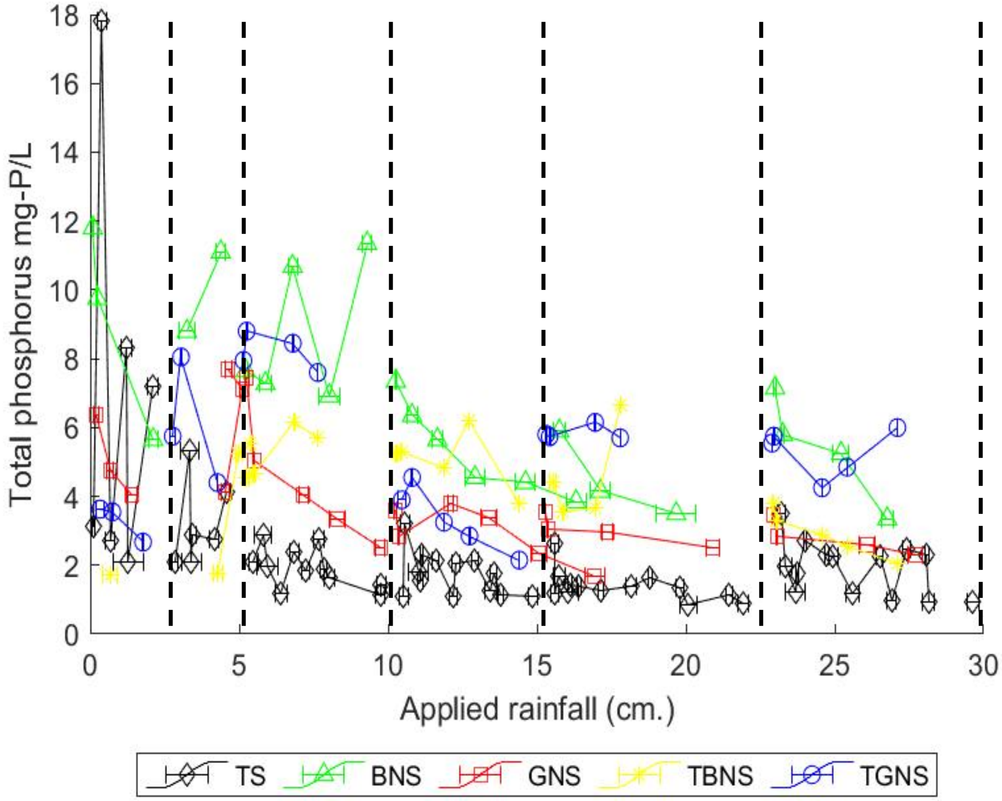

Figure 3-12: Phosphorus grab sample concentrations for all media applications in the greenhouse 25% slope study. Horizontal error bars represent the applied rainfall during the collection of sample. Large dashed vertical lines separate the individual applied rainfall events.

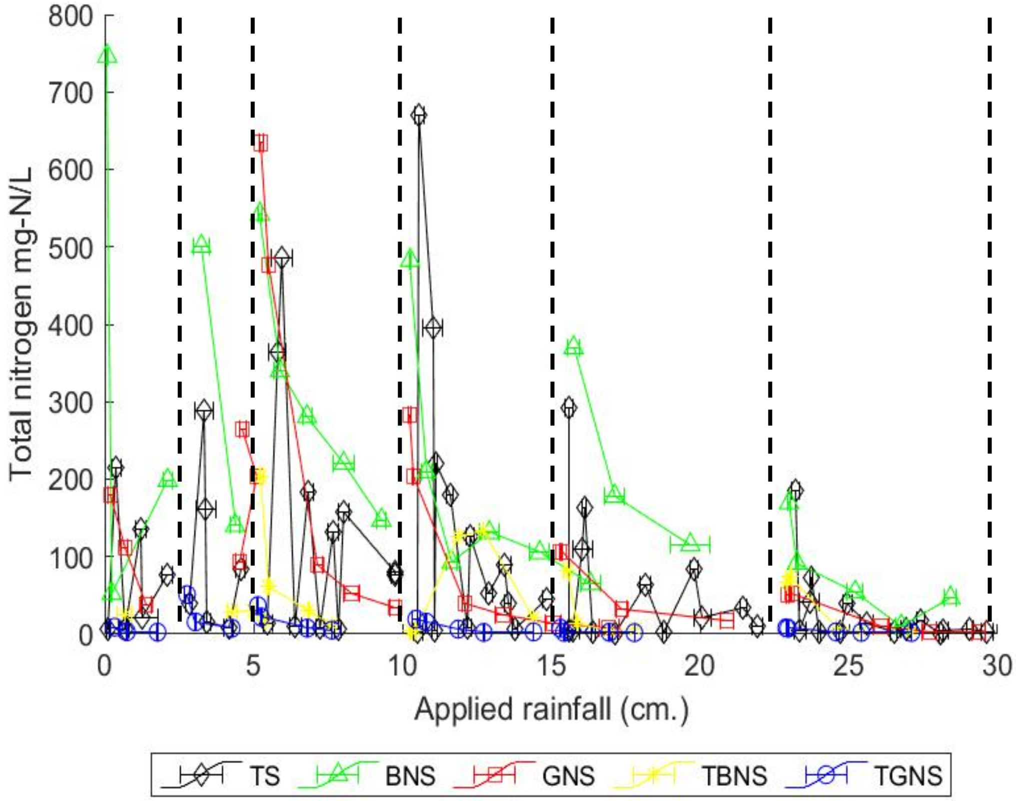

Figure 3-13: Nitrogen concentrations for all soil medium applications. Single applied rainfall events are connected, and each point represents an individual grab sample. Horizontal error bars represent the time to fill each sample bottle. Large dashed vertical lines separate the individual applied rainfall events.

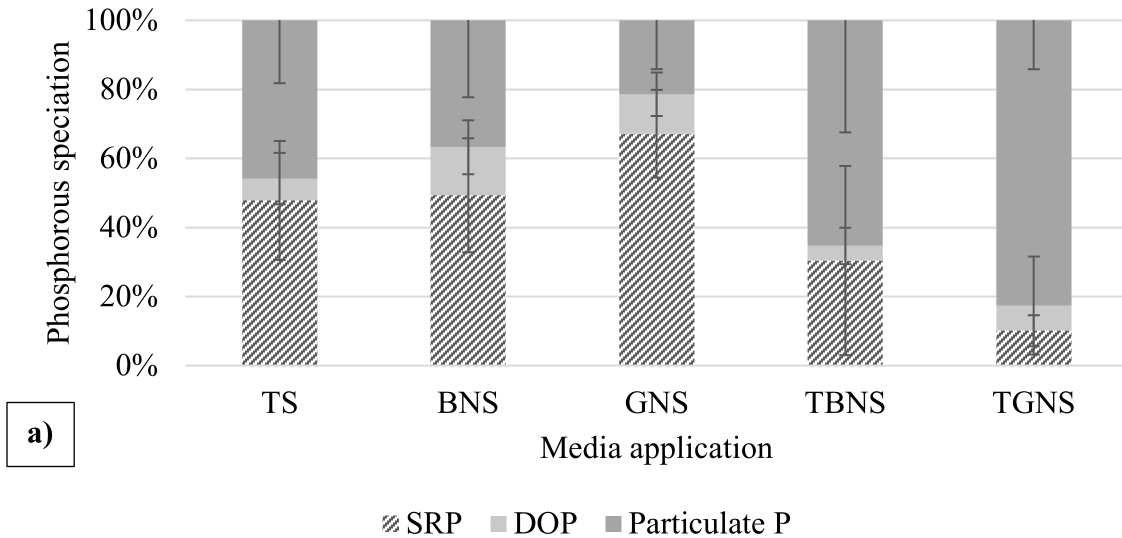

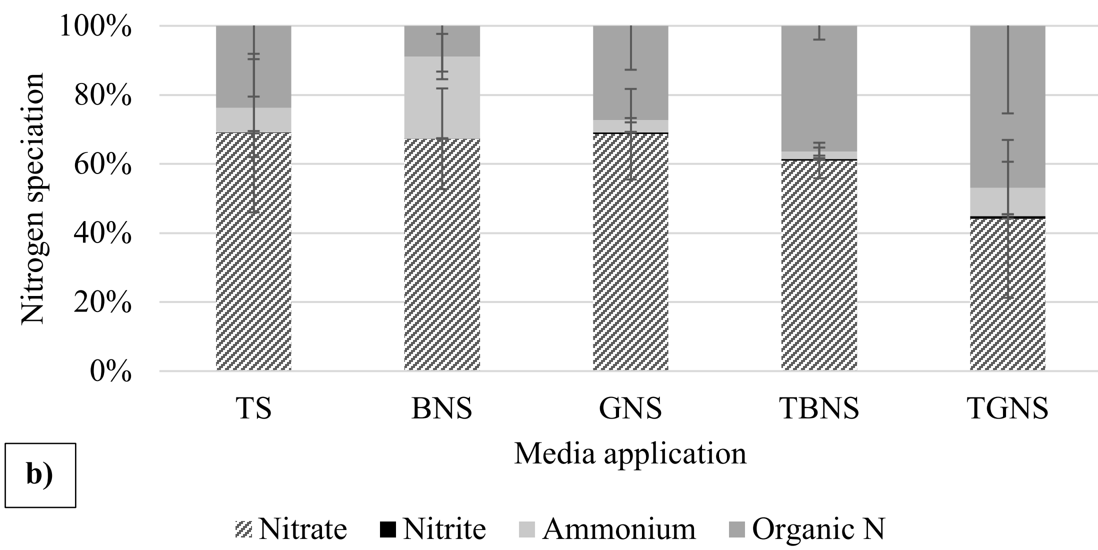

Figure 3-14: Average percent speciation of (a) phosphorus and (b) nitrogen for all media applications. Error bars represent the deviation over the entire trial. TS is presented as the average of all three trials.

Chapter 4: Effects of Slope Ratio, Straw Mulching, and Compost Addition on Permanent Vegetation Establishment and Runoff Quality Control

Dylan C. Owen[1], Allen P. Davis[2], and Ahmet H. Aydilek[3]

[1] Graduate Research Assistant, Dept. of Civil and Environmental Engineering, Univ. of Maryland, College Park, MD 20742.
[2] Professor and Charles A. Irish, Sr. Chair in Civil Engineering, Dept. of Civil and Environmental Engineering, Univ. of Maryland, College Park, MD 20742, USA.
[3] Professor, Dept. of Civil and Environmental Engineering, Dept. of Civil and Environmental Engineering, Univ. of Maryland, College Park, MD 20742, USA (corresponding author). E-mail: aydilek@umd.edu

4.1 Abstract

Soil erosion management is a major environmental challenge facing highway construction. A study was undertaken to analyze sustainable improvements to current standard procedures for final grade turfgrass establishment on disturbed soils. Using a series of greenhouse studies, compost and compost/topsoil blends with and without straw mulching were compared with a standard topsoil/straw/fertilizer practice in their ability to reduce soil and nutrient loss and improve the rate of green vegetation (GV) establishment at a variety of slope ratios. Straw mulching was seen to significantly improve GV establishment (64-93%), reduce runoff volume (22-99%), and reduce sediment and nutrient mass export (71-99% for sediment, 71-92% for nitrogen, and 66-99% for phosphorus). These reductions and improvements were largely attributed to the

physical barrier offered by the straw mulch layer. This layer improved water storage, reduced evaporation, reduced rainfall impact, and increased media surface roughness which resulted in reduced runoff velocity, soil splash and compaction, and increased available water for plant uptake. Composted amendment to the topsoil standard material with straw mulching, in general, increased hydraulic conductivity and improved soil aggregation and stability which reduced the total runoff volume (13-59%), sediment mass (64-98%), and nutrient mass export (6-82% nitrogen and 4-76% phosphorus). As slope ratio increased, export of both runoff volume and sediment and nutrient export increased while GV was seen to decline.

Keywords: Compost amendment, Vegetation establishment, Straw mulching, Erosion control, Slope ratio, Nutrient leaching

4.2 Introduction

The use of compost as a soil amendment for construction-related transportation projects has been studied and implemented across the U.S. (USEPA, 2003). Compost is a recycled, renewable resource that is high in organic and inorganic nutrients and can be readily found in many areas. Depending on the facility and location, feedstocks for composts can include food waste, yard waste (greenwaste), and treated wastewater sludge (biosolids). Each of these feedstocks results in a composted material with varying physical and nutrient compositions that can affect how well vegetation establishes and how effective the material performs as a stormwater management practice amendment (Diaz et al., 2007).

In general, compost addition to soils has shown increased porosity and decreased bulk density, which leads to an increase in soil stability, aggregation, hydraulic conductivity, and water holding capacity (Khaleel et al., 1981; Mitchell, 1997; Kirchoff et al., 2003; Duzgun et al., 2020). Composted material has also been used to improve vegetation establishment and reduce sediment runoff (Glanville et al., 2004; Harrell and Miller, 2005; Curtis and Claassen, 2007; Mukhtar et al., 2008; Hansen et al., 2012). Establishment of a healthy and dense ground cover plays a major role in minimizing nutrient and sediment runoff production (Pan and Shangguan 2006). Composted material and its benefits to plant nutrition and soil fertility are well-established (Darmody et al., 1983; O'Keefe et al., 1986; Sikora and Yakovchenko, 1996; Pascual et al., 1997). However, the use of compost as a stormwater management practice for erosion control has demonstrated mixed results; Glanville et al. (2004), Faucette et al. (2005), and Mukhtar et al. (2008) observed a reduction in runoff volume for compost-amended slopes when compared to non-mulched (no protective layer of straw or similar material) topsoil but substantially greater, 4-10-fold, nutrient concentrations were found in the runoff.

Research presented in Chapter 3 showed similar advantages and disadvantages to the use of compost in both field and greenhouse observations, with 2-9-fold increase in nutrients in runoff from compost layers compared to a standard topsoil with fertilizer and a straw mulch cover. An initial period within the first 25-35 cm of applied rainfall was identified where both vegetation establishment and 2-20-fold greater (than subsequent measurements) concentrations of total nitrogen and phosphorus occurred. This identified a critical period of nutrient and sediment loss that coincided with the initial vegetation establishment phase.

Each of the previous studies (Faucette et al., 2005; Mukhtar et al., 2008; Chapter 3) focused on the use of non-mulched composted material vis-à-vis some form of topsoil control, but none have analyzed composted material with additional stormwater management practices (e.g., straw mulching). To respond to this need, a series of greenhouse experiments carried out at a variety of slope ratios were designed to determine the implications of composted material amendment to current stormwater management practices with and without straw mulching. Straw mulching has shown improvements in vegetation establishment and runoff reduction through increased soil moisture, improved water storage, and reduced soil splash and compaction (Mannering and Meyer, 1963; Poesen and Lavee, 1991; Jordan et al., 2010; Liu et al., 2012). However, straw is an organic material that will decompose over time dependent on local climate and soil properties (Angers and Recous, 1997; Curtin et al., 2008). Thus, the rapid establishment of vegetation is essential to maintain the continued benefits seen with straw mulching.

The objectives for this study were to observe and identify critical elements involved in runoff generation and quality from (1) compost media application with straw mulch application, (2) variable ratio of compost/topsoil, and (3) variations in slope ratio percent. Metrics used to evaluate success of the medium were rapid and healthy growth of green vegetation (GV), reduced runoff volume, and reduced concentrations and total mass export of nutrients and sediments.

4.2.1 Materials and Methodology

4.2.2 Materials

Greenhouse studies were completed to analyze three variables associated with compost amendment for highway embankment stabilization; the effects of straw mulching, compost/topsoil mixing ratio, and embankment slope ratio. Table 4-1 has a detailed description of all slopes and media tested throughout the experiment. All compost/topsoil media ratios are based on volume; 2:1 topsoil: greenwaste (TG) and 2:1 topsoil: biosolids (TB) correspond to average dry mass compost of $9.3 \pm 1.4\%$ while 2:1 greenwaste: topsoil (GT) and 2:1 biosolids: topsoil (BT) correspond to average dry mass compost of $29 \pm 2\%$. Media were tested over four slopes, 5%, 17%, 25%, and 50%.

All media tested throughout the experiment adhere to Maryland Department of Transportation State Highway Administration (MDOT SHA) specifications. Topsoil was collected from a local landscaping facility, greenwaste compost was produced by Leafgro®, and biosolids compost was produced by the Aberdeen, Maryland wastewater treatment facility. Both composted materials were produced aerobically.

All surface media were seeded with an MDOT SHA turf grass mixture, from Chesapeake Valley Seed, of 95% tall fescue and 5% Kentucky bluegrass at a rate of 0.022 kg/m^2. Plots that received initial straw coverage (Table 4-1) were applied at 0.448 kg/m^2 with straw from a local home supply store. All treatments that received straw mulching had a minimum of 95% straw coverage prior to rainfall application, confirmed via image analysis. The topsoil standard media received additional fertilizer provided by

Keymar Fertilizer Inc. with an N: P: K ratio of 20: 16: 12 (83% ureaform with monoammonium phosphate and sulfate of potash) and applied at a rate of 0.022 kg/m^2.

4.2.3 Greenhouse experimental design

Two 1.8 m by 1.8 m platforms were used to test three medium applications at a time during the greenhouse experiments, each covering a 0.6 m wide by 1.8 m long section of the platform, as described in Chapter 3. Each of these sections was designed to capture surface runoff from a 5-cm deep media layer and allowed infiltrated water to exit the system; as seen in Figure 4-7a. Three Meter Group ECH2O 5TM Soil Moisture Sensors were placed within the media layers perpendicular to the surface to measure soil moisture at 10 minute intervals throughout the study.

The rainfall simulator design (Figure 4-7b and c; single 13 mm HH-30 W SQ Fulljet® nozzle at ~2.7 m height) presented in Chapter 3 was used in this research to produce uniform applied rainfall events. The duration and frequency of each applied rainfall event are shown in Table 4-2 for all designed plot studies. University of Maryland tap water was used for these experiments and was analyzed for nutrients throughout the study.

4.2.4 Plant Growth Analysis

Vegetation photos were captured via a Nikon D7100 digital camera with an AF-S DX NIKKOR 18-140mm f/3.5-5.6G ED VR lens in JPG format with the auto focus feature, maximum pixel size of 4000 x 6000, without a lens zoom, and at a hard sharpness and normal saturation. Images were captured regularly before each applied rainfall event, which occurred based on the schedule outlined in Table 4-2.

Each 1.8-m long greenhouse plot was divided into two sections (0.6 m x 0.9 m). Each of these sections produced one image at 0º and one at ~5º from vertical center. Total plot coverage was measured based on the method described in Chapter 2. Coverage results include green vegetation (GV), straw/dormant vegetation, and exposed soil. This method utilizes the decision tree algorithm along with image color, texture, and histogram of oriented gradients to classify pixel blocks within each image (Figure 4-8). The four total images were input into the algorithm and used to represent coverage for a single application at a single point in time. Coverage results are presented as GV establishment rate, which was determined via the change in GV percent per change in applied water.

4.2.5 Runoff Sampling and Water Quality

Applied rainfall used in the greenhouse studies was tap water supplied by the UMD greenhouse facility. The tap water had average nutrient concentrations of 1.9 ± 1.2 mg-N/L and 0.51 ± 0.52 mg-P/L with no measurable suspended solids. Much of the nitrogen was in the form of nitrate at $75 \pm 24\%$ and much of the phosphorus was soluble reactive phosphorus (SRP) at $81 \pm 29\%$. Before use, all glassware and plasticware were washed with Liquinox soap, rinsed with deionized (DI) water, placed in an acid bath for a minimum of 4 hours, rinsed with DI water, and allowed to air dry.

All surface runoff produced from applied rainfall was collected and analyzed for total suspended solids (TSS), nitrogen (total nitrogen (TN), ammonium (NH_4^+), nitrate

(NO_3^-), and nitrite (NO_2^{2-})), and phosphorus (total phosphorus (TP), soluble reactive phosphorus (SRP), and dissolved phosphorus (DP)). Where runoff volume was large enough, independent grab samples were taken throughout the duration of the event in 100-250 mL bottles. Occasionally, there were instances where runoff volume was not large enough for measurement of nutrient speciation or TSS.

Both TN and TP were measured using unfiltered, vortexed samples. All speciation measurements were taken after vacuum filtration through a 0.22-µm membrane. Samples that were not immediately measured were stored at 4°C.

Sediment was measured as total suspended solids and followed Standard Method 2540D (Eaton et al., 2005) using 30-50 mL samples. Some samples contained settleable solids, which were rinsed from the container with additional DI water to ensure all solids from the sample were accounted for. Inadequate runoff volume produced throughout the experiment for some treatments, especially biosolids at shallow slopes, limited the number of tests available per storm event. Because of this limitation, TN and TP were prioritized over TSS due to the reduced volume needed for those chemical tests. This resulted in a reduced number of TSS data points for some treatments.

All TN measurements were made using a Shimadzu SSM-5000A Total Organic Carbon/Total Nitrogen Analyzer. Nitrate measurements for filtered samples were measured using ion chromatography on a Dionex ICS-1100 with ASRS 4 mm suppressor and a Dionex IonPac AS22 column. Ammonium and nitrite were both measured using a SEAL AQ300 Discrete Nutrient Analyzer using Standard Method 4500-NH_3 H and Standard Method 4500-NO_2 B (Eaton et al., 2005), respectively. Both nitrate and TN standards were made using a 1000-ppm nitrogen as nitrate stock solution. Ammonium and nitrite standards ranged from 0 to 1 mg-N/L and were prepared from a 1000 mg-N/L stock solution produced from ammonium chloride (A649-500) and sodium nitrite (7632-00-0) stock solutions, respectfully. Organic N was calculated as total nitrogen minus all nitrogen speciation.

The persulfate oxidation method for phosphorus digestion was used, based on the Murphy and Riley (1977) colorimetric method to measure total phosphorus and dissolved phosphorus. SRP was measured in the same way without oxidation. TP, DP, and SRP were measured between 0 and 1 mg-P/L using a SEAL AQ300 Discrete Nutrient Analyzer. All standards were created using a stock solution of Lab Chem Inc. 1000-ppm phosphate as phosphorus. Particulate P was calculated as the difference between TP and DP; dissolved organic P (DOP) was calculated as the difference in DP and SRP.

4.2.6 Statistical Analysis

All grab sample bottle and cumulative sample bucket volumes were measured before sample testing. These volumes were then multiplied by the discrete concentrations measured for each sample/bucket and summed together to obtain the total mass of nutrient or sediment exported per applied rainfall event, which was summed for the total mass exported. The overall event mean concentration EMC was calculated as the total mass of nutrient or sediment exported after all applied storm events divided by the total volume of runoff produced, calculated as the sum of all discrete volumes.

All values are presented as the mean $\pm$ the standard deviation, unless otherwise stated. Statistical analysis was done within individual storm events for trends and significance as well as across all six storm events. Tests for data independence were done using the non-parametric one-tailed Wilcoxan rank-sum test to determine acceptance or rejection of the null hypothesis that the two samples were from the same set and equal (Hollander and Wolfe, 1999). The nonparametric Mann-Kendall Tau test was used to determine general increase or decrease in data values with the null hypothesis being no discernable trend in the sample data and sample concentrations do not change over the x-axis (Gibbons, 1985). A statistical significance level of 5% ($P<0.05$) was used to determine rejection of the null hypothesis for all statistics but p values are also included with results.

4.3 Results

4.3.1 Effects of Straw Mulching

4.3.1.1 Vegetation Establishment

Initial straw mulching had a substantial impact on vegetation establishment for all tested media at the 25% slope, which can be seen in the mean establishment rates presented in Figure 4-1a. The mean rates presented in Figure 4-1a are all statistically greater for straw-mulched media vis-à-vis non-mulched media ($p \leq 0.04$). Establishment rates for B, G, TB, and TG were 29-, 31-, 4.2-, and 4.6- fold greater with straw mulching than without, respectively. These differences are further exemplified when comparing final GV slope coverage after 60 days from seeding and 30 cm (330 L) of total applied water. At final ground coverage measurement all four compost media with straw mulching had greater than 95% GV cover; however, without straw mulching these same media only reached 29% GV for TGNS, 35% GV for TBNS, and 3% GV for both GNS and BNS.

Major benefits to straw mulching for GV establishment include physical protection of seeds and soil from solar radiation and additional moisture storage (deflection of solar radiation and an additional 'captured water' zone, Figure 4-2). The protection provided by the mulching can result in greater seed germination and reduced soil moisture evaporation, which provides more consistently available water for plant uptake (Adams, 1966; Hensler et al., 2001; Marcu et al., 2013). Supporting this theory, soil moisture readings taken prior to rainfall application in the greenhouse had as much as 35% greater volumetric water content with straw mulching than without.

4.3.1.2 Runoff Volume

The effects of straw mulching on runoff volumes are presented in Figure 4-1b for all media as total runoff (L) after 30 cm (330 L) of applied rainfall at the 25% slope. Error bars represent the range found from the duplicate (TB and TG) studies described previously. As seen in Figure 4-1b, straw mulching reduced runoff volume for all media tested. These runoff reductions were statistically significant for both TB with 98% reduction ($p = 0.05$) and TG with 99% reduction ($p = 0.001$), however, neither B (22% reduction) nor G (51% reduction) media showed statistical reductions in runoff volume ($p = 0.53$ and $p = 0.12$, respectively).

Rainfall impact and the transference of both kinetic energy (KE) and rainfall momentum lead to soil compaction, slaking, particle segregation and pore clogging through soil splash and sealing (Hillel, 2004; Armenise et al., 2018). As an example, Chapter 3 presented evidence of soil sealing for both TB and TG soil mixtures without straw mulching after 30 cm of applied rainfall (330 L). By incorporating the initial straw layer, rainfall KE and momentum was intercepted prior to soil impact, as evidenced by the lack of an increase in normalized volume runoff as a function of time for all straw mulched media.

Major water management mechanisms for the system studied are also demonstrated in Figure 4-2. The addition of straw mulching results in: KE dissipation from rainfall impact (the protective layer at A_2), increased surface roughness (surface runoff flows through the straw layer at B_2), and increased storage volume (identified by the additional 'captured water' in the straw layer) (Mannering and Meyer, 1963; Poesen and Lavee, 1991; Jordan et al., 2010; Liu et al., 2012). Each additive mechanism from straw mulching significantly decreases the effects of soil sealing and increases soil infiltration and runoff contact time with soil.

The Daily Morgan-Morgan Finney model provides information on runoff generation (Choi et al., 2017), and calculates KE as:

$$KE = R_{eff} * \{(1 - CC) * U_{DT} + CC * U_{LD}\} \tag{1}$$

where R_{eff} is the effective rainfall (mm) based on slope ratio, U_{DT} is an estimated KE of direct throughfall (rain that bypasses the coverage layer) based on the universal power law equation (Shin et al., 2016), U_{LD} is the leaf drainage KE based on plant height, and CC is the fraction of canopy cover. For all plant heights below 14 cm (i.e., short grass or straw layers), U_{LD} is equal to 0 and both R_{eff} and U_{DT} are constant for all tests on the 25% slope, thus KE is linearly related to canopy cover at a rate of R_{eff}*U_{DT}, which means that the 'canopy cover' provided by the straw mulching directly impacts the KE transfer to soil surfaces and high percent cover will significantly reduce KE effects.

Additionally, the Daily Morgan-Morgan Finney model identifies a modified Manning's roughness coefficient, *n'* (Petryk and Bosmajian, 1975), based on plant stem diameter (D) and number of stems per unit area (NV) as:

$$n' = \left(n^2 + \frac{D * NV * d^{4/3}}{2 * g}\right)^{1/2} \quad (2)$$

where n is Manning's roughness coefficient based on soil surface roughness, g is gravity, and d is flow depth. This roughness coefficient is inversely proportional to flow velocity by (Petryk and Bosmajian, 1975):

$$v = \left(\frac{1}{n'}\right) d^{2/3} * \sqrt{\tan{(S)}} \quad (3)$$

with S equal to slope ratio. By incorporating straw mulching, flow velocity is effectively reduced by the square root of straw diameter.

Because rainfall KE is reduced linearly with straw mulch canopy cover, soil splash, particle re-organization, and soil dispersion are less likely to occur. This reduces the potential for soil sealing which has been seen to significantly reduce infiltration, especially for lower organic matter materials like TB and TG, as discussed previously in Chapter 3. Lower flow velocity due to dense straw mulching (increased stems per unit area) will also lead to longer runoff contact time with the media surface, which will promote greater infiltration and lead to reduced surface runoff volume.

4.3.1.3 Sediment

Straw mulching effects on sediment export are presented in Figures 4-1c and 4-1d. Major reductions in sediment mass export and mean sediment EMC throughout the six applied rainfall events were seen for all media with straw mulching. The reduction in sediment mass export was statistically significant for TB ($p = 0.03$), TG ($p = 0.001$), and G ($p = 0.001$), but not for B ($p = 0.28$). The B media was not found to be statistically different with straw mulching due to reduced sample size for biosolids without straw mulching. Two applied rainfall events for this treatment did not produce runoff volume sufficient for accurate measurement of sediment. Straw mulching addition to the TB and TG treatments was the most effective with greater than 99% sediment reduction compared to non-mulched media. TB had total sediment mass export per unit area reductions, due to straw mulching, from 79 g-sediment/m^2 to 0.24 ± 0.23 g-sediment/m^2 and TG had reductions from 310 g-sediment/m^2 to 0.36 ± 0.071 g-sediment/m^2. For G and B, sediment export was reduced by 71% (2040 to 587 mg-sediment/m^2) and 99% (2981 to 40 mg-sediment), respectively.

The mass export of sediment presented in Figure 4-1c was not solely due to the volume reduction in runoff presented in Figure 4-1b. EMC reductions with straw mulching were seen for all tested media with mean percent reductions of 99% ($p = 0.06$), 50% ($p = 0.05$), 92% ($p = 0.002$), and 94% ($p = 0.001$) for B, G, TB, and TG, respectively (Figure 4-1d). Although not specifically analyzed for composts, significant reduction in sediment yield with straw mulching compared to non-mulched soils has been seen, consistently, in previous research (Jordan et al., 2010; Wang et al., 2011; Liu et al., 2012; Wang et al., 2015). The reduction in sediment loss seen here can largely be attributed to the reduction in KE and momentum transfer to the soil profile and the runoff flow velocity reduction, discussed previously.

Although compost addition has been shown to reduce sediment in soil runoff (Morgan, 1986; Poesen and Lavee, 1991; Shock et al., 1997; Faucette et al., 2007;

Muhktar et al., 2008; Gholami et al., 2012; Prosdocimi et al., 2016), it is still an exposed particle/media surface. As discussed previously for volume reduction, straw mulching reduced rainfall impact and the runoff flow velocity. With the reduced energy, particles in all media were less likely to detach and be conveyed through the surface flow, resulting in lower sediment transports.

4.3.1.4 Nutrients

The straw mulching effect on total mass export of nitrogen can be seen in Figure 4-3a. All tested media showed reduction in nitrogen mass export after straw addition, which was statistically significant for B ($p = 0.001$), G ($p = 0.013$), and TG ($p = 0.047$) but not for TB ($p = 0.15$). Both B and TB had the greatest reduction in nitrogen mass export of 92% and 89%, respectively. The soil sealing which occurred for TB described in Chapter 3 helps to explain the large difference in total mass reduction without statistical significance. Although overall reduction was very large for the TB media, initial applied rainfall events did not produce the increased nitrogen mass export found in the later applied events which lead to the lack of significance.

Lower total volume runoff largely resulted in reduced mass export for the straw mulched media tested, however, from Figure 4-3b, both the B and G media also showed a decrease in mean nitrogen EMC (87% for B and 22% for G). Some forms of nitrogen, specifically nitrate, are highly mobile in the environment. The EMC reductions seen for both composts can be attributed to the additional storage and conveyance of applied rainfall through the straw layer, as shown in Figure 4-2 and discussed previously, in contrast to flow through and over the soil media. Water passing on top of and through the straw layer, A_2 and B_2 in Figure 4-2, export significantly less mobile nitrogen than water that contacts and interacts directly with the media layer (A_1 and B_1 in Figure 4-2).

Unlike the B and G treatments, TB and TG saw an increase in average EMC from straw non-mulched to mulched media. The increase for TB and TG was likely due to dilution of EMC values by concentrations in the later phase of runoff. A 'first flush' is often attributed to storm events in which the initial runoff generated carries a disproportionately larger mass of nutrients than the later stages (Thornton and Saul, 1987). Due to greater runoff volume per storm, discussed previously, the EMC values generated by both TB and TG would be lower and more dominated by later phase runoff than a storm with less runoff volume on similar media.

The effects of straw mulching on phosphorus total mass export and mean EMC can be seen in Figures 4-3c and d. All media showed reductions in both mass export and EMC with straw mulching. Reduction in total mass export of phosphorus with straw mulching was the greatest for TB (99%) and TG (99%) which was largely due to runoff volume reductions. However, all media (including TB and TG) had reduced EMC values (mean values - B: 60% ($p = 0.002$), TB: 44% ($p = 0.09$), G: 57% ($p = 0.13$), and TG: 40%, ($p = 0.001$) with the addition of straw mulching; the reductions were statistically significant only for B and TG. These reductions likely resulted from blockage of the water and transported sediment from the media surface runoff by the straw layer. From both runoff volume and EMC reductions, B and G had 71% and 66% reductions in phosphorus mass export, respectively, with straw mulching.

Phosphorus is generally immobile in the environment due largely to its ability to readily adsorb onto soil particles. Thus, sediment export is the primary mechanism for phosphorus mobilization (Sharpley and Syers, 1979). In agreement with Sharpley and Syers (1979), the current study found good correlation between mass export of phosphorus and mass export of sediment via a power relationship with an R^2 of 0.79 (Figure 4-9), when all tested materials were analyzed (with and without straw mulching). This relationship is supported by both the Soil and Water Assessment Tool (SWAT) and the Chemicals, Runoff, and Erosion from Agricultural Management Systems (CREAMS) models which model phosphorus export in the sediment phase as a function of the phosphorus enrichment ratio which is a power function relationship based on the concentration of sediment in the runoff.

4.3.2 Effects of Compost Addition

4.3.2.1 Vegetation Establishment

Figure 4-4a gives GV establishment as a function of percent compost for both greenwaste and biosolids composts at the 25% slope. With straw mulching, no statistical differences were noted in rate of establishment; all materials reached 95% GV establishment by the end of the trial period. Although not statistically significant, compost addition initially showed improvement in growth rates for both compost materials, however, the rate reduced as compost percent increased. This was likely due to the positive relationship between compost addition and porosity, which likely led to faster evaporation and lower plant available moisture. Duzgun et al. (2020) found that compost from biosolids and greenwaste had 1-3 orders of magnitude greater saturated hydraulic conductivity and

124-127% greater wilting point values than in topsoil. Although compost addition provides a substantial amount of nutrients (as evidenced by the runoff nutrient concentrations and soil extractions), compost is also more prone to rapidly drying out due to the increased porosity. Chapter 3, however, noted that the drying process seen in the greenhouse was not evident in field application with shorter average drying periods and longer average rainfall events.

4.3.2.2 Runoff Volume

Figure 4-4b shows total runoff volume as a function of the various media types (with straw mulching). TS had greater total runoff volume (4.1 ± 1.8 L) than all compost-amended media except BTS (which had 13% greater runoff volume than TS; $p > 0.2$); this was statistically significant for BS ($p = 0.022$), TBS ($p = 0.023$), and TGS ($p = 0.026$), but not for GS ($p = 0.180$) or GTS ($p > 0.2$). The greatest reduction in total volume runoff occurred for BS, TBS, and TGS with reductions of 56%, 59%, and 64% respectively.

Runoff volume is largely influenced by the infiltration rate and the water holding capacity (calculated as the difference between field capacity and the initial soil moisture) of the media; faster infiltration with higher water holding capacity produces lower runoff volume. Duzgun et al. (2020) found that saturated hydraulic conductivity, field capacity, and maximum saturated water content were positively correlated to increased compost addition; values increased by 14-6170-fold, 1.5-2.6-fold, and 1.4-2.8- fold, respectively. With increased water storage and infiltration potential, compost addition was expected to have significantly reduced runoff volume compared to topsoil, which has been seen in

Faucette et al. (2007) and Mukhtar et al (2008) when compared to non-mulched topsoil. However, from Figure 4-4b there was not a clear trend in volume reduction with increased compost incorporation.

Chapter 3 discussed the effects of straw mulching on topsoil as compared to non-mulched compost. From this study, the benefits of straw mulching to the topsoil media outweighed the potential benefits of compost without straw mulching to volume reduction. The results also showed that some compost media without straw mulching showed evidence of soil sealing. Although compost media in this study were generally seen to reduce runoff volume, compared to topsoil, the straw mulching applied to all media likely played a larger role in runoff reduction (as discussed previously) than the compost media.

4.3.2.3 Sediment

The effects of compost addition on sediment loss can be seen in Figures 4-4c and d. These figures show that TS had greater total sediment mass export (1890 ± 1564 mg-sediment/m^2) and overall sediment EMC (589 ± 420 mg-sediment/L) than all compost amended treatments. Compared to TS, BS ($p = 0.008$) and TBS ($p = 0.04$) treatments showed the greatest reduction in sediment export (98% and 86%, respectively) and were the only treatments to have statistically significant overall EMC reductions of 96% ($p = 0.008$) and 83% ($p = 0.04$), respectively. Both BTS ($p = 0.20$) and GTS ($p = 0.39$) showed the least reduction in sediment runoff mass export at 53% and 8%, respectively. This reduction was consistent with previous studies which compared both non-mulched compost and non-mulched topsoil and found reductions in sediment runoff with compost addition (Morgan, 1986; Poesen and Lavee, 1991; Shock et al., 1997; Faucette et al., 2007).

Reduction in sediment loss may be attributed to improvements in aggregation within the media. Compost increased organic matter from 2.6% in TS to 47% and 39% in B and G, respectively. Organic matter improves soil aggregation through physicochemical clay and oxide interactions and by offering a healthy growing community for microorganisms that also bind soil (Hillel, 2005). Improved aggregate formation naturally resists the fragmentation, scouring, and dispersive forces from rainfall impact and overland flow, which leads to decreased sediment runoff.

4.3.2.4 Nutrients

The effects of compost addition on nitrogen and phosphorus export can be seen in Figure 4-5. Here, the standard TS media had a greater total mass export of both nitrogen (284 ± 243 mg-N/m^2) and phosphorus (8.7 ± 4.1 mg-P/m^2) than all other media, except BTS ($p = 0.40$) which had greater total mass export of both nitrogen (349 mg-N/m^2; $p = 0.4$) and phosphorus (9.9 mg-P/m2; $p = 0.4$).

Of the other mixtures, BS ($p = 0.001$), TBS ($p = 0.002$), and GTS ($p = 0.047$) all had statistically lower nitrogen mass export. BS (46 mg-N/m^2) and TBS (73 ± 53 mg-N m^2) had the greatest reduction in total mass export from TS of 82% and 72%, respectively. Phosphorus mass export, compared to TS, was statistically lower for BS ($p = 0.022$), TBS ($p = 0.001$), TGS ($p = 0.002$), and GTS ($p = 0.047$). Of these, TGS and TBS showed the greatest reduction in mean phosphorus mass export compared to TS, with reductions of 76% and 69%, respectively.

The reduction in total mass export of both nutrients compared to TS can largely be explained through volume reduction, as discussed previously. Further evidence of this can be seen in the shape of data presented in Figures 4-4b, 4-5a and 4-5c, which are similar. However, from the overall EMC graphs presented in Figures 4-5b and 4-5d, runoff concentrations were also reduced by 35-79% and 24-62% from the 134 ± 170 mg-N/L and 3.4 ± 3.4 mg-P/L TS nitrogen and phosphorus EMC, respectively.

Based on extraction data presented in Chapter 3 extractable N (KCl) and extractable P (Mehlich-3) were seen to increase with compost incorporation for biosolids (up to 19-fold for N and 6-fold for P) and extractable P was seen to increase for greenwaste incorporation (4-fold). From these numbers nutrient runoff concentrations would be expected to increase from TS with compost addition, which was seen in non-mulched media in that study. However, the extraction data presented in Chapter 3 does not account for the additional fertilizer applied at 0.022 kg/m^2 to the TS treatment.

At a ratio of 20:16:12, applied at 0.022 kg/m^2, and a bulk density of 0.94 ± 0.2 g/cm^3, calculated from the tested slopes, this would result in an additional 92 mg-N/kg extractable N and 73 mg-P/kg from the fertilizer. Additionally, the Mehlich-3 extraction is a strong acid method that has been shown to strip orthophosphate as well as organic P from the soil medium (Cade-Menun et al., 2018). Compost is often considered a slow release fertilizer because most nutrients held within compost are in the form of inaccessible organic matter, which is held tightly in the soil structure and is decomposed into more mobile forms over time. As such, values from the extraction will likely over predict the available phosphorus from highly organic rich soils, like pure compost (47% and 39% organic matter for B and G, respectively).

Combining the extractable N and P values for TS (Owen et al., 2020b) and the calculated additional fertilizer, the new TS extractable N and P values would be 275 mg-N/kg and 220 mg-P/kg, respectively. Additionally, if the organic matter content, which would not be readily available for plant uptake or aqueous runoff, were assumed to contribute to the reported extractable P values then final available P would be the extraction value minus the percent organic content. With these manipulations, nitrogen extractions for all media (except BS) become 30-70% lower than TS. While phosphorus extractable values were still calculated to be greater for compost than TS, values were reduced to 2- fold greater versus the initially stated 4- (greenwaste) and 6- fold (biosolids). Although extractions would predict greater phosphorus export, the reduction in sediment loss, which was seen to be highly correlated with phosphorus export (discussed previously), from the system likely played a major role in reducing the phosphorus export from the TS medium.

From previous research, non-mulched compost was found to reduce mass export of nitrogen and phosphorus when compared to non-mulched topsoil (Faucette et al., 2007; Muhktar et al., 2008; Hansen et al., 2012). Although this was not found in Chapter 3 for non-mulched compost compared to straw-mulched topsoil, the addition of straw mulch to both the control and composted media produced similar results to the previous research.

4.3.3 Effects of Slope Ratio

4.3.3.1 Vegetation Establishment

Figure 4-6a shows mean GV establishment rates as a function of slope ratio for the tested media. For TS, GNS, and BNS, a negative statistical trend was found for growth rates with respect to increasing slope ratio. The lack of growth at steeper slopes was likely due to moisture availability after infiltration. From the 5% to the 50% slope, gravitational head increased by 12%, causing reduced soil moisture, which led to a 3.5-4.2% decrease in establishment rate, seen in Figure 4-6a.

4.3.3.2 Runoff Volume

The effects of slope ratio on runoff volume are presented in Figure 4-6b. The runoff volume generation was seen to statistically increase with slope ratio increase. The other media (GNS, BS, TGS, and TBS) also showed similar increases, but did not have statistically different runoff values at the varying slope ratios ($p \geq 0.1$). The revised universal soil loss equation (RUSLE) predicts that a steeper slope will result in greater runoff volume (Renard et al., 1997), due to gravity acting on ponding water; the contact time a water surface has moving across the soil surface is reduced based on the cosine of slope angle. This general trend was also captured in this data.

4.3.3.3 Sediment

The effects of slope ratio on total mass export of sediment are presented in Figure 4-6c. Although sediment export was seen to be positively correlated (over all media) with slope ratio, as discussed previously, sediment transport is strongly affected by rainfall impact and overland flow rate and volume. Based on the volume generated with slope ratio increase, discussed previously, greater volumes at higher slope ratios naturally lead to greater sediment runoff. Additionally, with increased slope ratio, the rainfall angle of impact decreases (closer to parallel with the soil surface) which may lead to higher lateral force on sediment splash particles and greater horizontal movement of soil particles.

4.3.3.4 Nutrients

Total mass export of nitrogen as a function of slope ratio is presented in Figure 4-6d for all media tested. Similar to runoff volume and sediment export, nitrogen mass export was seen to generally increase with slope ratio increase. Nitrogen increase with slope ratio was a function of plant uptake and immobilization, runoff volume increase, and sediment export. At steeper slopes, GV was seen to decline, runoff volume increased, and sediment export increased which translated directly to increased nitrogen export. TS at the 50% slope (for example) showed significant increase in sediment export (30-fold from the 25% slope), with that export came an increase in organic N (particulate) and ammonium (which readily adsorbs to clay and fine particles) of 12% and 6%, respectively (Sparks, 2003).

Figure 4-6e shows the effects of slope ratio change on total mass phosphorus export for the tested media. Like sediment and nitrogen, phosphorus was seen to generally increase with slope ratio. Phosphorus mass export increased statistically with slope increase from the 5-25% slopes to the 50% slope ($p \leq 0.002$) for TS, from the 5% slope to the 50% slope ($p = 0.01$) for GNS, and from the 5-17% slopes to the 25-50%

slopes ($p \leq 0.002$) for BNS. BS, TBS, and TGS were not found to be statistically different between 17% and 25% slopes. Like nitrogen, phosphorus export is controlled by plant uptake and immobilization, runoff volume, and sediment export, however, for phosphorus the dominant mechanism for transport is sediment, as discussed previously. As sediment was seen to increase with slope ratio (Figure 4-6c), it was not surprising to find phosphorus mass export increase as well.

4.4 Conclusions

Three water quality parameters along with digital GV growth analysis were used to analyze the application of both biosolids- and greenwaste-derived composts for the purpose of slope stabilization along highway embankments. Straw mulching, percent compost mixing with topsoil, and slope ratio were varied to understand the effects and impacts of compost addition.

Straw mulch addition resulted in improved GV establishment (4-33-fold faster rates) and reductions in runoff volume (64-99% reduction), total sediment mass export (71-99.9% reduction), total nitrogen mass export (71-92% reduction), and total phosphorus mass export (66-99% reduction). With the addition of straw mulching, a second protective storage layer was added above the media. This layer provided additional water storage for plant uptake and physical protection of the planting media from solar radiation and the soil media from rainfall impact.

The addition of the straw layer completely minimized the impact of various mixtures of compost. While the addition of the straw produced a major impact, the makeup of the media layer below had a much lower statistical impact on the parameters measured. Compost addition increased soil organic matter content, saturated hydraulic conductivity, water holding capacity, and soil aggregation while having similar (after accounting for additional fertilizer application for topsoil) extractable nutrients compared to the standard topsoil practice. Although compost addition (with straw mulching) was not seen to significantly affect GV establishment when compared to topsoil, in this study, the improved hydraulic conductivity and water holding capacity resulted in increased water infiltration; which generally reduced runoff volume by 13-64% compared to the standard topsoil practice. The increased soil aggregation with compost addition resisted the destructive properties of rainfall runoff and resulted in 8-98% reduction in sediment export compared to standard topsoil. Nitrogen and phosphorus are strongly related to runoff volume and sediment export, both of which were seen to be reduced in this study. From the media tested (excluding BTS) compost addition was seen to reduce nitrogen mass export by 6-82% and phosphorus mass export by 4-76% when compared to the topsoil standard.

The gravitational head within the media was varied by altering the slope ratio. This resulted in up to a 12% modeled difference (based on the highest and lowest slope ratios tested herein) in available water for plant growth resulting in a 3.5-4.2% decrease in GV establishment rate. Slope ratio during a rainfall event affects the gravitational force on the generated runoff and rainfall impact angle. With greater slope ratio, there was an increase runoff velocity and lateral particle dispersion forces. This led to reduced runoff contact time for infiltration and increased soil particle displacement. From the results obtained, slope ratio was positively correlated to both runoff volume and sediment export. Both nitrogen and phosphorus mass export were also seen to increase with increasing slope ratio. As export of both nutrients are a function of vegetation establishment (which was reduced with slope ratio increase), runoff volume and sediment export (both increased with slope ratio increase), these results were not surprising.

It is strongly recommended that straw mulching be used for all treatment applications regardless of compost percent; this treatment was shown to reduce total runoff volume, sediment and nutrient yield, and improve vegetation establishment for all tested media. The use of compost with straw mulching was seen to perform statistically similar to TS or better for all tested media. Based on the similar results obtained herein to TS, compost may be a viable alternative to the standard TS medium for slope stability applications. Both BS and TBS showed the greatest improvement to the TS standard with 79% and 78% reduction in mass export of sediment and nutrients and 56% and 59% reduction in runoff volume. Slope ratio changes greatly affected the total mass export for each medium tested. In general, runoff generation increased, and vegetation establishment decreased with slope ratio increase.

4.5 List of Tables

Table 4-1: List of all tested slopes and treatments. Some slopes were repeated and are represented by a multiplier (eg. x2). Media treatments: topsoil with straw and fertilizer (TS), biosolids (B), 2:1 biosolids: topsoil (BT), 2:1 topsoil: biosolids (TB), greenwaste (G), 2:1 greenwaste: topsoil (GT), 2:1 topsoil: greenwaste (TG). With straw mulching is denoted by an additional S and without is an NS.

5% Slope	**17% Slope**	**25% Slope**	**50% Slope**
TS	TS	TS x3	TS
BNS	BNS, BS	BNS, BS	BNS
GNS	GNS	GNS, GS	GNS
	TBS	TBS x2, TBNS	
	TGS	TGS x2, TGNS	
		GTS	
		BTS	

4.6 List of Figures

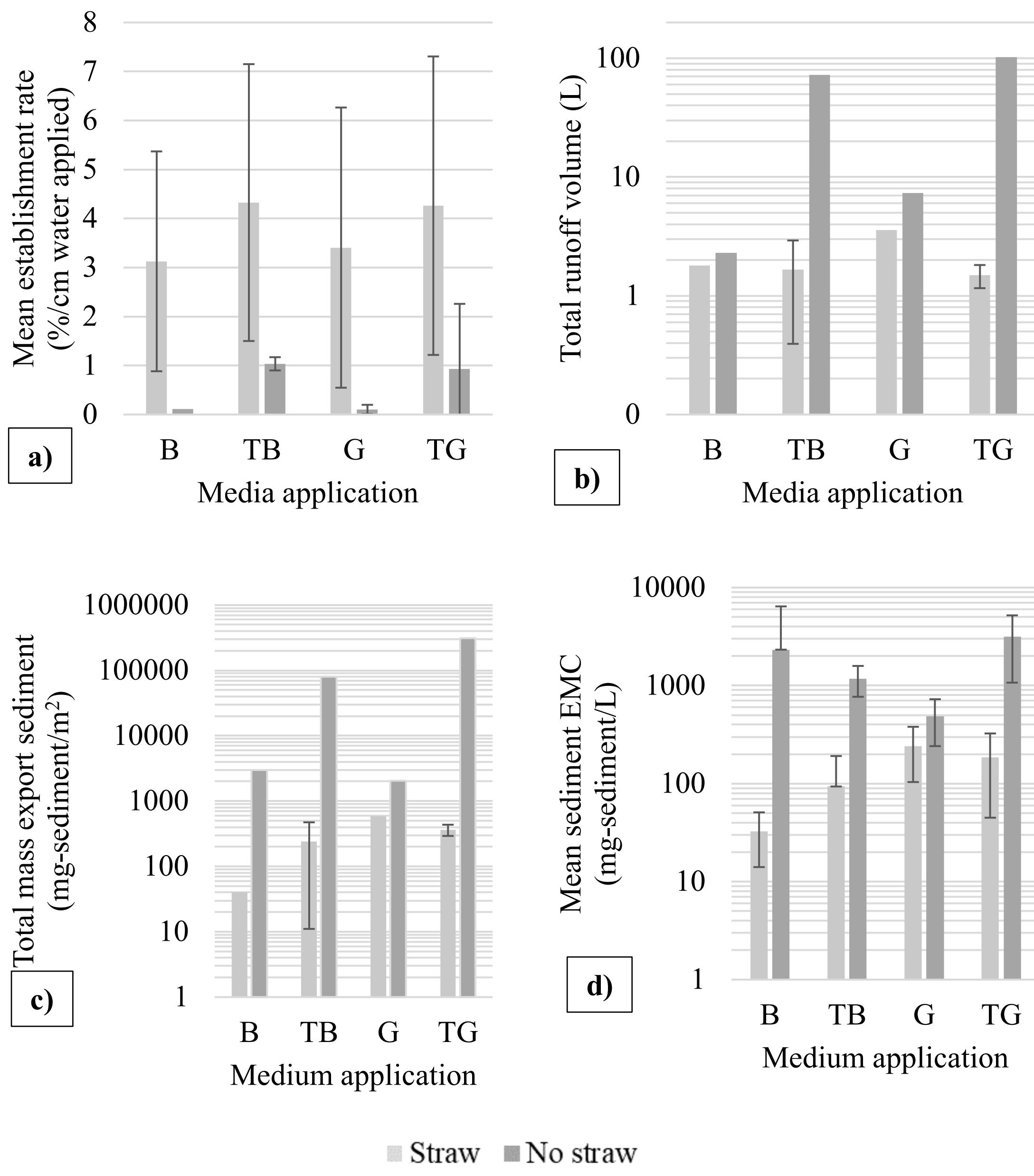

Figure 4-1: Effects of straw coverage at a 25% slope after 30 cm. of applied rainfall (330 L) on a) green vegetation establishment, b) total runoff volume (log scale), c) total mass export of sediment (log scale) and d) mean sediment EMC (log scale). B = biosolids, TB = 2:1 topsoil: biosolids, G = greenwaste, TG = 2:1 topsoil: greenwaste.

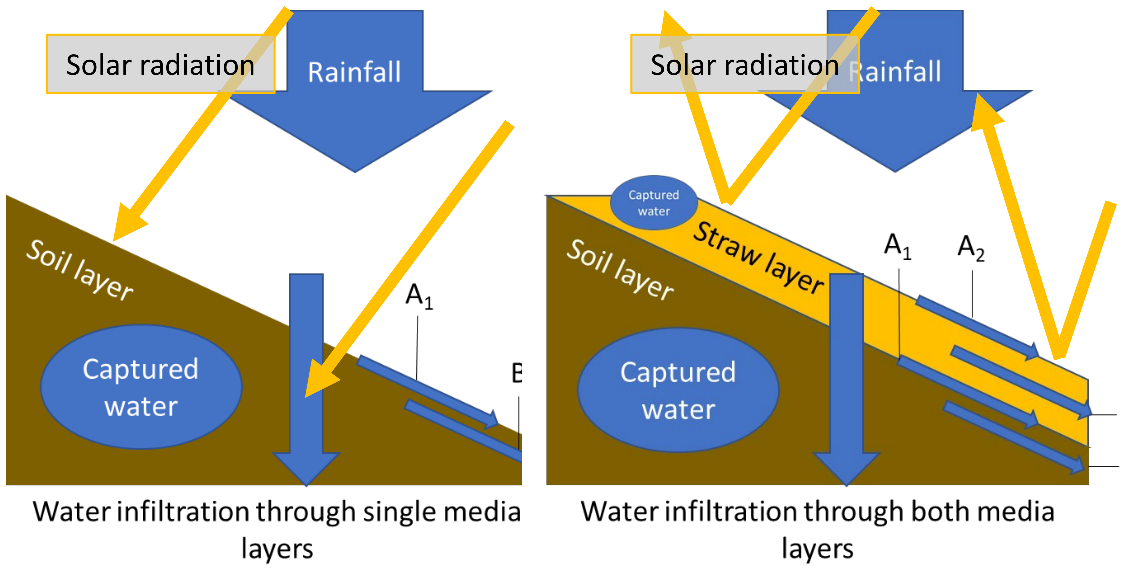

Figure 4-2: Theoretical diagram of solar energy transfer and water runoff generation from no straw mulching and straw mulching. A_1 is surface flow from the soil layer, B_1 is subsurface flow through the soil layer. A_2 is surface flow through the straw layer and B_2 is subsurface flow through the straw layer.

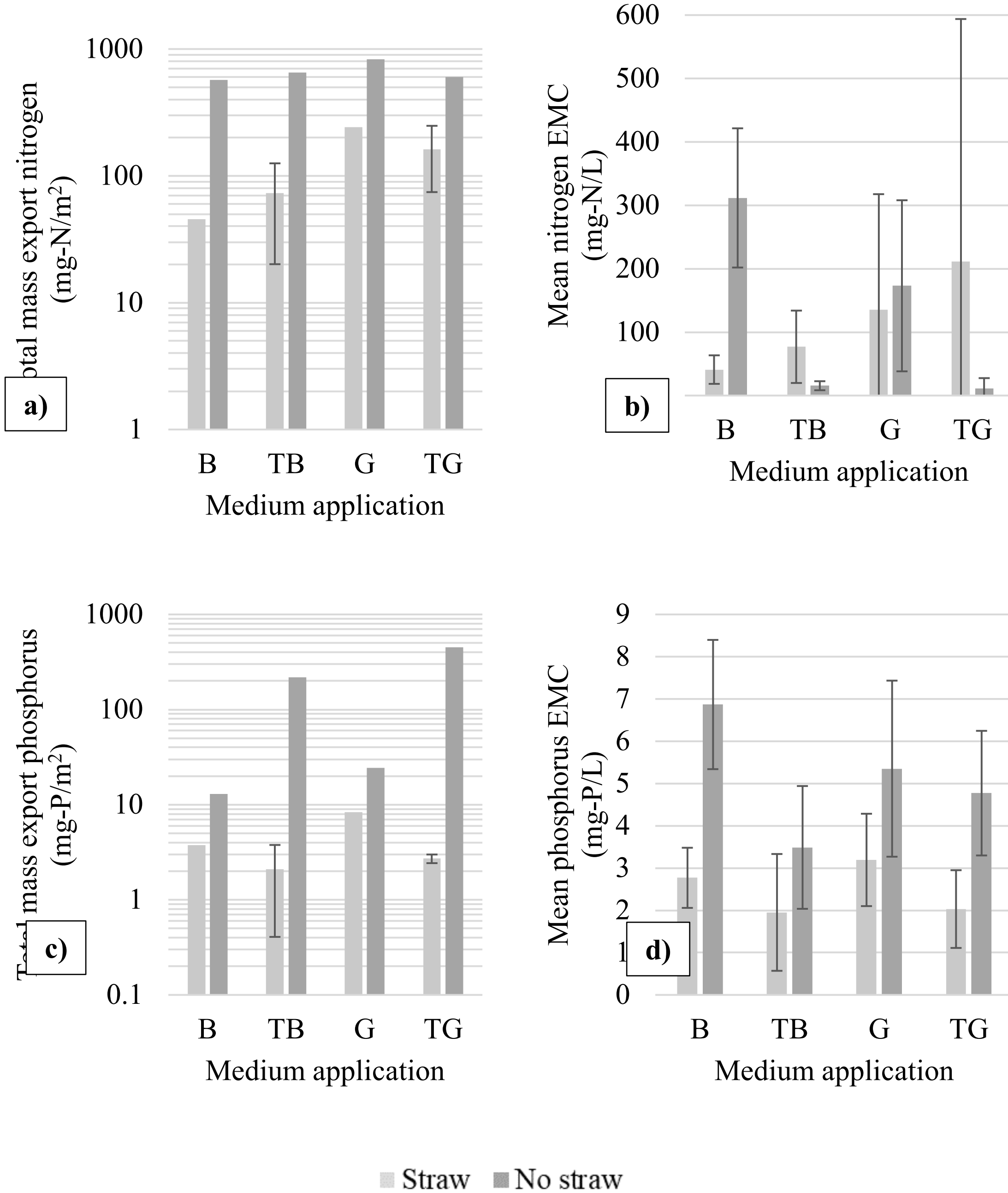

Figure 4-3: Effects of straw coverage at a 25% slope after 30 cm. of applied rainfall (330 L) on a) total mass export of nitrogen, b) mean nitrogen EMC, c) total mass export of phosphorus and d) mean phosphorus EMC. B = biosolids, TB = 2:1 topsoil: biosolids, G = greenwaste, TG = 2:1 topsoil: greenwaste.

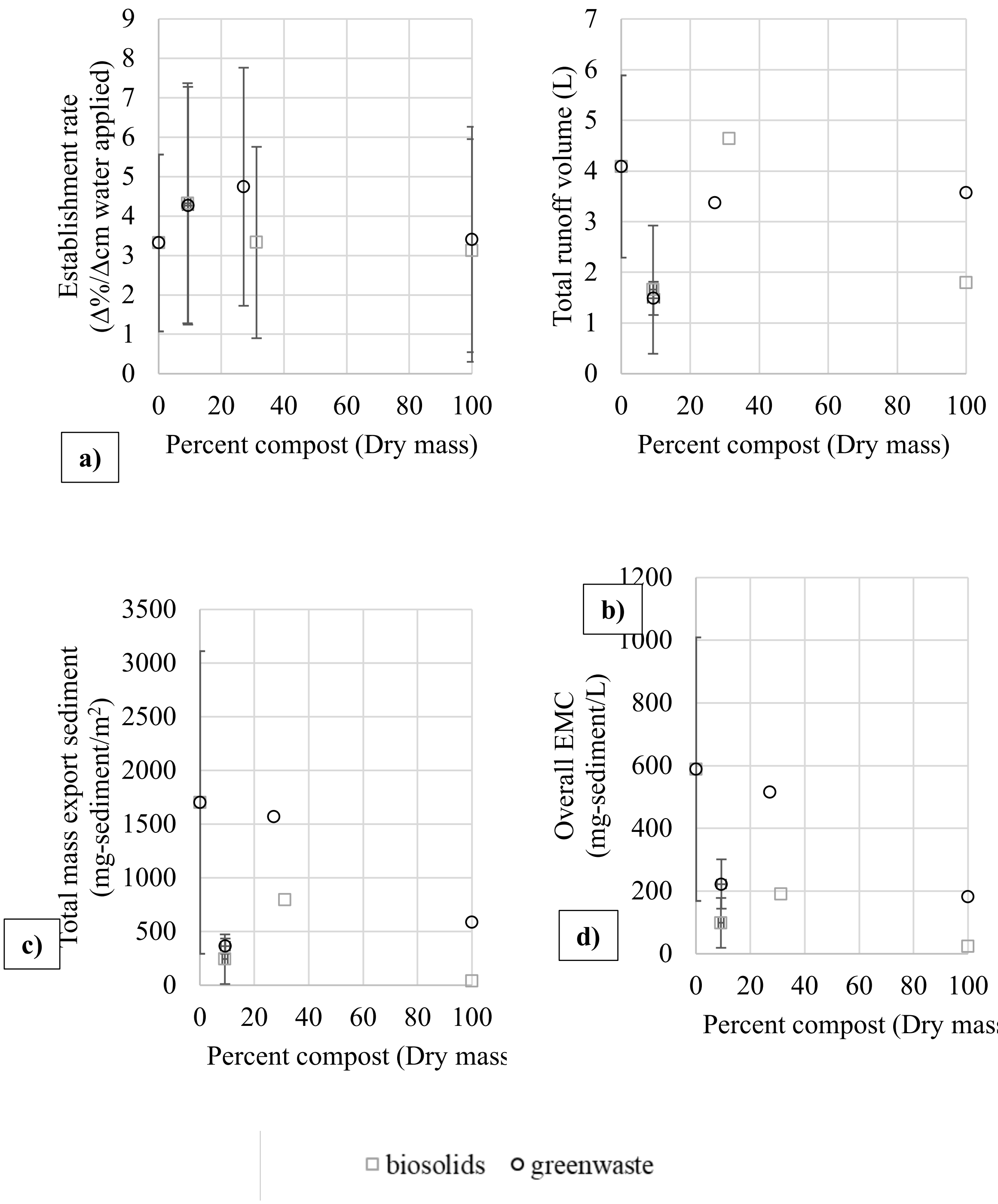

Figure 4-4: Effects of compost addition (with straw) at a 25% slope after 30 cm. of applied rainfall (330 L) on a) green vegetation establishment, b) runoff volume, c) total mass export of sediment and d) mean sediment EMC. 0% compost (TS = topsoil/fertilizer), 9% compost (TBS = 2:1 topsoil: biosolids and TGS = 2:1 topsoil: greenwaste), 29% compost (BTS = 2:1 biosolids: topsoil and GTS = 2:1 greenwaste: topsoil), 100% compost (BS = biosolids and GS = greenwaste).

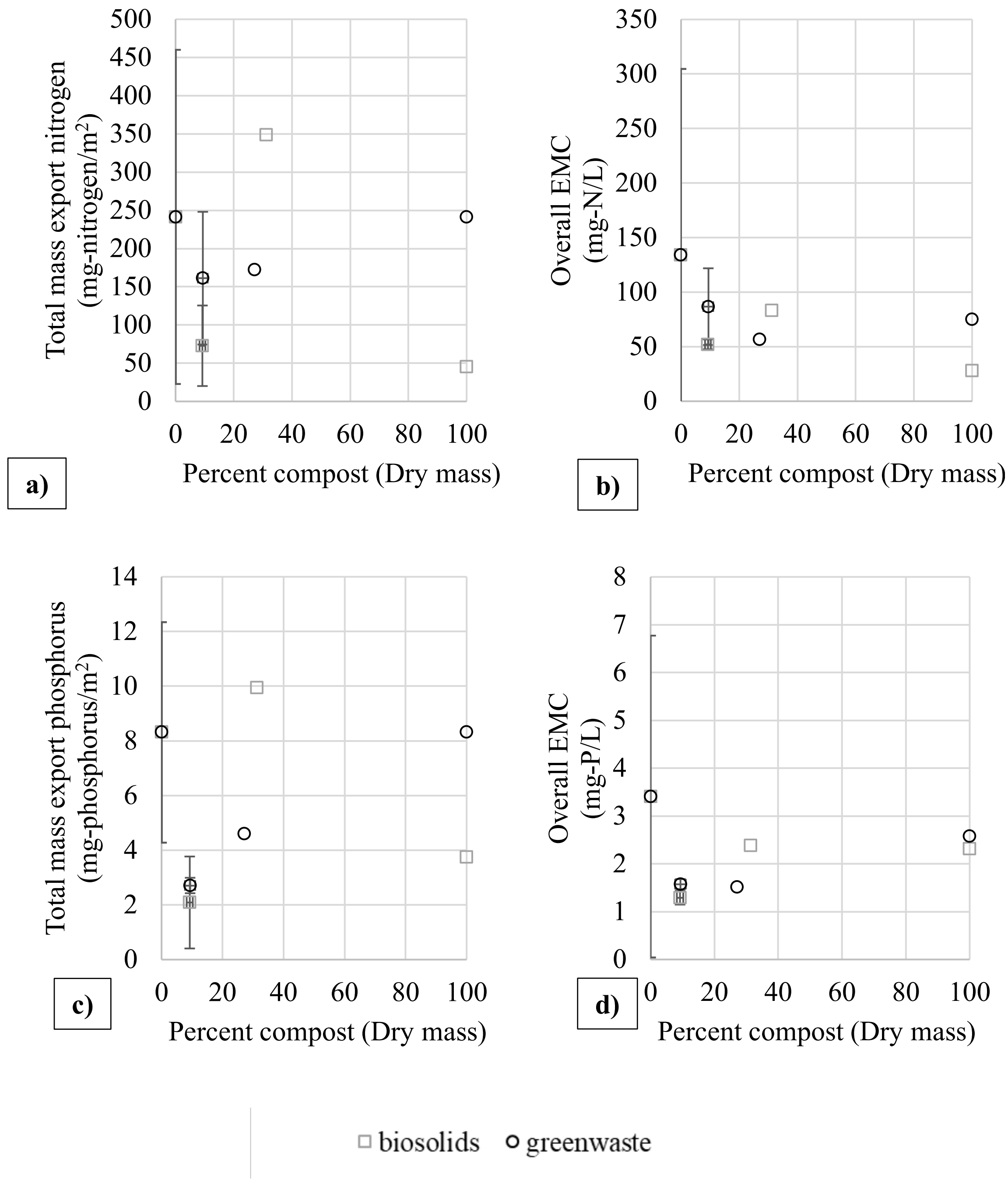

Figure 4-5: Effects of compost addition at a 25% slope (with straw) after 30 cm. of applied rainfall (330 L) on a) total mass export of nitrogen, b) mean nitrogen EMC, c) total mass export of phosphorus and d) mean phosphorus EMC. 0% compost (TS = topsoil/straw/fertilizer), 9% compost (TBS = 2:1 topsoil: biosolids and TGS = 2:1 topsoil: greenwaste), 29% compost (BTS = 2:1 biosolids: topsoil and GTS = 2:1 greenwaste: topsoil), 100% compost (BS = biosolids and GS = greenwaste).

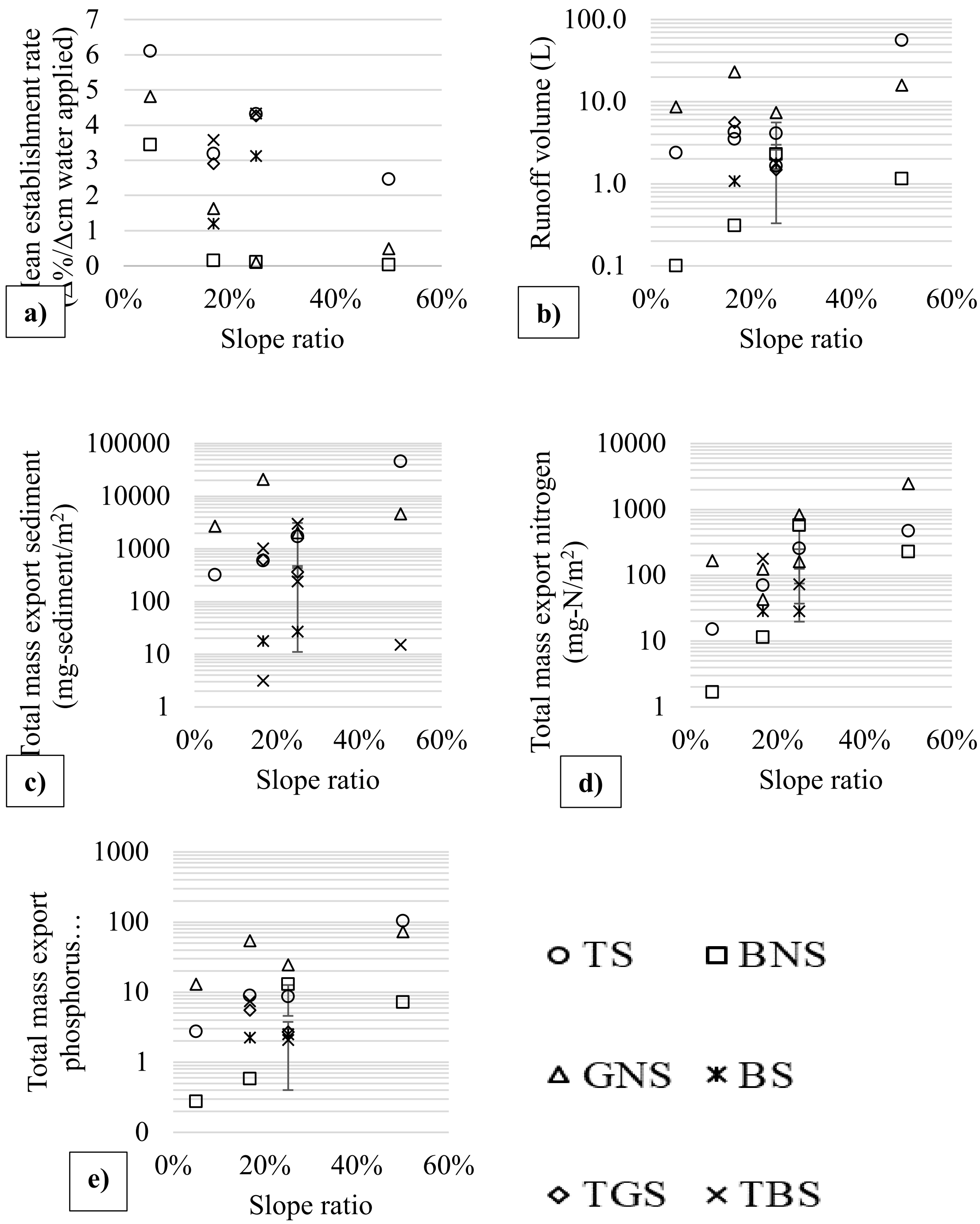

Figure 4-6: Effects of slope ratio at a 25% slope after 30 cm. of applied rainfall (330 L) on a) green vegetation establishment, b) runoff volume, c) total mass export of sediment, d) total mass export of nitrogen, and e) total mass export of phosphorus. TS = topsoil//straw/fertilizer, BNS = biosolids without straw, GNS = greenwaste without straw, BS = biosolids with straw, TGS = 2:1 topsoil: greenwaste without straw, and TBS = 2:1 topsoil: biosolids with straw.

4.7 Supplemental Information

Table 4-2: Synthetic stormwater application schedule and durations for greenhouse simulations.

Days since seeding	0-2	6-8	13-15	20-22	27-29	34-36
Duration	15-min	15-min	30-min	30-min	45-min	45-min
Rainfall Volume (cm.)	2.5	2.5	5.1	5.1	7.6	7.6
Accumulated Rainfall (cm.)	2.5	5.1	10	15	23	30

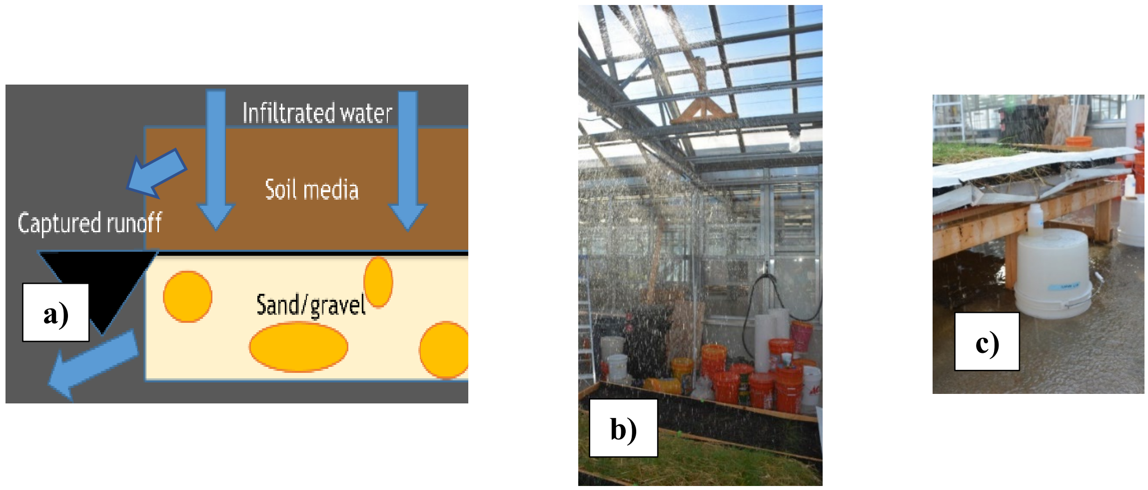

Figure 4-7: (a) Rainfall simulator with a single jet nozzle to produce synthetic rainfall which produced surface runoff collected in (b) sample bottles at the base of the slope. (c) the cross-sectional view of the runoff setup. Runoff was captured in the gutter system for collection and analysis with a rain guard to protect the effluent from dilution due to applied rainfall.

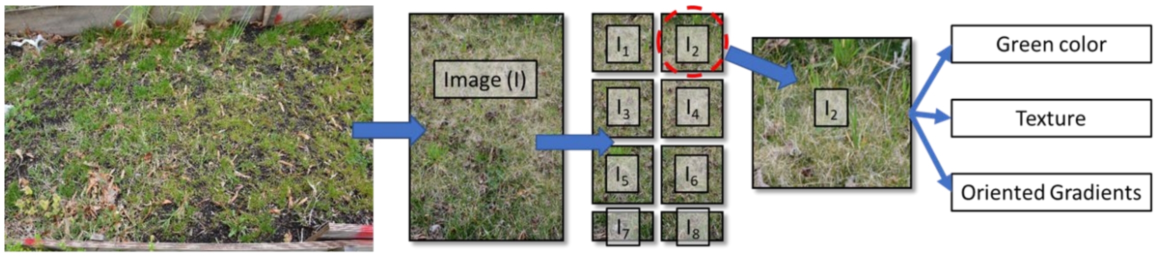

Figure 4-8: Flow chart of (left to right) the original image captured, cropping to the region of interest, segmentation into pixel blocks, and extractions of feature descriptors for algorithm input.

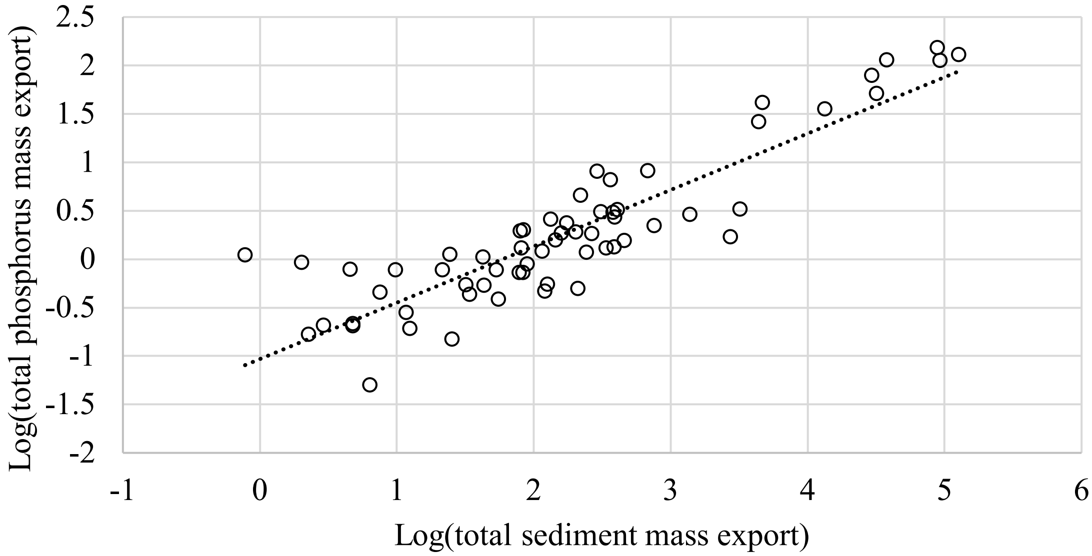

$y = 0.58 * x - 1.03$ $R^2 = 0.79$

Figure 4-9: Phosphorus mass export as a power function of sediment mass export.

Chapter 5: Conclusions and Recommendations

This research was designed to analyze and identify different elements involved in the application of a compost medium as a SMP for erosion control on highway slopes. Three water quality parameters (sediment, nitrogen, and phosphorus) along with digital GV growth analysis were used to quantify the effects of biosolids- and greenwaste-derived compost application on slope stabilization. Straw mulching, compost mix ratios with topsoil, and slope ratio were altered to further understand the effects of compost addition at both the greenhouse and field size scales.

An automated ground cover measurement tool using readily available software tools for standard JPEG images was created for the purposes of quantifying GV growth in an objective and repeatable fashion. The tool was successfully optimized to produce accurate and quantitative ground cover data with limited processing power requirements and rapid responses to limited input information. Three different image feature descriptors (color, texture, and oriented gradients) were chosen to represent image blocks which were used to assess alternative modeling options and to ultimately train a decision tree algorithm for classification purposes.

Results from this algorithm showed good correlation for all three coverage classifications with R-squared values of 0.86, 0.87, and 0.96 for green vegetation, straw/dormant vegetation, and exposed soil, respectively. However, the average absolute value of the difference between manual and algorithm-derived classifications was 2.4, 3.3, and 1.2 times, respectively, greater than the average standard deviation between manual observations. The algorithm was less successful for images containing both green vegetation and straw/dormant vegetation (~50:50 coverage of each), $20 \pm 2\%$ average difference between manual and algorithm, but performed successfully for all other ground cover configurations, $2 \pm 1\%$ average difference between manual and algorithm. Based on correlation, this method was a suitable determinant of ground coverage data.

Both field and initial greenhouse studies were conducted in parallel for the purposes of analyzing non- straw mulched composted media to a standard topsoil with straw and fertilizer and identifying critical elements for further greenhouse study based on objective three. From field observations, greenhouse experimental design was tailored to focus on the initial growth stage where low GV and high nutrient loss was identified. The field study received continued monitoring beyond the initial phase of establishment to identify any trends in runoff quality.

Using the image algorithm derived for the purpose of ground cover analysis, three distinct growth periods were seen in the field element of this project. After initial establishment, GV growth in the field showed few statistical differences among the different media applications. During the initial establishment phase, BNS (87% vs 38-62% at 69 days) at the HA site and TS (100% vs 61-73% at 73 days) at the UM site had statistically higher GV growth rates than other non-straw mulched applications. GV establishment in the greenhouse without straw mulch (25% slope, 30 cm water, 60 days) failed to increase above 35% for compost mixtures and 77% for TS. It was hypothesized that this was due to moisture loss in the compost amended materials which had greater porosity and higher wilting points. Straw mulching improved GV establishment by 4-33-fold for all media with no statistical differences between rates of establishment. Slope ratio increase was seen to negatively affect grass establishment (60-99% reduction in GV as slope increased from 5% to 50%) likely due to reduced soil moisture from gravimetric filtration.

Runoff volume was reduced with both straw and compost addition. Volume runoff for all composted materials was significantly reduced with straw application, by 64-99%, with the most successful reductions occurring for TB and TG. All compost amended media with straw mulching (except BTS with 13% higher runoff volume than TS) reduced runoff from TS by 13-64%. As slope ratio declined, runoff generation was seen to decline by 46-96% (from the 50% to 5% slope).

In the field and greenhouse, sediment loss was not seen to be correlated with total rainfall application or vegetation growth. Straw and compost addition were seen to decrease sediment mass transport. This was most significant for both TB and TG which saw sediment EMC and mass reductions of 92-99.9%, largely attributed to runoff volume reductions. With straw mulching, compost addition to TS reduced sediment mass export and EMC with the BS and TBS treatments showing the greatest sediment reduction 74-98%, due to increased infiltration and soil aggregation from compost addition. Slope ratio increase showed 2-140- fold increase in sediment yield from 5% to 50% slopes.

A major issue facing the use of composted material as a SMP has been the increased export of nutrients. Similar issues (increasing EMCs with increased compost addition) were found in the 'initial phase' greenhouse studies without straw mulching, but not through extended field observation which showed statistically similar concentrations (1-3 mg-P/L phosphorus and 3-5 mg-N/L nitrogen). Straw mulching significantly reduced mass export of both nitrogen (71-92%) and phosphorus (66-99%) but did not consistently reduce EMC (both TB and TG had 4-17% increase in nitrogen

EMC, attributed to decreased runoff volume more affected by the ‘first flush’). With the addition of straw mulching, compost amendments reduced mass export of nitrogen and phosphorus from the standard TS (except BTS which exported 36% more nitrogen and 15% more phosphorus) largely attributed to volume runoff reduction and additional storage and water transport pathways provided by the straw. BS and TBS were the most effective at export reduction of nitrogen and phosphorus (57-82%). Nitrogen (14-140-fold) and phosphorus (5-37-fold) mass export both increased with slope ratio from the 5% to 50% slopes.

According to both field and greenhouse observations, compost addition has the potential to greatly reduce overall runoff volume, nutrient loss, and sediment loss compared to fertilized topsoil. However, compost is highly rich in nutrients and was seen to export both phosphorus and nitrogen at high concentrations without straw mulching. It is strongly recommended that straw mulching (or some other equally effective cover) be used for all treatment applications regardless of compost percent. At a 25% slope, compost addition with straw mulching showed similar or improved runoff generation, runoff quality, and vegetation establishment to TS (except BTS). Both BS and TBS showed the greatest improvement to the TS standard with 56-79% reduction in runoff volume and mass export of sediment and nutrients. Slope ratio changes greatly affected the total mass export for each medium tested in inconsistent ways. However, the runoff and vegetation establishment reduction benefits of compost addition, analyzed in detail at the 25% slope, may be less evident at shallower slopes and more evident at steeper slopes.

5.1 Recommendations for Future Research

The image classification process developed in this work used pre-determined pixel block sizes to segment images in order to reduce computational time. It is possible that an attempt to segment the image into objects (vis-à-vis the set pixel bocks proposed here) prior to algorithm training and object classification may improve the performance of the algorithms; however, this change may also increase the computational need and classification time, which could offset potential benefits.

The soil mixtures tested through this study produced a range of runoff water quality results that did not show strong correlation to compost: topsoil ratios. However, with inclusion of additional compost: topsoil mixtures a trend in data may yield an optimal ratio for minimizing runoff volume and increasing runoff quality. Furthermore, only straw mulching as an additional SMP was used with compost application, which showed significant improvements in all examined performance criteria; using other SMPs may yield better results (e.g., geotextiles or silt fences). Water treatment residual and activated charcoal have been seen to reduce phosphorus and nitrogen concentrations in a variety of SMPs; investigation into compost amended with these or other materials may also yield reduced nutrient export.

References

Abrahams, A D, A J Parson, and P J Hirsch. 1992. "Field and laboratory studies of resistance to interrill overland flow on semi-arid hillslopes, southern Arizona." *Overland flow* 1-23.

Abrahams, A D, A J Parson, and P J Hirsch. 1992. "Field and laboratory studies of resistance to interrill overland flow on semi-arid hillslopes, southern Arizona." In *Overland Flow: Hydraulics and Erosion Mechanics*, by A J Parson and A D Abrahams, 1-23. London: UCL Press.

Allred, B, G Brown, and J Bigham. 2007. "Nitrate mobility under unsaturated flow conditions in four initially dry soils." *Soil Science* 172;27-41.

Allred, B, G Brown, and J Bigham. 2007. "Nitrate mobility under unsaturated flow conditions in four initially dry soils." *Soil Science* 172: 27-41.

Armenise, E, R Simmons, S Ahn, A Garbout, S Doerr, S Mooney, C Sturrock, and K Ritz. 2018. "Soil seal development under simulated rainfall: structural, physical, and hydrological dynamics." *Journal of Hydrology* 556: 211-219.

Armenise, E, R Simmons, S Ahn, A Garbout, S Doerr, S Mooney, C Sturrock, and K Ritz. 2018. "Soil Seal Development Under Simulated Rainfall: Sturctural, Physical, and Hydrological Dynamics." *Journal of Hydrology* 211-219.

Arya, L M, and J. F Paris. 1981. "A physico-empirical model to predict the soil moisture characteristic from particle-size distribution and bulk density data." *Soil Science Society of America Journal* 1023-1030.

Arya, L M, and J. F Paris. 1981. "A physico-empirical model to predict the soil moisture characteristic from particle-size distribution and bulk density data." *Soil Science Society of America Journal* 45 (6): 1023-1030.

2020. "Atmospheric Integrated Research Monitoring Network." National Atmospheric Deposition Program.

Bauer, T, and P Strauss. 2014. "A rule-based image analysis approach for calculating residues and vegetation cover under field conditions." *Catena* 113: 363-369.

Bauer, T., & Strauss, P. 2014. "A rule-based image analysis approach for calculating residues and vegetation cover under field conditions." *Catena* 363-369.

Bohn, H, B McNeal, and G O'Connor. 1985. *Soil Chemistry.* 2nd. New York, NY: John Wiley & Sons.

—. 1985. *Soil Chemistry, end Ed.* New York, NY: John Wiley & Sons.

Booth, D T, S E Cox, and R D Berryman. 2006. "Point sampling digital imagery with "samplepoint"." *Environmental Monitoring and Assessment* 123: 97-108.

Booth, D. T., S. E. Cox, and R. D. Berryman. 2006. "Point sampling digital imagery with "samplepoint"." *Environmental Monitoring and Assessment* 123: 97-108.

Bresson L, Koch C, Le Bissonnais E, Barriuso E, Lecomte V. 2001. "Soil Surface Structure Stabilization by Municipal Waste Compost Application." *Soil Science Society of America* 1804-1811.

Bresson, L, C Koch, E Le Bissonnais, E Barriuso, and V Lecomte. 2001. "Soil surface structure stabilization by municipal waste compost application." *Soil Science Society of America Journal* 65 (6): 1804-1811.

Burgos-Artizzu, X. P., A. Ribeiro, A. Tellaeche, G. Pajares, and C. Fernández-Quintanilla. 2009. "Improving weed pressure assessment using digital images from an experience-based reasoning approach." *Computers and Electronics in Agriculture* 60 (1): 176-185.

Burgos-Artizzu, X. P., Ribeiro, A., Tellaeche, A., Pajares, G., & Fernández-Quintanilla, C. 2009. "Improving weed pressure assessment using digital images from an experience-based reasoning approach." *Computers and Electronics in Agriculture* 176-185.

Burgos-Artizzu, Xavier P, Angela Ribeiro, Alberto Tellaeche, G Pajares, and C Fernandez-Quintanilla. 2010. "Analysis of natural images processing for the extraction of agricultural elements." *Image and Vision Computing* 138-149.

Castle, S. 2009. "Soil inorganic nitrogen: KCl extraction." In *Aridlands Ecology Lab Protocol*. Boulder: University of Colorado.

Chaganti, V, and D Crohn. 2014. "Evaluation of compost blankets for erosion control and runoff water quality on a constructed hillslope in southern california." *Transactions of the ASABE.* 403-416.

Cimbala, John M. 2011. "Outliers." *Penn State University.*

Crogger, C. 2005. "Potential compost benefits for restoration of soils disturbed by urban development." *Compost Sci. Util.* 243-251.

Crogger, C. 2005. "Potential compost benefits for restoration of soils disturbed by urban development." *Compost Science & Utilization* 13 (4): 243-251.

Curtis, M, and V Claassen. 2007. "Using compost to increase infiltration and improve the revegetation of a decomposed granite roadcut." (JOURNAL OF GEOTECHNICAL AND GEOENVIRONMENTAL ENGINEERING) 133 (2).

Curtis, M, and V Claassen. 2007. "Using compost to increase infiltration and improve the revegetation of a decomposed granite roadcut." *Journal of Geotechnical and Geoenvironmental Engineering* 133 (2): 215-218.

Daniel, Wayne W. 1990. *Applied nonparametric statistics.* PWS-Kent Publ.

—. 1990. *Applied nonparametric statistics.* 2nd. Boston: PWS-Kent Publ.

Davis, A P, and R H McCuen. 2005. *Stormwater management for smart growth.* Springer, New York.

Diaz, L., M. De Bertoldi, and W. Bidlingmaier. 2007. *Compost science and technology.* Elsevier.

Duley, F. 1939. "Infiltration of water into soils as influenced by surface seal development." *Soil Science Society of America* 60-64.

Duzgun, O, M Hatipoglu, and A Aydilek. 2020. "Geotechincal properties of compost amended topsoils for use on highway slopes." *Environmental Geothnics Report 20-1, University of Maryland, College Park, MD* 85.

Edwards W, Larson W. 1969. " Infiltration of water into soils as influenced by surface seal development." *Trans ASAE* 463-465.

Edwards, L, J R Burney, G Richter, and A H MacRae. 2000. "Evaluation of compost and straw mulching on soil-loss characteristics in erosion plots of potatoes in prince edward island, canada." *Agriculture, Ecosystems and Environment* 81 (3): 217-222.

Faucette, L., J. Governo, C. Jordan, B. Lockaby, H. Carino, and R. Governo. 2007. "Erosion control and storm water quality from straw with pam, mulch, and compost blankets of varying particle sizes." *Journal of Soil and Water Conservation* 62(6), 404-413.

Faucette, L.B., C.F. Jordan, L.M. Risse, M.L. Cabrera, D.C. Coleman, and L. T. West. 2005. "Evaluation of stormwater from compost and conventional erosion control practices in construction activities." *Journal of Soil and Water Conservation.* 60 (6): 355-362.

Faucette, L.B., Jordan, C.F., Risse, L.M., Cabrera, M.L., Coleman, D.C., and West L.T. 2005. "Evaluation of Stormwater from Compost and Conventional Erosion Control Practices in Construction Activities." *Journal of Soil and Water Conservation.* 355-362.

Fu, X, M Shao, X Wei, and R Horton. 2009. "Effects of two perennials, fallow and millet on distribution of phosphorous in soil and biomass on sloping loess land, China." *Catena* 77; 200-206.

Gee, C., J. Bossu, G. Jones, and F. Truchetet. 2008. "Crop/weed discrimination in perspective agronomic images." *Computers and electronics in agriculture* 60 (1): 49-59.

Gee, Ch, J Bossu, G Jones, and F Truchetet. 2008. "Crop/weed discrimination in perspective agronomic images." *Computers and electronics in agriculture* 49-59.

Genet, M, A Stokes, T Fourcaud, and J Norris. 2010. "The influence of plant diversity on slope stability in a moist evergreen deciduous forest." *Ecological Engineering* 36 (3): 265–75.

Genet, M, A Stokes, T Fourcaud, and J Norris. 2010. "The Influence of Plant Diversity on Slope Stability in a Moist Evergreen Deciduous Forest." *Ecological Engineering* 36(3): 265–75.

Glanville, T. D., R A Persyn, T L Richard, J M Laflen, and P. M. Dixon. 2004. "Environmental effects of applying composted organics to new highway embankments: Part 2. Water quality." *Transactions of the ASAE* 47 (2): 471-478.

Glanville, T. D., R. A. Persyn, T. L. Richard, J. M. Laflen, and P. M. 2004. "Environmental effects of applying composted organics to new highway embankments: Part 2. Water quality." *Trans. ASAE* 471-478.

Glasbey, C.A., and G.W., Horgan. 1995. *Image Analysis for the Biological Sciences.* New York: Wiley.

Glasbey, C.A., Horgan, G.W.,. 1995. *Image Analysis for the Biological Sciences.* New York: Wiley.

Gonzalez, R C, R E Woods, and S L Eddins. 2003. *Digital Image Processing Using MATLAB.* New Jersey: Prentice Hall.

Gonzalez, R. C., R. E. Woods, and S. L. Eddins. 2003. *Digital Image Processing Using MATLAB.* New Jersey: Prentice Hall.

Hairsine P., Rose C. 1991. "Rainfall detachment and deposition: sediment transport in the absence of flow-driven." *Soil Science Society of America Journal* 320-324.

Hairsine, P., and C Rose. 1991. "Rainfall detachment and deposition: sediment transport in the absence of flow-driven." *Soil Science Society of America Journal* 55 (2): 320-324.

Hamuda, E., Glavin, M., & Jones, E. 2016. "A survey of image processing techniques for plant extraction and segmentation in the field." *Computers and Electronics in Agriculture* 184-199.

Hamuda, E., M. Glavin, and E. Jones. 2016. "A survey of image processing techniques for plant extraction and segmentation in the field." *Computers and Electronics in Agriculture* 125: 184-199.

Hansen, N E, D M Vietor, C L Munster, R H White, and T L Provin. 2012. "Runoff and nutrient losses from constructed soils amended with compost." *Applied and Environmental Soil Science.*

Harrell, M, and G Miller. 2005. "Composted yard waste affects soil displacement and roadside vegetation." (HortScience) 40 (7): 2157-2163.

Harrell, M, and G Miller. 2005. "Composted yard waste affects soil displacement and roadside vegetation." *Hortscience* (HortScience) 40 (7): 2157-2163.

Hatton, TJ, NE West, and PS Johnson. 1986. "Relationships of error associated with ocular estimation and actual total cover." *Journal of Range Management* 39:91-92.

Hay, GJ, T Blaschke, DJ Marceau, and A Bouchard. 2003. "A comparison of three image-object methods for the multiscale analysis of landscape structure." *ISPRS Journal of Photogrammetry and Remote Sensing* 57:327-345.

Hillel, D. 2004. *Introduction to Environmental Soil Physics.* Elsevier.

Hsieh, Y, K Grant, and G Bugna. 2009. "A field method for soil erosion measurements in agricultural and natural lands." *Journal of Soil and Water Conservation* 374-382.

Hsieh, Y, K Grant, and G Bugna. 2009. "A field method for soil erosion measurements in agricultural and natural lands." *Journal of Soil and Water Conservation* 64 (6): 374-382.

Hu, J B, M X Dai, and S T Peng. 2018. "An automated (novel) algorithm for estimating green vegetation cover fraction from digital image: UIP-MGMEP." *Environ Monit Assess* 190: 687.

Hu, J. B., M. X. Dai, and S. T. Peng. 2018. "An automated (novel) algorithm for estimating green vegetation cover fraction from digital image: UIP-MGMEP." *Environ Monit Assess* 190 (11): 190: 687.

Humphry, J.B, T.C Daniel, DR Edwards, and A.N Sharpley. 2002. "A portable rainfall simulator for plot-scale runoff studies." *Applied Engineering in Agriculture* Vol. 18(2): 199-204.

Humphry, J.B, T.C Daniel, DR Edwards, and A.N Sharpley. 2002. "A portable rainfall simulator for plot-scale runoff studies." *Applied Engineering in Agriculture* 18 (2): 199-204.

Jordán, A., L.M. Zavala, and J. Gil. 2010. "Effects of mulching on soil physical properties and runoff under semi-arid conditions in southern Spain." *Catena* 81:77-85.

Kennedy, KA, and PA Addison. 1987. "Some considerations for the use of visual estimates of plant cover in biomonitoring." *Jounal of Ecology* 75:151-157.

Kennedy, KA, and PA Addison. 1987. "Some considerations for the use of visual estimates of plant cover in biomonitoring." *Jounal of Ecology* 75: 151-157.

Khaleel, K., K R Reddy, and M R. Overcash. 1981. "Changes in soil physical properties due to organic waste applications: A review." *Journal of Environmental Quality* 10, 133-141.

Khaleel, K., K R Reddy, and M R. Overcash. 1981. "Changes in soil physical properties due to organic waste applications: A review." *Journal of Environmental Quality* 10: 133-141.

Kirchoff, Christine J., Joseph F. Malina, and Michael E. Barrett. 2003. "Characteristics of composts: moisture holding and water quality improvement." *CRWR Online Report 03-09.*

Kirchoff, Christine J., Joseph F. Malina, and Michael E. Barrett. 2003. "Characteristics of Composts: Moisture Holding and Water Quality Improvement." *CRWR Online Report 03-09.*

Kranz, C, R McLaughlin, A Johnson, G Miller, and J Heitman. 2020. "The effects of compost incorporation on soil physical properties in urban soils - A concise review." *Journal of Environmental Management* 261.

Kropff, M, J Wallinga, and L Lotz. 1997. *Precision Agriculture: Spatial and Temporal Variability of Environmental Quality.* Chester: Wiley.

Laflen, J. M., Amemiya, M., & Hintz, E. A. 1981. "Measuring crop residue cover." *Journal of Soil and Water Conservation* 341-343.

Laflen, J. M., M. Amemiya, and E. A. Hintz. 1981. "Measuring crop residue cover." *Journal of Soil and Water Conservation* 36 (6): 341-343.

Liu, Q Q, and V P Singh. 2004. "Effect of microtopography, slope length and gradient, and vegetative cover on overland flow through simulation." *J. Hydrol. Eng.* 9; 375-382.

Liu, Q Q, and V P Singh. 2004. "Effect of microtopography, slope length and gradient, and vegetative cover on overland flow through simulation." *Journal of Hydrologic Engineering* 9 (5): 375-382.

Liu, Q. Q., and V. P. Singh. 2004. "Effect of microtopography, slope length and gradient, and vegetative cover on overland flow through simulation." *Journal of Hydrologic Engineering* 9 (5): 375-382.

Liu, Y, Y Tao, K Wan, G Zhang, D Liu, G Xiong, and F Chen. 2012. "Runoff and nutrient losses in citrus orchards on sloping land subjected to different surface mulching practices in the Danjiangkou Reservoir area of China." *Agricultural water management* 34-40.

Liu, Y, Y Tao, K Wan, G Zhang, D Liu, G Xiong, and F Chen. 2012. "Runoff and nutrient losses in citrus orchards on sloping land subjected to different surface mulching practices in the Danjiangkou Reservoir area of China." *Agricultural Water Management* 110: 34-40.

Lottes, P, M Horferlin, S Sander, and C Stachniss. 2017. "Effective Vision-based Classification for Separating Sugar Beets and Weeds for Precision Farming." *Journal of Field Robotics* 1160-1178.

Lottes, P., M. Horferlin, S. Sander, and C. Stachniss. 2017. "Effective Vision-based Classification for Separating Sugar Beets and Weeds for Precision Farming." *Journal of Field Robotics* 34 (6): 1160-1178.

Luscier, J, W Thompson, J Wilson, B Gorham, and L Dragut. 2006. "Using digital photographs and object-based image analysis to estimate percent ground cover in vegetation plots." *Front Ecol Environ* 4(8):408-413.

Luscier, J., W. Thompson, J. Wilson, B. Gorham, and L. Dragut. 2006. "Using digital photographs and object-based image analysis to estimate percent ground cover in vegetation plots." *Frontiers in Ecology and the Environment* 4 (8): 408-413.

MDOTSHA. 2019. "Standard specifications for construction and materials." *Maryland Department of Transportation State Highway Administration.*

MDOTSHA. 2019. "Standard Specifications for Construction and Materials." *Maryland Department of Transportation State Highway Administration.*

Meyer, G. E., & Camargo-Neto, J. 2008. "Verification of color vegetation indices for automated crop imaging applications." *Computers and Electronics in Agriculture* 282-293.

Meyer, G. E., and J. Camargo-Neto. 2008. "Verification of color vegetation indices for automated crop imaging applications." *Computers and Electronics in Agriculture* 63 (2): 282-293.

Meyer, G.E., T.W. Hindman, and K Lakshmi. 1998. "Machine vision detection parameters for plant species identification." *SPIE 3543, Precision Agriculture and Biological Quality.* Bellingham, WA.

Meyer, L.D. 1965. "Simulator of rainfall for soil erosion research." *Transactions of the ASAE* 8(1): 63-65.

Meyer, L.D. 1965. "Simulator of rainfall for soil erosion research." *Transactions of the ASAE* 8 (1): 63-65.

Mitchell, D. 1997. "State highway departments find it pays to use compost." *Bio Cycle* 38 (8): 67-72.

Mitchell, D. 1997. "State Highway Departments Find it Pays to Use Compost." *Bio Cycle* 38(8), 67-72.

Montalvo, M, J M Guerrero, J Romeo, L Emmi, M Guijarro, and G Pajares. 2013. "Automatic expert system for weeds/crops identification in images from maize fields." *Expert systems with applications* 75-82.

Montalvo, M., J. M. Guerrero, J. Romeo, L. Emmi, M. Guijarro, and G. Pajares. 2013. "Automatic expert system for weeds/crops identification in images from maize fields." *Expert Systems with Applications* 40 (1): 75-82.

Morgan, J, S Gergel, and N Coops. 2010. "Aerial Photography: A Rapidly Evolving Tool for Ecological Management." *BioScience* 60:47-59.

Mortensen, A. K., Dyrmann, M., Karstoft, H., Nyholm Jørgensen, R., Gislum, R. 2016. "Semantic segmentation of mixed crops using deep convolutional neural network." *CIGR-AgEng conference.*

Mortensen, A. K., M. Dyrmann, H. Karstoft, R. N. Jorgensen, and R. Gislum. 2016. "Semantic segmentation of mixed crops using deep convolutional neural network." *International Conference of Agricultural Engineering.* Aarhus: Denmark. 1-6.

Mukhtar, S, M.L McFarland, and C.A Wagner. 2008. "Runoff and water quality from inorganic fertilizer and erosion control compost treatments on roadway sideslopes." *Transactions of the ASABE* Vol. 51(3):927-936.

Mukhtar, S, M.L McFarland, and C.A Wagner. 2008. "Runoff and water quality from inorganic fertilizer and erosion control compost treatments on roadway sideslopes." *Transactions of the ASABE* 51 (3): 927-936.

Mutchler, C, C Murphree, and K Mcgregor. 1994. *Laboratory and Field Plots for Erosion Research. Soil Erosion Research Methods.* Delray Beach, FL: St. Lucie Press.

Neeser, C, A Martin, P Juroszek, and D Mortensen. 2000. "A Comparison of Visual and Photographic Estimates of Weed Biomass and Weed Control." *Weed Technology* 14:586-590.

Neitsch, S. L., J. G. Arnold, J. R. Kiniry, and J. R Williams. 2011. *Soil and water assessment tool theoretical documentation version 2009.* Texas Water Resources Institute.

Northwest Alliance for Computational Science and Engineering. 2013. *PRISM Climate group.* 6. Accessed 3 2019. www.prism.oregonstate.edu.

Pan, Chengzhong, and Z Shangguan. 2006. "Runoff hydraulic characteristics and sediment generation in sloped grassplots under simulated rainfall conditions." *Journal of Hydrology* 178-185.

Pandey, A, S K Himanshu, S K Mishra, and V P Singh. 2016. "Physically based soil erosion and sediment yield models revisited." *Cantena* 595-620.

Pandey, A., S. K. Himanshu, S. K. Mishra, and V. P. Singh. 2016. "Physically based soil erosion and sediment yield models revisited." *Cantena* 147: 595-620.

Patrignani, A, and T Ochsner. 2015. "Canopeo: Apowerful new tool for measuring fractional green canopy cover." *Agronomy Journal* 107 (6): 2312-2320.

Patrignani, A.,&Ochsner, T. E. 2015. "Canopeo: Apowerful new tool for measuring fractional green canopy cover." *Agronomy Journal* 2312-2320.

Reinsch, C, D Admiraal, B Dvorak, C Cecrle, T Franti, and J Stansbury. 2007. "Yard waste compost as a stormwater protection treatment for construction sites." *Water Environment Research* 868-876.

Renard, K, G Foster, D Weesies, D McCool, and D Yoder. 1997. *Predicting Soil Erosion by Water: A Guide to Conservation Planning With the Revised Universal Soil Loss Equation (RUSLE).* Tucson, AZ: USDA, Southwest Watershed Research Center.

Renard, K. G., G. R. Foster, G. A. Weesies, D. K. McCool, and D. C. Yoder. 1997. *Predicting soil erosion by water: A guide to conservation planning with the revised universal soil loss equation (RUSLE).* Tucson: US Department of Agriculture.

Riegler-Nurscher, Peter, Johann Prankl, Thomas Bauer, Peter Strauss, and Heinrich Prankl. 2018. "A machine learning approach for pixel wise classification of residue and vegetation cover under field conditions." *Biosystems Engineering* 188-198.

Riegler-Nurscher, Peter, Johann Prankl, Thomas Bauer, Peter Strauss, and Heinrich Prankl. 2018. "A machine learning approach for pixel wise classification of residue and vegetation cover under field conditions." *Biosystems Engineering* 169: 188-198.

Robinson, C, M Ghaffarzadeh, and R Cruse. 1996. "Vegetative Filter Strip Effects on Sediment Concentrations in Cropland Runoff." *Journal Soil and Water Conservation* 50(3):227-230.

Sander, G C, P B Hairsine, C W Rose, D Cassidy, J Y Parlange, W L Hogarth, and I G Lisle. 1996. "Unsteady soil erosion model, analytical solutions and comparison with experimental results." *Journal of Hydrology* 351-367.

Sander, G C, P B Hairsine, C W Rose, D Cassidy, J Y Parlange, W L Hogarth, and I G Lisle. 1996. "Unsteady soil erosion model, analytical solutions and comparison with experimental results." *Journal of Hydrology* 178: 351-367.

Shelton, C. H., R. D. von Bernuth, and S. P. Rajbhandari. 1985. "A continuous–application rainfall simulator." *Transactions of the ASCE* 28 (4): 1115-1119.

Shin, S, S Park, and B Choi. 2016. "Universal power law for relationship between rainfall kinetic energy and rainfall intensity." *Advances in Meteorology* 2016: 1-11.

Singh, V. 1996. *Kinematic Wave Modeling in Water Resources: Surface Water Hydrology.* New York, NY: Wiley.

Snedecor, George W, and William G Cochran. 1989. *Statistical Methods.* Eighth Edition: Iowa State University Press.

Society for Range Management, Task Group on Unity in Concepts and Terminology. 1995. "New concepts for assessment of rangeland condition." *Journal of Range Management* 48:271-282.

Society for Range Management, Task Group on Unity in Concepts and Terminology. 1995. "New concepts for assessment of rangeland condition." *Journal of Range Management* 48: 271-282.

Sparks, D. 2003. *Environmental Soil Chemistry.* Elsevier.

2005. *Standard methods for the examination of water and wastewater.* Vol. 21. Washington, DC: New York: American Public Health Association.

Strauss, P., D. Swoboda, and W. E. H. Blum. 2003. "“How effective is mulching and minimum tillage to control runoff and soil loss? A literature review”." In *Twenty-Five Years of Assessment of Erosion*, by D., Cornelis, W. Gabriels, 545-550. Belgium: Ghent University.

Strauss, P., Swoboda, D. and Blum, W. E. H. 2003. "“How effective is mulching and minimum tillage to control runoff and soil loss? A literature review”." In *Twenty-five years of assessment of erosion*, by D., Cornelis, W Gabriels, 545-550. Belgium: Ghent University.

Sykes, J. M., A. D. Horrill, and M. D. Mountford. 1983. "Use of visual cover assessments as quantitative estimators of some British woodland taxa." *Journal of Ecology* 71 (2): 437-450.

Sykes, J. M., Horrill, A. D., & Mountford, M. D. 1983. "Use of visual cover assessments as quantitative estimators of some British woodland taxa." *Journal of Ecology* 437-450.

Thornton, R, and A Saul. 1987. "Temporal variation of pollutants in two combined sewer systems." *Proceedings of the 4th International Conference on Urban Storm Drainage.* Lausanne, Switzerland. 51-52.

Todd, L R, Kommedahl, T. 1994. "Image analysis and visual estimates for evaluating disease reactions of corn to Fusarium stalk rot." *Plant Dis.* 876-878.

Todd, L. R., and T. Kommedahl. 1994. "Image analysis and visual estimates for evaluating disease reactions of corn to Fusarium stalk rot." *Plant Disease* 78 (9): 876-878.

United States. Natural Resources Conservation Service. Soil Science Division. 2017. *Soil survey manual (Fourth, Ser. United States department of agriculture handbook, number 18).* United States Department of Agriculture.

USEPA. 2003. *Compost use on state highway applications.* Washington D.C: US Environmental Protection Agency.

Viessman, W, M Hammer, E Perez, and P Chadik. 2009. *Water Supply and Pollution Control.* Upper Saddle River, NJ: Pearson Prentice Hall.

Vukovic M., Soro A. 1992. *Determination of Hydraulic Conductivity of Porous Media from Grain-size Composition.* Littleton, Colorado: Water Resources Publications.

Wang, J, G Lu, X Guo, Y Wang, S Ding, and D Wang. 2011. "Effects of straw mulch and balanced fertilization on nitrogen loss from farmland in chaohu lake region." *Nutrient Cycling in Agroecosystems* 101, 93-106.

Welch, BL. 1947. "The generalization of "student's" problem when several different population variances are involved." *Biometrika* 28-35.

Welch, BL. 1947. "The generalization of "student's" problem when several different population variances are involved." *Biometrika* 34 (1/2): 28-35.

Woebbecke DM, Meyer GE, Von Bargen K, Mortensen DA. 1995. "Color indices for weed identification under various soil, residue, and lightning conditions." *Trans. ASAE* 259-269.

Woebbecke, D M, G E Meyer, K Von Bargen, and D A Mortensen. 1995. "Color indices for weed identification under various soil, residue, and lightning conditions." *Transactions of the ASAE* 38 (1): 259-269.

Zimdahl, R L. 1993. *Fundamentals of Weed Science.* San Diego: Academic Press.

—. 1993. *Fundamentals of Weed Science.* San Diego: Academic Press.

Zimdahl, R L. 1988. "Management in Agroecosystems, Ecological Approaches." 145-155. Boca Raton, FL: CRC Press.

Zimdahl, R. L. 1988. "The Concept and Application of the Critical Weed-Free Period." In *Management in Agroecosystems: Ecological Approaches*, by A. Miguel and M. Liebman, 145-155. Boca Raton, FL: CRC Press.